An e-Compendium on

50 YEARS OF ENERGY RESEARCH

at ICAR - Central Institute of Agricultural Engineering, Bhopal

celebrating 50 ICAR-CIAE 1976-2026
Golden Years of Engineering in Indian Agriculture


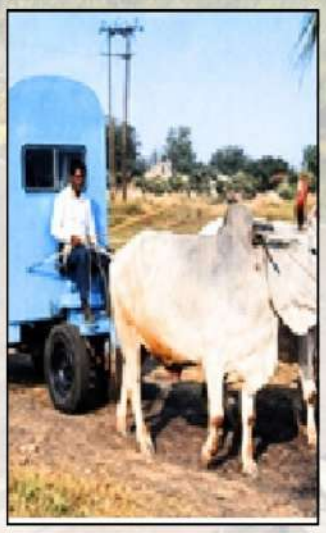





A RETROSPECTIVE (1975–2025)

Honouring five decades of innovation, impact and stewardship in agricultural energy systems.

ICAR-Central Institute of Agricultural Engineering
Nabi bagh, Berasia Road, Bhopal-462038 (M.P.)

CIAE Technical article number: CIAE/AEPD/TB/2026/424

An e-Compendium on

50 Years of Energy Research

AtICAR-Central Institute of Agricultural Engineering, Bhopal

A Retrospective (1975–2025)

Honouring five decades of innovation, impact and stewardship in agricultural energy systems.

Edited by:

Sandip Mandal
Sandip Gangil
Kamendra

Published by:

Director, Central Institute of Agricultural Engineering, Nabibagh, Berasia Road, Bhopal – 462038

Foreword

The Central Institute of Agricultural Engineering (CIAE), Bhopal has completed five decades of dedicated service to the nation through research, development, and innovation in agricultural engineering. Among its many areas of contribution, energy research has remained a cornerstone, supporting agricultural mechanization, resource efficiency, and sustainable rural development. Over the years, the Institute has addressed the evolving energy needs of Indian agriculture through systematic research on farm power sources, renewable energy technologies, and energy-efficient systems suited to diverse agro-climatic conditions.

This e-compendium has been brought out to document and showcase the 50 years of energy research accomplishments at CIAE, highlighting significant technological developments, research milestones, and their impact on agricultural productivity and sustainability. The chapters presented in this volume reflect the collective efforts of scientists, engineers, and technical staff who have contributed to advancing knowledge and developing practical solutions for the farming community and allied sectors.

By compiling these research outcomes in a digital format, the e-compendium aims to serve as a valuable reference for researchers, students, policymakers, and development professionals, while also preserving the institutional legacy of CIAE in the domain of agricultural energy. It is hoped that this publication will not only provide insights into past achievements but also inspire future research and innovation aligned with national priorities and emerging challenges in energy and agriculture.

I applaud the editorial team and contributors for their efforts in bringing out this e-compendium and extend my best wishes for its wide dissemination and effective utilization.

Director, CIAE

About the compendium

This e-compendium presents a comprehensive account of research and development efforts in the field of agricultural energy and biomass utilization, undertaken over the years. It covers a wide spectrum of studies ranging from village energy surveys and assessment of energy equivalents to advanced approaches for energy management in agriculture, providing a holistic understanding of energy use patterns, efficiency, and optimization at farm and rural levels. The compendium documents methodologies and findings that have supported informed planning, technology selection, and sustainable energy interventions in rural areas.

The volume also includes significant research contributions on biomass densification technologies, such as briquetting and pelleting, aimed at improving the handling, storage, and utilization efficiency of agricultural residues. Emerging and alternative liquid biofuel technologies form an important component of this compendium, encompassing work on algal biofuels, ethanol, and butanol production. In addition, research on thermochemical conversion processes (including combustion, gasification, and pyrolysis) and biochemical conversion routes (such as anaerobic digestion and fermentation) is presented to highlight diverse pathways for energy recovery from biomass. Other related research on biomass utilization and value addition has also been included, reflecting integrated and multidisciplinary efforts toward sustainable and renewable energy solutions for agriculture and rural development.

Editors

Acknowledgements

We thank the Directors, scientific and technical staff past and present, partner organizations, funding agencies, farmer collaborators, and administrative teams whose sustained support made fifty years of research and outreach possible.

CONTENTS

CHAPTER – 1

1. Introduction

Energy is a critical driver of agricultural productivity, sustainability, and rural development. Over the past five decades, the Central Institute of Agricultural Engineering (CIAE), Bhopal has played a pioneering role in advancing energy research for the diverse and evolving needs of Indian agriculture. Since its inception, the Institute has consistently contributed to the development, evaluation, and dissemination of energy-efficient technologies aimed at enhancing farm mechanization, optimizing resource use, and promoting environmentally sustainable practices.

This technical bulletin documents 50 years of energy research at CIAE, Bhopal, highlighting key milestones, innovations, and technological breakthroughs achieved. It presents a comprehensive overview of research outcomes that have strengthened energy security, reduced drudgery, improved efficiency, and supported climate-resilient agricultural systems.

1.1 Rural energy system

An analysis of rural energy distribution indicates that out of a total consumption of approximately 11.42×10^{12} kcal, nearly 65% is derived from non-commercial sources, about 15% from human and animal power, and only 20% from commercial energy. This distribution implies that nearly 80% of rural energy demand is met through renewable sources, underscoring the central role of indigenous and naturally replenished energy systems in agricultural and rural livelihoods.

The sun is the primary source of energy for almost all processes on Earth. Solar energy drives atmospheric circulation, wind patterns, ocean currents, and the hydrological cycle through evaporation and precipitation. Through photosynthesis, plants capture solar energy and store it in the form of carbohydrates, proteins, fats, oils, cellulose, and lignin. Humans and animals depend on plant biomass, directly or indirectly, to meet their metabolic energy needs. Over geological timescales, plant and animal residues are transformed into coal and petroleum, which now constitute major energy sources for modern industrial society.

Within agricultural systems, energy is supplied through a wide range of sources, including human and animal labour, solar radiation, wind, biomass, coal, fertilizers, seeds, agro-chemicals, petroleum products, and electricity. Energy sources that deliver usable energy directly to the production system through mechanical, chemical, or biological processes are categorized as direct energy sources. These include human labour, animal power, petroleum fuels, and electrical energy. In contrast, indirect energy sources represent energy invested in the

manufacture or production of inputs such as seeds, farmyard and poultry manure, fertilizers, agro-chemicals, and agricultural machinery.

Energy sources may also be classified based on their replenishment period. Renewable energy sources are those that are replenished over relatively short time spans and include human and animal power, solar energy, wind, biomass, and organic manures. Non-renewable energy sources, such as petroleum products, require extremely long periods for regeneration and are finite in nature.

1.2 Energy Equivalents

From an economic perspective, energy sources that are locally available and obtained at relatively low cost are termed non-commercial energy sources, while cost-intensive sources such as petroleum products and electricity are classified as commercial energy sources. To enable systematic comparison and assessment of different energy inputs in agricultural research, energy equivalents are commonly expressed in megajoules (MJ). These equivalents, presented in Table 1.1, provide a standardized basis for evaluating energy use efficiency and sustainability across agricultural systems.

Table 1.1: Equivalents for various sources of energy

Particulars	Units	Equivalent energy, MJ	Remarks
A. INPUTS			
1. Human labour			
Adult man	Man-h	1.96	1 Adult woman = 0.8
Women	Woman-h	1.57	Adult man
Child	Child-h	0.98	1 Child = 0.5 Adult man
2. Animals			
Bullocks	Pair-h	14.05	Body weight above 450 kg
Large	Pair-h	10.10	Body weight above 350-450 kg
Medium	Pair-h	8.07	Body weight less than 350 kg
He-buffalos	Pair-h	15.15	He-buffalo = 1.5 medium bullock
Camel or Horse	Animal-h	10.10	Camel or Horse = medium bullock pair
Mules and other small animals	Animal-h	4.04	Small animal = 0.4 medium bullock pair
3. Diesel	Litre	56.31	
4. Petrol	Litre	48.23	
5. Electricity	kWh	11.93	
6. Machinery			
Electric motor	kg	64.80	Distribute the weight of the machinery equally over the total life span of the
Prime movers other than electric motors (including self-propelled machines)	kg	68.40	

Farm machinery excluding self-propelled machines	kg	62.70	machinery (in hours). Find the use of machinery (hours) for the particular operation for crop
7. Seed			
Output of crop production system and not processed			Same as that of output of crop production system
Output of crop production system and is processed before using it for seed (e.g. potato, groundnut, cotton, etc.)			Add 1.5, 1.0 and 0.5 MJ/kg for potato, groundnut and other seed respectively to the equivalent energy of the product of crop production system

B. OUTPUTS

1. Main Product			
Cereal crops such as Wheat, Maize, Sorghum, Bajra, Barley, Oats, Paddy (not Shelled Rice)	kg (dry mass)	14.7	The main output is grains
Pulses such as Mash, Moong, Lentil, Arhar, Soyabean, Peas, Beans, etc.	kg (dry mass)	14.7	The main output is grains
Oilseeds such as Cotton seed, Groundnut Pods (not Shelled), Sesamum, Rape Seed, Mustard, Linseed, Sunflower seeds, etc.	kg	25.0	The main output is seed except for groundnut, where it is pods
Sugarcane (harvested mass)	kg	5.3	The main output is cleaned canes
Vegetables			
a) Root or Tuber vegetables High Food values: Sweet Potato, Topica, etc.	kg	5.6	
Medium Food values: Colocasia, Potato etc.	kg	3.6	
Low food values: Carrot, Radish, Onion, Beetroot, etc.	kg	1.6	
b) Fruit or seed vegetables Broad Beans, Cluster beans, Ladyfinger, Musk Melon, Water melon etc.	kg	1.9	
Gourd family vegetable: Cucumber family, Drumstic Giant, Green Papaya, Pumpkin, Tomato, Chillies etc.	kg	0.8	
c) Leave Vegetables: Cabbage, Spinach, Green Mustard Leaves, etc.	kg	1.2	
Fruits			
a) Higher food values: Tamarind, Grapes, etc.	kg	11.8	

b) Low Food values: Fruit, Guava, Mango, Amla, Apple, Peach, Ber, Chiku, Cashew fruit, Citrus, etc.	kg	1.9	
Fiber Crops: Cotton, Sunheamp, Sunflex, Jute etc.	kg (dry mass)	11.8	Main Product is fibre
Fodder Crops: Berseem, Lucerne, Senji, Oats, Maize, Bajra, Sorghum, Cowpeas, Guara, Napier etc.	kg	18.0	The main product is dry or green fodder
Green Manuring Crops: Dhaincha, Cowpeas, Sunheamp, etc.			Energy equivalent to the amount of nutrients added to the soil through green manuring
Fuel Crops: Sunheamp, Dhaincha, etc.	kg (dry mass)	18.0	The main product is fuel wood
Crops for Fodder, Fuel & Green manuring Crops			
a) Fodder from cereal crops: Maize, Oats, Bajra, Sorghum, etc.	kg (dry mass)	14.7	The main output is seed
b) Other Fodder Crops (Berseem, Lucerene, Senji, Guara, etc.) Fuel crops and green Manuring Crops	kg (dry mass)	10.0	The main output is seed
2. By Product			
Straw, Vines, etc.	kg (dry mass)	12.5	
Stalks, Cobs, Fuelwood, Fruits, Vines, Plant Wood etc.	kg (dry mass)	18.0	
Leaves, Vines and Straw from vegetables	kg (dry mass)	10.0	
Cotton seed	kg (dry mass)	25.0	
Fibre crop seed other than cotton and fuel crops seed	kg (dry mass)	10.0	
Sugarcane Leaves & Tops	kg (dry mass)	16.1	
3. Animal Production System			
Milk			
Buffalo	kg	4.9	
Cow, Goat etc.	kg	2.8	
Eggs (Whole)			
Duck	kg	7.58	
Hen	kg	7.41	
Meat (Cleaned)			
Poultry	kg	4.56	
Mutton	kg	4.94	
Fish	kg	4.26	
Dung (dry)	kg	18.0	

Source: Singh et al., 1996

1.3. Trends in use of Agricultural Inputs

The use of agricultural inputs in India has shown a consistent upward trend over the years (Fig. 1.1a). The consumption of seeds increased from 918 thousand tonnes in 2000–01 to 2773.4 thousand tonnes in 2010–11 and further to 4451.1

thousand tonnes in 2022–23, reflecting the growing adoption of high-yielding and improved seed varieties. The use of agrochemicals also increases from 17,407.02 thousand tonnes in 2000–01 to 29,854.72 thousand tonnes in 2021–22, showing intensified input use for crop protection (Fig. 1.1b). Similarly, the consumption of electricity for agricultural purposes increased from 84,729 GWh in 2000–01 to 126,377 GWh in 2010–11 and further to 228,451 GWh in 2021–22, indicating more use of electric power for irrigation and mechanized operations in farming. The trend in use of agricultural inputs shows that the total volume of inputs over the years has increased substantially (Fig. 1.1c).

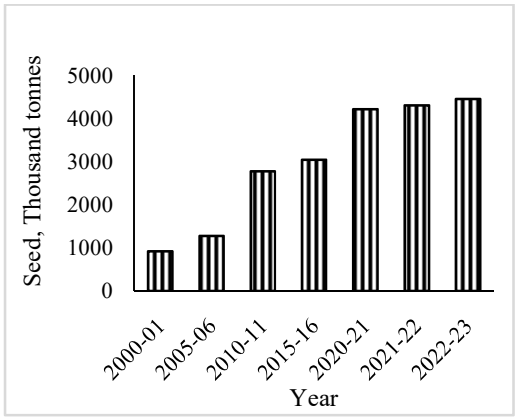

(a) Seed

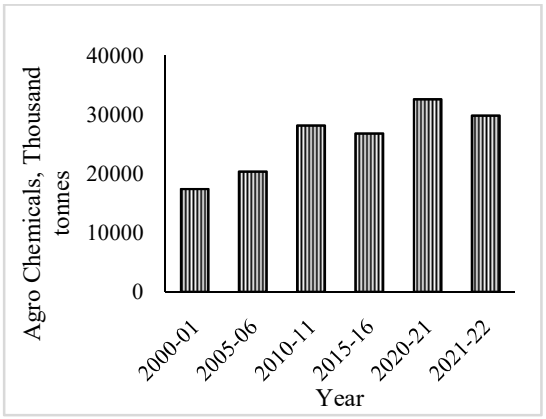

(b) Agro chemical

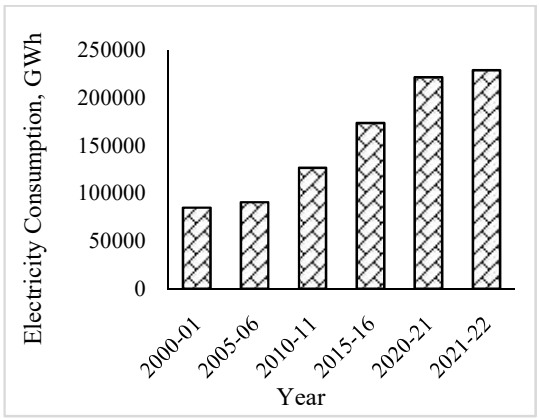

(c) Electricity consumption in agriculture

Fig. 1.1 Trends in use of agricultural inputs (Agricultural statistics at a Glance, 2024)

CHAPTER – 2

2. Farm Power Sources

Farm power is a critical input for carrying out agricultural operations in a timely, efficient, and economical manner. Traditionally, agriculture relied on human and animal power, which continues to play an important role, particularly in small and marginal farming systems. With technological advancement, mechanical power sources such as diesel engines, tractors, and power tillers have become dominant, significantly enhancing operational capacity and field efficiency. In parallel, the increasing use of electrical power has supported irrigation, post-harvest processing, and on-farm energy applications. In recent decades, growing emphasis on sustainability has led to the integration of renewable energy sources, including solar, biomass, and biogas, to supplement conventional power systems. Research on farm power sources focuses on optimizing the appropriate mix of these energy inputs to improve productivity, reduce drudgery, enhance energy use efficiency, and promote environmentally sustainable agricultural development.

2.1 Agricultural Workers

The population of agricultural workers has shown a fluctuating trend over the years. In 1971–72, there were about 125.7 million workers engaged in agriculture, which increased steadily to 263.1 million by 2011–12 due to population growth and dependence on agriculture. However, a significant decline was observed in the following decade, with the number dropping to 228.53 million by 2021–22 (Fig.2.1a). This decrease indicates a gradual shift of the workforce from agriculture to non-agricultural sectors and the increasing mechanization of farm operations, reducing the dependence on human labour.

2.2 Draught Animals

The population of draught animals has shown a consistent decline over the decades, highlighting the gradual replacement of animal power with mechanical sources. In 1971–72, there were about 78.41 million draught animals, which reduced to 64.09 million by 2001–02 and further down to 27.52 million by 2021–22 (Fig. 2.1b). This sharp decline demonstrates the declining role of animal power in farm operations due to the increasing availability and affordability of tractors, power tillers, and other mechanical power sources.

2.3 Power Tillers

The population of power tillers has increased steadily over the years, reflecting their growing importance in small and medium-scale farming. Starting from a negligible number of 0.016 million in 1971–72, the population increased to 0.123 million by 2001–02 and reached 0.508 million by 2021–22 (Fig. 2.1c). This steady rise shows the adoption of power tillers as a suitable mechanization option,

particularly for smallholders and farmers in hilly and coastal regions where tractors are less feasible.

2.4 Tractors

Tractors have emerged as the dominant source of mechanical power on Indian farms. The tractor population grew exponentially from 0.168 million in 1971–72 to 2.546 million by 2001–02, and further to 9.173 million by 2021–22 (Fig. 2.1d). This sharp increase highlights the rapid mechanization and modernization of Indian agriculture, driven by the need for higher efficiency, timeliness of operations, and enhanced productivity.

2.5 Diesel Engines

The use of diesel engines has also shown a rising trend, especially for irrigation and stationary farm operations. The population grew from 1.443 million in 1971–72 to 5.981 million in 2001–02 and reached 9.157 million by 2021–22 (Fig. 2.1e). Although their growth has slowed in recent years due to the expansion of electric motor usage, diesel engines continue to play a significant role in regions where electricity supply is unreliable or insufficient.

2.6 Electric Motors

Electric motors have shown the highest rate of growth among all stationary power sources, indicating the increasing electrification of rural areas. The population increased from 1.535 million in 1971–72 to 9.508 million in 2001–02 and reached a remarkable 21.392 million by 2021–22 (Fig. 2.1f). This rise reflects improved access to electricity for irrigation and other farm operations, contributing significantly to the mechanization of Indian agriculture.

2.7 Farm power availability and share of farm power sources

The farm power availability in India has steadily increased over the years (Fig. 2.2). It was 0.372 kW/ha in 1971–72, which increases to 1.711 kW/ha in 2011–12 and further increased to 3.045 kW/ha in 2021–22 due to the rapid adoption of tractors, power tillers and other modern agricultural machinery, along with increased use of electrical and renewable energy sources in farming operations.

2.8 Share of farm power sources

The share of different farm power sources in India has changed significantly over time, showing a clear transition from animate to mechanical and electrical power (Fig. 2.3). In 1971–72, draught animals contributed about 56.99% of the total power, while tractors, diesel engines, and electric motors together accounted for around 30.65%, and human power contributed 12.10%. By 2011–12, the share of draught animals declined sharply to 7.83%, whereas tractors, diesel engines, and electric motors contributed 47.00%, 17.25%, and 21.39%, respectively, indicating a

dominance of mechanical and electrical sources. In 2021–22, tractors became the major source with 63.44% of total power, followed by electric motors at 18.64% and diesel engines at 12.08%, while the combined share of human and animal power reduced to only 5.16%, reflecting the near-complete mechanization of Indian agriculture (Mehta *et al*., 2023).

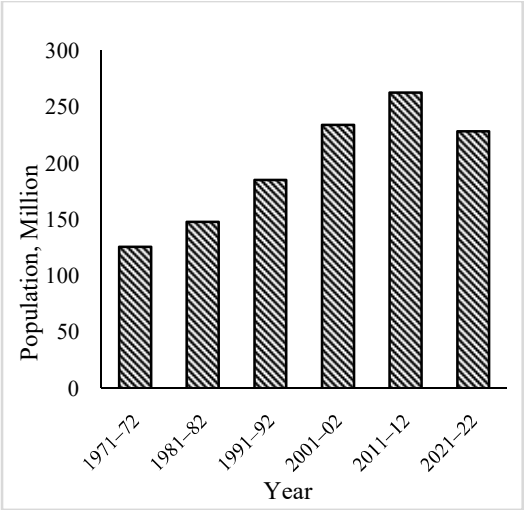

(a)Agricultural Workers

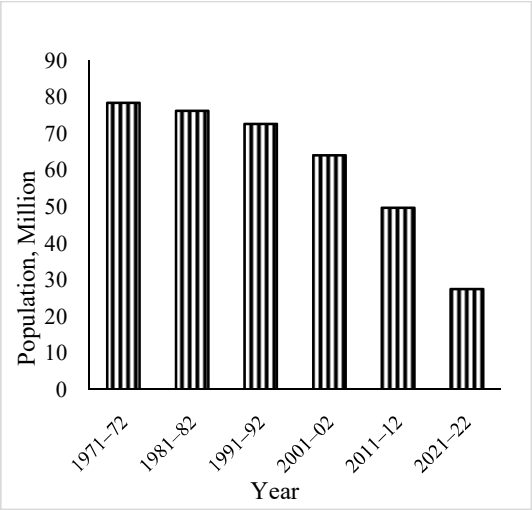

(b)Draught Animals

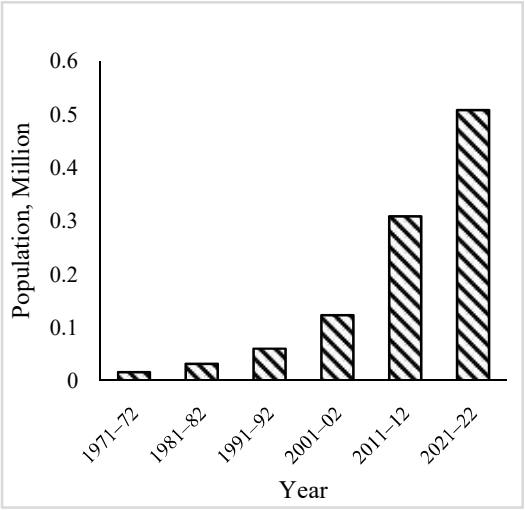

(c)Power Tillers

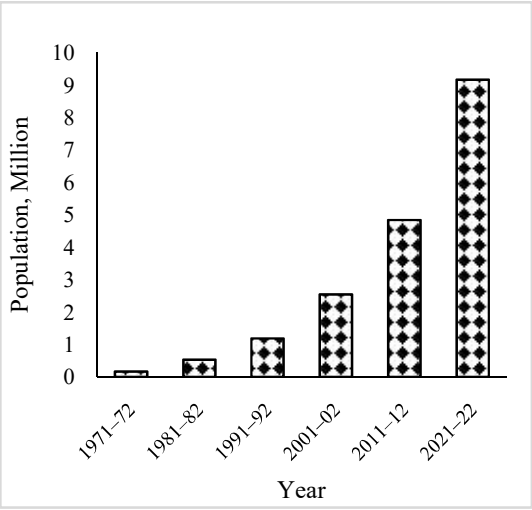

(d) Tractor

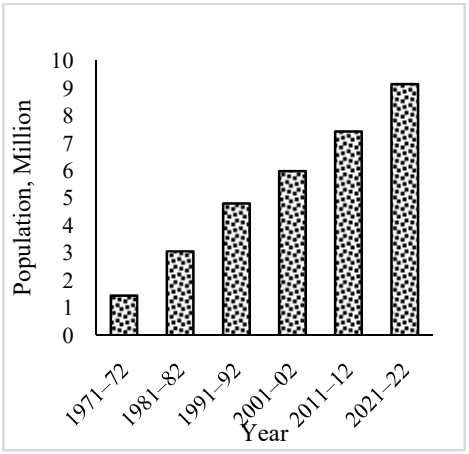

(e) Diesel Engines

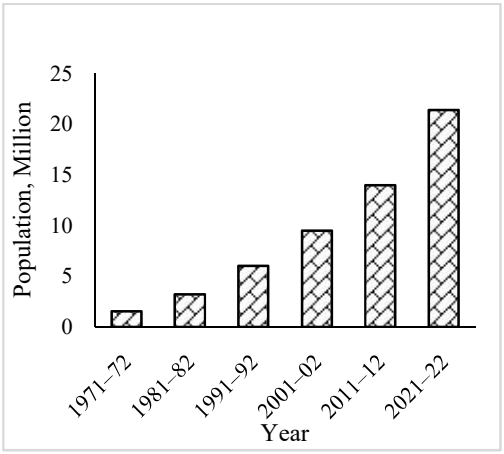

(f) Electric Motors

Fig. 2.1 Farm Power Sources (Mehta et al., 2023)

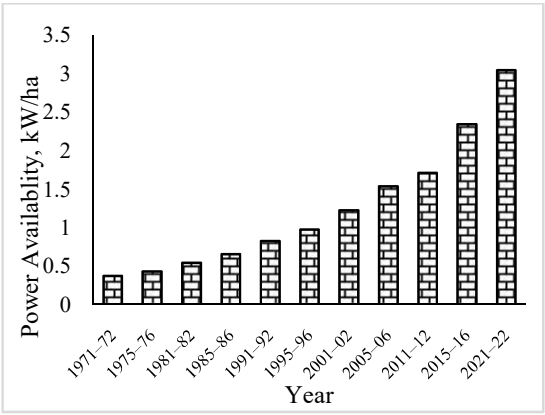

Fig. 2.2 Total Farm Power Availability (Mehta et al., 2023)

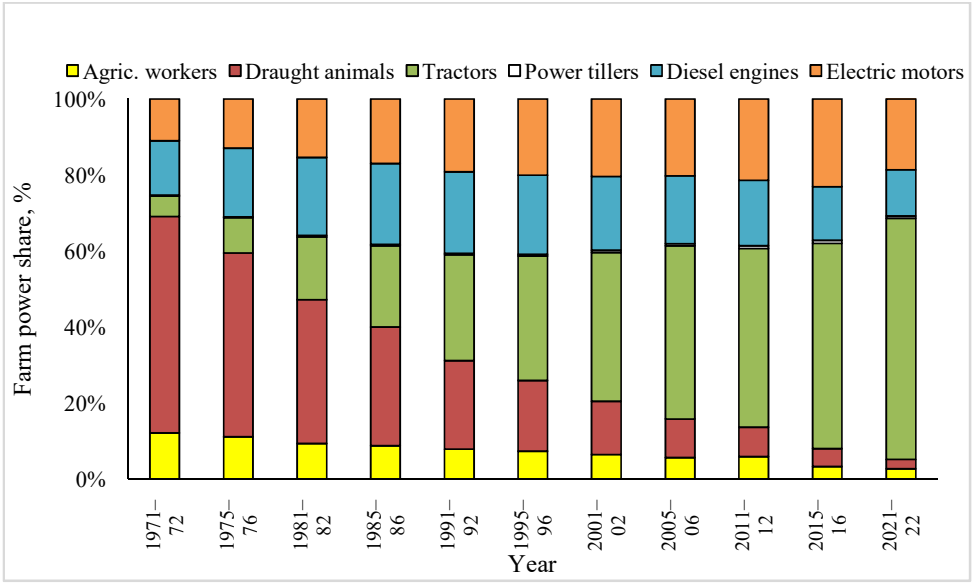

Fig. 2.3 Share of farm power sources(Mehta et al., 2023)

The share of tractive power over total farm power in India has increased significantly over the years, reflecting the rapid mechanization of agricultural operations (Table 2.1). In 1971–72, the total farm power was 52.13 MkW, with 68.96% contributed by animate sources and 31.04% by electromechanical sources, while tractive power constituted only 5.38% of the total. By 2011–12, total farm power had risen to 241.22 MkW, with animate power declining to 13.62% and electromechanical power increasing to 86.38%, resulting in a higher tractive power share of 46.83%. In 2021–22, total farm power reached 424.32 MkW, with electromechanical sources dominating at 94.84% and tractive power contributing 63.45%, indicating a major shift toward mechanical traction and widespread use of tractors and power tillers in Indian agriculture.

Table 2.1: Share of tractive power over total farm power in India

Year	Total farm power (MkW)	Animate power (%)	Electromechanical power (%)	Tractive over total power (%)
1971–72	52.13	68.96	31.04	5.38
1981–82	76.36	47.23	52.77	16.51
1991–92	118.29	31.76	68.24	28.29
2001–02	172.44	20.69	79.31	39.51
2011–12	241.22	13.62	86.38	46.83
2021–22	424.32	5.16	94.84	63.45

(Source: Mehta et al., 2023)

In the agriculture sector, high-speed diesel (HSD) consumption was 575 thousand tonnes in 2014–15 and increased to 723 thousand tonnes in 2017–18, reflecting higher farm mechanization and increased agricultural activities during this period (Fig. 2.4). However, by 2023–24, consumption had decreased to 413 thousand tonnes, indicating improved efficiency of farm machinery, better fuel management practices, and a gradual shift toward alternative energy sources in agriculture.

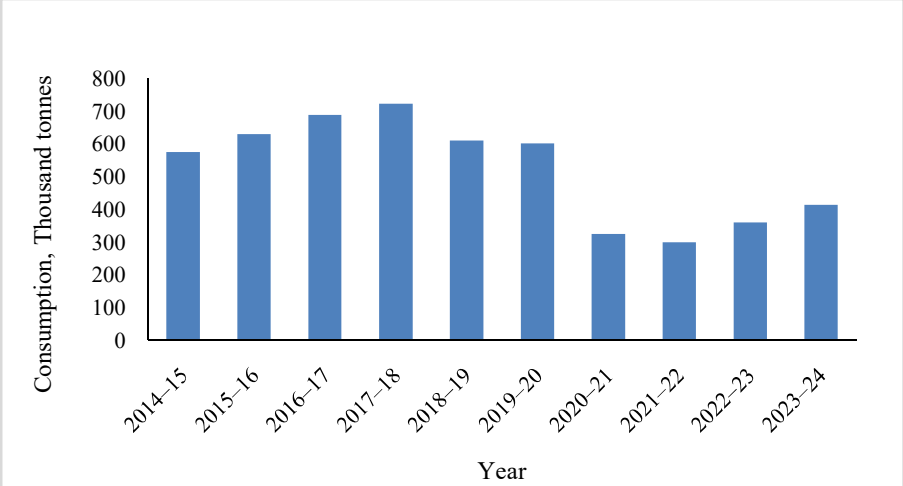

Fig.2.4 Consumption of High Speed Diesel (Source: Anonymous, 2024 b)

Unit farm power has been used as one of the indicators for assessing the growth of mechanization (Nowacki, 1978). Relationship between growth in food grain yield and unit farm power therefore, was considered appropriate for estimating farm power requirement. This could be represented by a quadratic equation given below:

$$Y_{fg} = 325 \pm 1675X_p - 449X_p^2, (R^2=0.97) \quad \text{... (2.1)}$$

Where X_p = All India average potential availability of farm power, kW/ha

Actual use of farm power especially in the case of mechanical and electrical depend upon availability of fuel and electricity as discussed by Singh and De (1999). Usually 35% of the total yearly use of the tractor is for field operation and for remaining time transport of men and material.

The equation was also developed based on State average use of inputs and expressed as;

$$Y_{fgs} = 1122 + 126.47X_{ps}, (R^2 = 0.81) \quad \text{... (2.2)}$$

Where, X_{ps}= Average potential power available in different states, kW/ha.

It revealed that farm power upto 0.80 kW/ha does not have much influence on yield, and other inputs have greater influence.

CHAPTER - 3

3. Energy and Resource Assessment in Village Ecosystem

3.1 Assessment of Village Islamnagar (1980-81)

In order to assess the energy needs of a village by the different categories of farmers and to study the extent of self-sufficiency/deficiency in food, feed, fuel and fiber and also the extent of recycling/utilization pattern of agricultural biomass in the Village ecosystem, the Institute conducted an Energy Census and Resource Assessment Survey of the village Islamnagar in the District of Bhopal in 1981. This survey became the basis for planning, implementation and monitoring of an integrated energy and nutrient supply system since April 1984. The survey revealed a total population of 1529 across 224 households, with a balanced human–animal population ratio of nearly 1:1. Agriculture was the major livelihood activity, with 48.6% irrigated and 51.4% rainfed area. The Rabi season dominated cultivation (87.6%), with wheat and paddy as major crops.

The village ecosystem utilized diverse energy sources for different activities. Total available energy was mainly derived from non-commercial renewable sources (80.7%), followed by commercial energy (17.0%) and animate energy (2.3%). Out of the total energy consumed, 83.8% was used for domestic activities, 10.25% for agricultural inputs, 4.66% for crop production, 0.49% for post-harvest operations, and 0.84% for cattle raising.

For crop production, the energy contribution was from seed (33.6%), fertilizer (19.9%), diesel (19.3%), machinery (15.2%), electricity (6.6%), animal (4.2%), and human labour (1.2%). Tractor-operated farms consumed more energy (9909 MJ/ha) than bullock-operated farms (4170 MJ/ha). In domestic energy use, firewood (59.1%) and dung cakes (37.2%) were the dominant fuels, with limited reliance on kerosene and electricity. The village was self-sufficient in cereals, vegetables, sugarcane, and milk but deficient in pulses (32%) and oilseeds (71%).

3.1.1 Energy and Material Flow in Village Ecosystem

Fig. 3.1 shows the total energy and material flow within the village ecosystem, highlighting the interrelationship among land, water, livestock, and human resources, with the sun as the primary energy source. It also reflects the import of industrial goods and the exchange of food materials within and outside the ecosystem. The output–input ratios were 13.70 for crop production, 0.54 for animal raising, and 0.0055 for human activities, indicating high energy productivity in crop-based systems compared to other sectors.

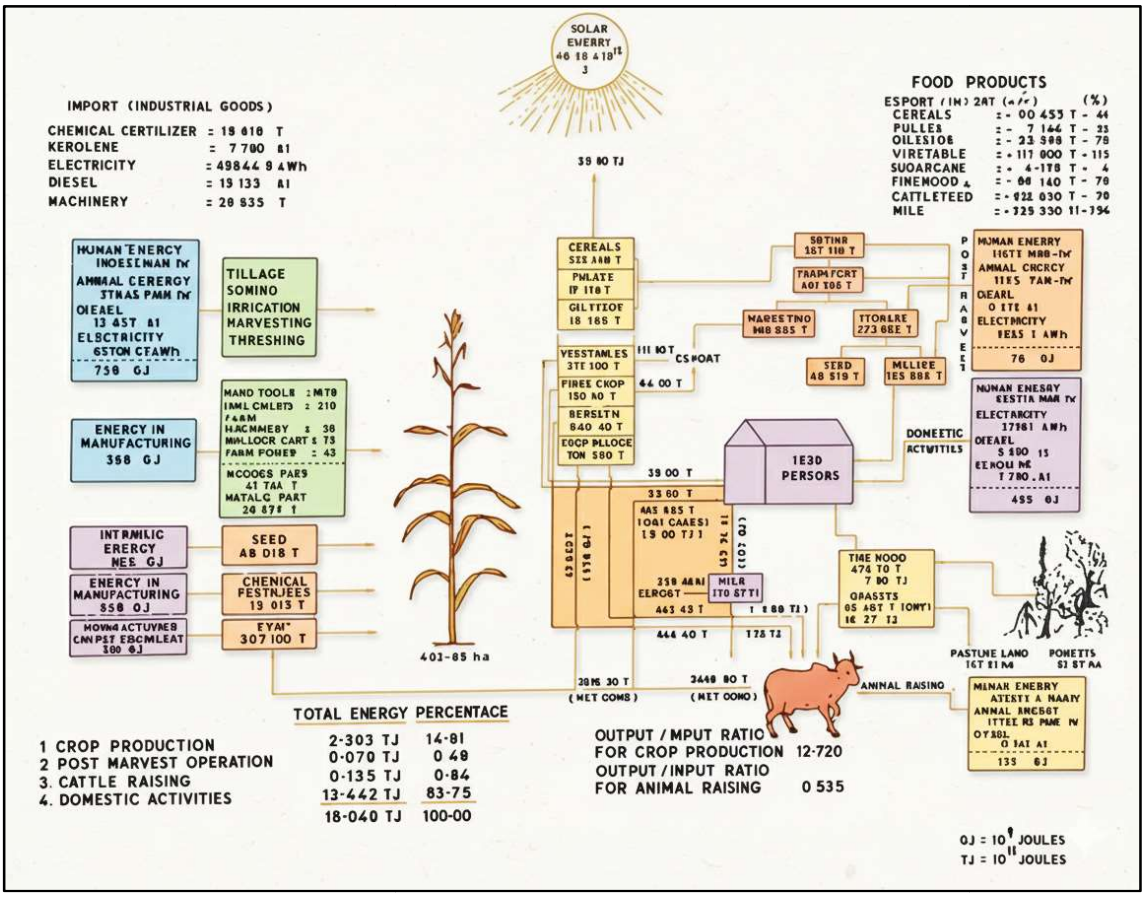

Fig. 3.1 Annual Energy Flow in Village Eco-system

3.1.2 Solar Energy Flow in the Village Ecosystem

The village of Islamnagar annually receives approximately 46,600 TJ of solar energy, out of which 40.44 TJ is effectively converted into food, feed, fuel, and fibre. To facilitate this conversion, the ecosystem utilizes 0.27 TJ from chemical fertilizers, 0.37 TJ from machinery, 0.46 TJ from diesel, and 0.16 TJ from electricity. The net human energy output is 0.22 TJ, which represents only 0.0055 of the total biological conversion from solar energy. Fig. 3.2 depicts the utilization of solar energy and its flow in the village ecosystem through various stages.

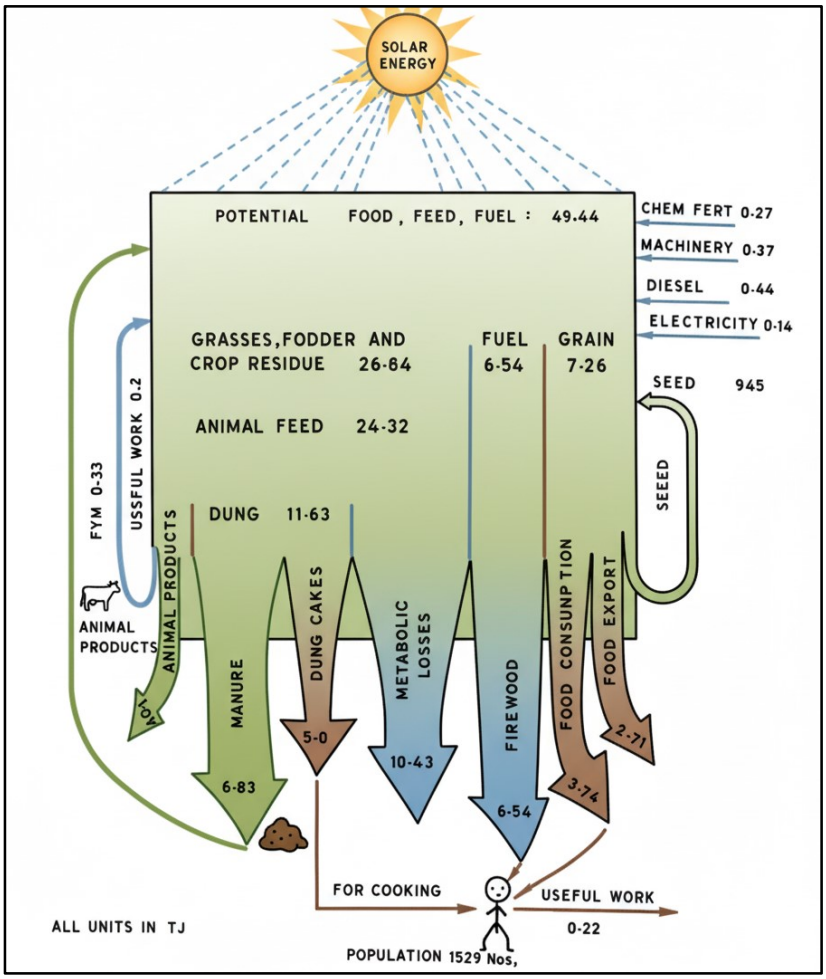

Fig. 3.2 Solar Energy Flow in Village Eco-system (Islamnagar)

3.1.3 Planning for Self-Sufficiency in Fuelwood Supply

The annual consumption of fuelwood and cow dung for cooking in the village was 473 tonnes and 448 tonnes, respectively. To reduce dependence on these resources, efforts were made to improve the thermal efficiency of traditional stoves and install individual and community biogas plants. It was estimated that 50 individual and three community biogas plants could meet about 58% of the cooking energy demand and supply essential nutrients for crop production. So far, 44 individual and one community biogas plant have been installed, and 150 households have adopted smokeless stoves, minimizing the 20% fuelwood deficit.

To enhance energy efficiency and reduce dependence on conventional fuels, several technological interventions were implemented in the village. These included improved cookstoves, solar devices, and biogas systems for both individual and community use. The major techniques introduced and their outcomes are summarized in Table 3.1.

Table 3.1: Techniques Introduced for Improving Energy Efficiency in Village Islamnagar

S. No.	Technique Introduced	Description / Activities	Outcome / Benefit
1	Smokeless Chullahs (Improved Cookstoves)	160 smokeless stoves were distributed among village households to reduce fuelwood consumption and indoor smoke.	Improved thermal efficiency, reduced fuelwood use, and better indoor air quality.
2	Solar Cookers	69 solar cookers were procured from MP UrjaVikas Nigam, Bhopal and demonstrated in the village. Used for cooking dal, rice, vegetables, fish, cakes, kheer, etc.	Reduced dependence on conventional fuels; promoted use of renewable solar energy.
3	PV Street Lighting System	5 photovoltaic (PV) street lights (Model RES 2012 VPB) were installed in Mastipura hamlet of Islamnagar with assistance from MP UrjaVikas Nigam.	Improved rural lighting and safety; reduced kerosene and electricity use.
4	Individual Biogas Plants	44 biogas plants of 7 different designs (KVIC, Janta, PAU, Deenbandhu, Pragati, Capsule, etc.) with 1–8 cum/day capacity were installed. Beneficiaries trained in operation and maintenance.	Met about 40–60% of cooking energy needs; reduced dung cake use and improved waste utilization.
5	Community Biogas Plants	3 community biogas plants (KVIC design) of 85, 35, and 35 cum capacity were set up with support from the Department of Non-Conventional Energy Sources and MP UrjaVikas Nigam. One 85 cum plant commissioned in July 1988 supplied gas to 62 families.	Provided clean cooking fuel for multiple households; reduced fuelwood pressure; promoted community energy self-sufficiency.

3.1.4 Planning for Self-Sufficiency in Fodder and Crop Production

In village Islamnagar, the total fodder availability was 1928 tonnes (dry weight) against a requirement of 2740 tonnes, resulting in a 29.7% deficit. To overcome this, 38 ha of hillock land and 1 ha of Panchayat land were used for afforestation, while 10 ha were planted with high-yielding grasses such as Cenchrussetigerus and Cenchrusciliaris. A 1 ha grass nursery was also established to supply slips to farmers, demonstrating the potential to meet about 77% of the annual fodder deficit (812 tonnes).

For achieving self-sufficiency in pulse and oilseed production, land reallocation planning was carried out based on standard dietary requirements. The proposed reallocation of cultivated land under different crops to enhance production and economic returns is presented in Table 3.2.

Table 3.2: Tentative reallocation of land under different crops

S. No.	Crop	Original Allocation		Proposed Allocation	
		Kharif	Rabi	Kharif	Rabi
1	Wheat	-	275.6	-	18.4
2	Paddy	33.4	-	33.4	-
3	Bengal gram	-	24.2	-	43.4
4	Groundnut	9.7	-	95.1	-
5	Maize	7.0	-	7.0	
6	Soybean	2.0		33.81	-
7	Mustard	-	-	-	32.3

3.1.5 Developmental Activities in Village Islamnagar

To improve agricultural productivity and livelihood opportunities in Islamnagar, several developmental interventions were undertaken focusing on irrigation, water conservation, fish farming and post-harvest processing.

Hydram Lift Irrigation System -to meet the irrigation requirement of the village, two Laxmi make double-pipe hydram units (12"×12"×2½") were installed on the Patra River at Shyampur site, utilizing the existing stop dam and foundation. These systems helped lift water efficiently without external energy input, ensuring sustainable irrigation for nearby fields.

Water Harvesting and Recycling System-for enhancing water availability, an energy-efficient water harvesting and recycling system was developed at the village pond site. A detailed grid survey at 10 m spacing and contour mapping at 0.2 m interval were conducted. The pond, spread over 3.6 ha, required 2,34,492 m^3 of earthwork and increased its storage capacity from 3.53 ha-m to 7.14 ha-m. This intervention expanded the irrigated command area from 17 ha to 40 ha, recording a 135% increase.

Fish Farm/Culture in 0.5 ha Private Pond -to diversify farm income, a fish farming unit was established by converting a 0.5 ha low-lying area into a pond. It was stocked with 7,000 fingerlings of silver carp and catala. Encouraged by the profitability, the farmer expanded the activity to 20 ha, producing 100–125 kg of fish daily and developing a major fish seed production center for species like Rohu, Katla, Bighead, and Silver Carp.

Post Harvest Operation and Equipments-for value addition and employment generation, a plan for post-harvest operations and agro-processing was implemented. The identified operations included cleaning, grading, drying, milling, dehusking, oil extraction, straw alkali mixing, briquetting, and rice puffing. The total cost of processing all farm produce locally was Rs. 2.06 lakh, with an additional gain of Rs. 13.02 lakh, resulting in a net profit of Rs. 10.96 lakh and a benefit-cost ratio of 53:1. Even processing only the produce earlier exported outside the village yielded a profit of Rs. 6.44 lakh. To support these activities, an Agro-Processing Centre was established and operated by the KrishiVigyan Kendra (KVK), CIAE, Bhopal.

3.1.6 Energy Flow Modelling for Village Ecosystem

Linear programming model of solar energy flow in village Islamnagar

A linear programming model was conceptualized for village level analysis after a through scanning of data available for village Islamnagar for the year 1980-81. The objective function of model design was to optimize the solar energy harvest through various food crops, vegetables and fodder crops and a set of constraint equation explaining the limitations of farmers with regard to land, labour material inputs, electricity, diesel, food consumption pattern and market constraints. The following equations shown the objective functions:

$$\sum_{C=1}^{C=20} (E_C + E_{CR} \times R_C) \times X_C \times Y_C = Z \quad \ldots (3.1)$$

Where,

C	=	Crop Index
E	=	Energy equivalent of crop C (GJ/kg)
E_{CR}	=	Energy equivalent of crop residue of crop C (GJ/kg)
R_C	=	Residue to grain ratio of crop C
Y_C	=	Average grain yield of crop C (kg/ha)
X_C	=	Area under crop C (ha)
Z	=	objective function (to be maximized)

Based on the village resources availability (1980-81), following constraints identified for sensitivity and post optimal analysis.

Rabi land constraints: 317.7 ha of total arable land sown in Rabi season, therefore, Rabi land area constraint can he given by equation:

$$\sum_{c} X_C \leq 317.7 \text{ ha} \quad \ldots (3.2)$$

Where, c= 1, 2, 5, 6, 13, 14, 15, 20

Kharif land constraint : only 86.2 ha of total arable land (405.7 ha) is sown in Kharif season, Kharif land constraint can be given by equation:

$$\sum_{c} X_C \leq 86.2 \text{ ha} \quad \ldots (3.3)$$

Where, c = 3,4,7,8,9,1041,12,26,17,18,19

Irrigated land constraint: In both Rabi and Kharifseasons farmers could irrigate 196.3 ha of land, therefore,

$$\sum_{c} X_C \leq 196.3 \text{ ha} \quad \ldots (3.4)$$

Where, c = 1,3,5,7,11,13,16,17,19,20

Operational energy constraint: Direct energy was expended by human labourers, draft animals electricity and diesel in various farm operations carried out on different crops. The supply constraints of these energy expenditures for the year 1980-81 were;

$$\sum_{c} H_C X_C \leq 8032.495 \text{ kWh} \quad \ldots (3.5)$$

$$\sum_{c} A_C X_C \leq 28081.782 \text{ kWh} \quad \ldots (3.6)$$

$$\sum_{c} C_C X_C \leq 99124.645 \text{ kWh} \quad \ldots (3.7)$$

Where,

H_C = Human energy expenditure on crop C (kWh/ha)
A_C = Animal energy expenditure on crop c (kWh/ha)
C_C = Commercial energy (electricity + diesel) expenditure on crop (kWh/ha)
C = 1 to 20

The greater than or equal to sign for human energy and animal energy are due to this easy and excessive availability in the village Islamnagar. But commercial energy is obviously a less than or equal to constraint.

Seed, human consumption and market constraints on production

Based on seed human consumption, marketed quantity and total production of various crops, vegetables and fodder crops of the year 1980-81. The following constraint equations have been derived:

Seed constraint:

$$\sum_{c} S_C X_C \leq 4905 \text{ kg} \quad \ldots (3.8)$$

Where,

S_C = Seed rate for crop C (kg/ha)
c = 1 to 20

Cereal constraint:

$$\sum_{c} Y_c X_c \leq 339345 \text{ kg} \quad \ldots (3.9)$$

Where,

Y_C = average yield of crop c (kg/ha)
c = 1,2,3,4,7,8,11,12

Pulse constraint:

$$\sum_{c} Y_C X_C \leq 17178 \text{ kg} \quad \text{... (3.10)}$$

Where,

c = 5,6,13,14

Oilseed constraint:

$$\sum_{c} Y_C X_C \leq 10795 \quad \text{... (3.11)}$$

Where,

c = 9,10,15,17,18

Sugar constraint:

$$\sum_{c} Y_C X_C \leq 120000 \text{ kg} \quad \text{... (3.12)}$$

Where,

c = 16

Vegetable constraint:

$$\sum_{c} Y_C X_C \leq 13300 \quad \text{... (3.13)}$$

Where,

c = 19

Crop residue and fodder constraint:

$$\sum_{c} Yer..X_C \leq 835370 \text{ kg} \quad \text{... (3.14)}$$

Where,

Yer = Crop residue yield of crop c (in the case of Berseem, Yer is total crop yield), kg/ha

c = 1 to 20

Fertilizer constraints

Based on fertilizer application rates for various crops, vegetables and fodder. The following constraints were developed on the basis of NPK application rates and their supply levels:

$$\sum_{c} N_C X_C \leq 7757.50 \text{ kg} \quad \text{... (3.15)}$$

$$\sum_{c} P_C X_C \leq 3431/10 \text{ kg} \quad \text{... (3.16)}$$

$$\sum_{c} K_C X_C \leq 3046.90 \text{ kg} \quad \text{... (3.17)}$$

Where,

N_C = Nitrogen application rate for crop c (kg/ha)

P_C = Phosphate application rate for crop c (kg/ha)

K_C = Potassium application rate for crop c (kg/ha)
c = 1 to 20

The right-hand sides of equation 15, 16 and 17 shows the total supply of N, P and K from both purchased fertilizer and farm yard manure for the year 1980-81.

The model was tested and validated for the base year 1980-81. Model evolved represented the state of agricultural production of the base year which were used for sensitivity and post-optimal analysis. It depicted an experimental set up on which a number of experiments could be carried out. Therefore, to a planner the most obvious experiment would be to study the response agricultural production with respect to changes in the area cultivated in both the season and their implications on various resources. The above response was measured in terms of solar energy harvest through various crops, vegetables and fodder.

3.1.7 Impact of technological inputs on productivity of land, animals, machines and human beings in village Islamnagar

The energy census and resource assessment survey was repeated in 1986 to assess the impact of introduction of various technologies on the productivity of land, animals, machines and human beings and the socioeconomic changes that may have taken place during the intervening period of five years. The following are the salient observations:

- Livestock population increased by 13.5%, indicating better animal management and resource utilization.
- Irrigated area increased from 403 ha to 438 ha, leading to a enhance in cropping intensity from 99.5% to 130.8%.
- Fertilizer consumption and overall grain production (cereals, oilseeds, pulses) increased notably, improving land productivity.
- Tree plantations on hillocks showed a 25.76% survival rate, with Subabool having the highest survival among species.
- Around 110 tonnes of fuelwood were generated from surviving trees and regenerated rootstocks, supporting local energy needs.
- Out of 44 domestic biogas plants, 40 were functional, though many operated below capacity due to limited cattle dung availability.
- The study emphasized linking biogas plants with fodder production to ensure a continuous supply of feedstock.
- Among three community biogas plants, one 85 m^3 plant was operational, providing cooking energy and nutrient-rich slurry for crops.
- Overall, the technological interventions enhanced the efficiency of land, livestock, and machinery, promoted renewable energy use, and improved agricultural and socio-economic sustainability in Village Islamnagar.

3.2 Assessment of village BarkhedaNathu in Bhopal District (1995-96)

The energy assessment of village BarkhedaNathu was conducted with the aim to assess the energy use pattern and resource availability of village ecosystem in respect of production agriculture, post-harvest operations, domestic & animal raising activities and to examine extent of self-sufficiency for food, fodder & animal waste in village ecosystem along with assessment of biomass recycling. The socio-economic and infrastructural constraints of village were also identified. One hundred sixty families of villagers were assessed by conducting extensive survey through a common questionnaire and verification of observations through actual measurements. The assessed households included 48.1% landless, 11.3% marginal, 21.2% small, 11.3% medium and 8.1% large respondents with total population of 884 consisting of 26.92% male, 24.44% female and 48.64% children. The livestock strength in village was recorded to be 378 whose maximum share (28.3%) was owned by small respondents. On an average each family had 2.36 livestock.

The village has total geographical area of 698.98 ha out of which only 28.66% (200.36 ha) was recorded to be owned by 83 (51.9%) respondents. Maximum land (43.1%) was owned by large farmers. In general, land available per family was 1.25 ha.Study revealed that only 144.81 ha of area was cropped during 1995-96 and the major crop was wheat sown on area of 108.50 ha (74.92% of total cropped land). The cropped land distribution between Rabi and Kharif season was 91.54% and 8.46%, respectively during 1995-96.

The villagers were having various conventional as well as improved agricultural machinery. The hand tools such as sickles, spade, axe, khurpi were well distributed amongst all categories of respondents. Sickles were maximum (374) in numbers amongst all hand tools possessed by villagers followed by 326 khurpies, 171 spades, 154 axe, 9 hand operated chaff cutter and 8 pacha. There were 35 bullock carts in village of which 14 was owned by small farmers. The tractor operated machineries was mostly owned by large farmers followed by medium households. Viewing the power source machineries, village has been found to have 14 tractor, two diesel engine and 53 electric motors.

3.2.1 Production Agriculture

The various energy input in crop production includes animate (human and animal), diesel, electricity, seed, fertilizer and machine. Animate energy along with diesel and electricity is direct energy and other can be placed in indirect energy for crop production.

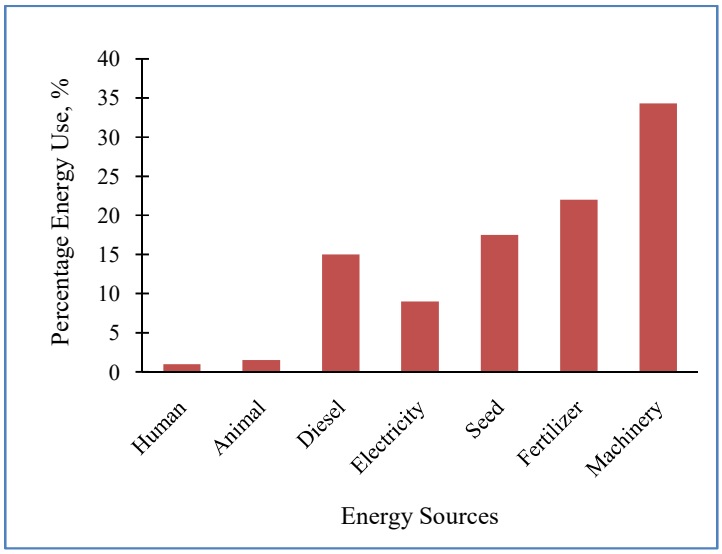

Fig. 3.3 Percentage Share of Energy Sources in CropProduction (BarkhedaNathu)

Table 3.3 indicates comprehensive statement of energy expenditure on various farms and from various energy sources. Total energy input of 1916.5 GJ was calculated for village BarkhedaNathu in 1995-96 on total cropped are of 144.79 ha. The percentage share of different energy sources has been shown in Fig. 3.3.The ratio of indirect to direct energy was computed as 1.5, 1.8, 1.8, 4.7 for marginal, small, medium and large category, respectively.

Table 3.3: Energy input for crop production in BarkhedaNathu (1995-96)

S. No.	Energy Sources	Energy use in production agriculture, MJ/ha				Total
		Category				
		Marginal	Small	Medium	Large	
I. Direct Energy						
a.	Human	143	149	126	79	116
b.	Animal	1158	229	170	17	210
c.	Diesel	2341	1304	1752	2430	1932
d.	Electricity	923	1452	1370	913	1184
A. Sub Total (a+b+c+d)		**4565**	**3134**	**3418**	**3439**	**3442**
II. Indirect Energy						
x.	Seed	2173	1811	2332	2590	2290
y.	Fertilizer	3414	2620	2807	3113	2921
z.	Machinery	1200	1102	1115	10331	4584
B. Sub Total (x+y+z)		**6787**	**5593**	**6254**	**16034**	**9795**
Grand Total (A+B)		**11351**	**8727**	**9672**	**19473**	**13237**

3.2.2 Animal Raising

Only 18.1% (i.e. 160 Nos.) of the total population, with an MFC ratio of 5.8:6.5:1, were engaged in animal-raising activities. Among them, the highest proportion (27.5%) belonged to the small farmer category, while the marginal group contributed the largest share (29.41%) of its population to this sector. The animal-raising activities in village BarkhedaNathu required 187.6 human hours per year per livestock. The annual human hours spent per livestock were 241.1, 149.1, 156.5, 208.0, and 194.0 hours for landless, marginal, small, medium, and large farmers, respectively. The human energy expenditure per livestock was estimated at 33.6 MJ, with the total human energy input to the animal-raising sector amounting to 12.7 GJ. Fig.3.4 illustrates the percentage share of various energy sources utilized in animal-raising activities.

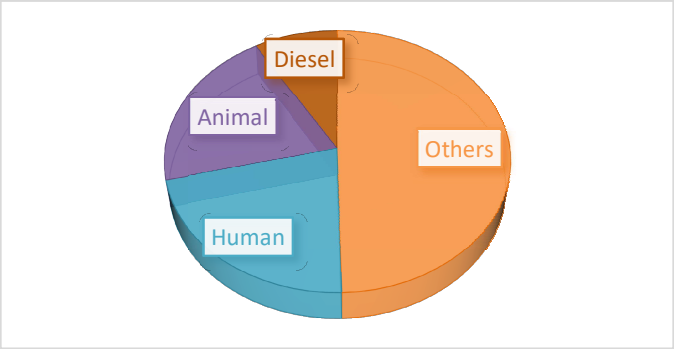

Fig. 3.4 Percentage Share of Energy Sources in Animal Raising (BarkhedaNathu)

3.2.3 Post Harvest Practices

The energy consumed to store and transportation of agricultural produce were assessed. It was assessed that 0.2 animal-h/q/km were required to transport the agricultural produce from field or threshing yard to storage point whereas tractor mode transportation needed 0.01 tractor- h/q/km. There were consumption of 0.17 man-h/q to load and unload the foodgrains. The marketing transportation by bullock cart consumed 0.15 animal-h/q/km whereas 0,45 tractor min/q/km when tractor trailer was used for transport. The bicycle for transporting the agricultural produce required 1.0 man-h/q/km with maximum carrying capacity of 40 kg. The human energy for spreading and collecting 10 q of produce a total 12 man-h was needed. The human hour requirement as 20 man-min/100 kg of produce was assessed for cleaning and filling the grain in storage structures. There were three flour mills in village out of them one was solely used by owner family for its own purpose. The energy consumption of these mills was estimated. The energy for milling 100 kg grain was estimated 17.0, 21.0 and 14 MJ for wheat, gram and paddy respectively. Total electrical consumption for milling operation was calculated to be 82.4 GJ. On an average villager has to move the crop residue from their field to storage point by 10 km. Total energy in post-harvest sector was estimated to be 247.3 GJ. Fig. 3.5 shows the source wise energy consumption in post-harvest sector of village BarkhedaNathu.

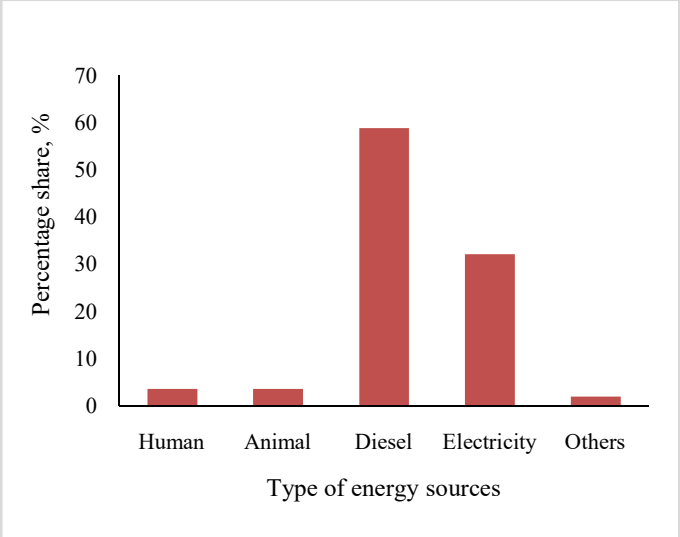

Fig. 3.5 Percentage Share of various Energy Sources for Post Harvest Operations (BarkhedaNathu)

3.2.4 Domestic Sector

The various energies consumed in domestic sector is given in Table 3.4.These energy sources were classified in three categories i.e. human energy, commercial &non-commercial energy.

Table 3.4: Annual Domestic Energy Consumption, MJ per capita

Category	Fuelwood	Dungcake	Kerosene	Electricity	Human	Total
Landless	6485	1714	516	76	55	8847
Marginal	9527	2811	698	327	47	13411
Small	5644	1766	428	135	37	8009
Medium	4840	1852	524	130	32	7378
Large	7753	3285	492	187	31	11751
Total	**6488**	**2044**	**510**	**137**	**44**	**9223**

Total human-h utilization for domestic activities of village per head was estimated to be 243.4 annually. The cooking activity was found to consume maximum human time as 251.2 h/day out of total human time expenditure as 589.4 h/day in domestic activities. The annual per capita fire wood and dung cake consumption was computed as 3.9q and 2.0q, respectively. The overall dung cake consumption in domestic activities was computed 3.0 kg/day for each family and 0.5 kg/day/person. The share of kerosene for cooking was computed as 34.9% and for lighting 65.1%. The annual per capita kerosene consumption was calculated to be 7.7litre and 4.1 litre for lighting and cooking, respectively. The per capita annual consumption of electrical power was 11.5 kWh for domestic activities.

The expenditure of non-commercial energy was computed to be 146.9 kJ/day/family and 26.6 kJ/day/capita. The annual utilisation of commercial energy in domestic sector of village BarkhedaNathu was found to be 3571.7 MJ per family and 644.6 MJ per head. The activity wise energy expenditure is given in Table 3.5.

Table 3.5: Activity wise energy expenditure in domestic sector (1995-96)

Activity	Total (GJ)	%
Cooking	7716.45	94.60
Lighting	414.39	5.10
Fuel gathering	9.99	0.10
Cleaning & Washing	5.34	0.08
Baby care	3.06	0.05
Fetching water	4.32	0.07

3.2.5 Identification of Constraints

The following infrastructural and socio-economic constraints/problems were assessed:

- Erratic & undependable rains.
- Irrigation water scarcity
- Undulated hilly and rocky area
- Collection of firewood is also a tedious job for rural women and children. This is the major problem for lower land holding categories and land less families.
- Sanitation of residential area was also very poor. At the other
- end, the primary medical services are also not satisfactory as indicated by villagers.
- There is soil erosion in the village because of sloppy land. Villagers also expressed their concern on the complicated process for attaining the loan from various finance agencies.

3.2.6 Total energy utilization for village BarkhedaNathu

Table 3.6 shows the comprehensive energy utilization in village BarkhedaNathu during 1995-96. The percentage share of energies from direct energy sources, for various rural sector shown in Fig. 3.6.

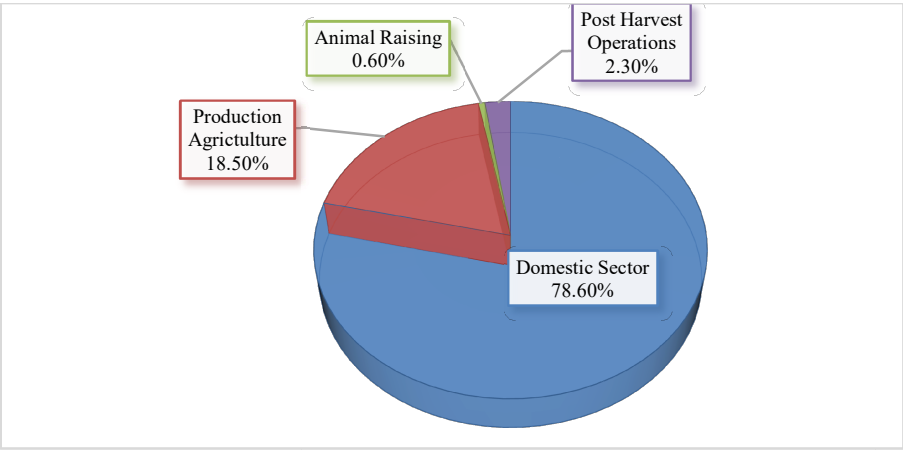

Fig. 3.6 Percentage Energy Consumption in various sectors (BarkhedaNathu)

Table 3.6: Total energy input in village BarkhedaNathu (1995-96)

Energy Soruce	Crop Production	Domestic Sector	Animal Raising	Post Harvest Activities	Total(GJ)
Human	16.8	38.6	12.7	7.2	75.3
Animal	30.4	-	11.9	7.5	49.8
Diesel	279.8	-	5.0	144.2	429.0
Electricity	171.4	120.9	-	82.4	374.7
Seed	331.5	-	-	-	331.5
Fertilizer	422.9	-	-	-	422.9
Firewood	-	5735.7	-	-	5735.7
Dungcake	-	1807.2	-	-	1807.2
Kerosene	-	450.6	-	-	450.6
Others	663.7	-	29.1	6.0	698.8
Total	**1916.5**	**8153.0**	**58.7**	**247.3**	**10375.5**

The village invested around 10.4 TJ energy in its four major rural activities. The share of energy for domestic sector was 78.6%. The rest of the energy was 18.5%, 0.6% and 2.3% for production agriculture, animal raising and post-harvest operations, respectively. The energy inflow in domestic and crop production sector was of 25.3 MJ and 5.9 MJ per capita per day, respectively. Per capita consumption of fuel wood, dung cake and kerosene was assessed as 1.1 kg/day, 0.5 kg/day and 0.03 L/day, respectively. The cooking is the maximum energy consuming activity out of all rural activities requiring nearly 74.3% of total energyused in village.

Analysis for sufficiency and deficiency indicated the village was in surplus of cereals (22.9%) and milk (by 32.8%) in reference to recommended diet level. The pulses, oils, vegetables and sugarcane were in deficit in 1995-96 by 28.2%, 100.0%, 21.6% and 16.0%, respectively. The import of cereals and milk must be discouraged and the system be adopted to enhance the export of both of these commodities. Level of present import of pulses and sugarcane must be lower down and the export is not advisable. The import of vegetables and fat/oils must more be enhanced to attain the self-sufficiency in village at recommended diet level.

The village was deficit in fodder by 43.7% and surplus in case of firewood by 36.3% as compared to assessed consumption. Fodder deficiency in village must be given due consideration. The use of better and nutritive varieties of grasses in village may be beneficial. Also, the reduced recycling of crop residue may provide the reduction in fodder deficit. Fire wood availability is higher in village than its required consumption. Thus, the energy from surplus fire wood may be used to provide other commercial energies to unload the energy import in village. The improved technologies to use the surplus firewood may be introduced.

The crop residue and animal waste recycled in soil by 42.1% and 59.0%, respectively, against estimated productions of 513 tonnes for crop residue and 1292 tonnes for dung. Improved renewable technologies must be introduced in village to reduce the energy use by burning of cow dung cakes. The efficiency of dung use may be increased by using biogas plants and the higher nutrient input to village soil will be available in form of slurry. The whole recommended process will certainly lead to higher animal waste recycling to soil along with the better and efficiency trapping of energy content of animal waste. The human time requirement for firewood collection activity was found higher for landless and marginal respondents. As the

operation is not efficient in its own, the use of solar cookers may be recommended to avoid the pressure on forests and to reduce the fire wood collection time.

CHAPTER - 4

4.Development of Animal Energy Gadgets and Technologies

Indian farming system basically consists of small and scattered holdings. Inspite of rapid growth of agricultural mechanization in recent years, the draught animals, available as progenies of the milch animals, continue to be the major power source for field operations on small and marginal farms. In the slopy hill regions and on marginal, small and semi medium farms up to 4 ha, the draught animals will remain the main power source for a long time, besides human power.

4.1Bench-mark Survey on Utilization of Animal Power

Bench-mark surveys on utilization of animal power in three selected villages of Nabibagh, Palasi and Islamnagar near Bhopal, done during 1985-87 have shown that the utilization of draught animals in all these villages was low as shown in Table 4.1.The survey was conducted using standard proforma.

Table 4.1: Average use of a pair of bullocks of selected farmers in three villages (1985-1987)

Name of Village	No. of farmers	No. of bullocks	Area (ha)	% area shown		Crop Intensity (%)	Average use of a pair of bullock in a year (hrs.)	% Utilization operation wise		
				Kharif (%)	Rabi (%)			Tillage (%)	Sowing (%)	Transport (%)
Nabibagh	6	6	27.18	45.25	84.80	130.05	285	74.45	17.40	8.15
Palassi	15	17	76.39	12.97	79.97	92.02	238	70.26	15.82	13.92
Islamnagar	19	21	48.70	50.49	92.92	143.41	319	71.12	9.78	19.10
							281	71.94	14.33	13.73

This survey has revealed the following points:

- The use of draught animals in the villages surveyed was low. They were used mainly for tillage, sowing and transport operations.
- The animals were not used much for transport purposes, as these villages were connected by roads.
- When idle time was more than time taken for actual work, animal transport was economical.
- The use of animals was high during seedbed preparation, sowing, harvesting and threshing time when they were used from 8-10 hours daily with 1-2 h rest in between morning and afternoon sessions. No definite work rest cycle was followed by the farmers. The use of draught animals for about 8 months was very little.
- Unless the use of draught animals was increased from their present level, they would prove to be uneconomical as compared to other sources of power.
- There was need to develop implements for operations for which they were not being used in order to increase the utilization of draught animal power.

- Only bullocks were used as draught animals in the region, Majority of the farmers owned non-descript breeds of animals while few farmers had Malvi breed of bullocks.
- The health status of animals in most cases was from poor to satisfactory as they were fed with mainly dry straw and allowed to graze during lean periods.
- Traditional wooden yoke was used with the bullocks.

The survey was again repeated in those villages during 1992-93 (Table4.2).This survey revealed that the population of draught animals in those villages have gone down slightly as a few farmers have purchased tractors. However, the annual utilization of draught animals has increased slightly due to less number of animals available in the villages.

Table 4.2: Average use of a pair of bullocks by the farmers in three villages (1992-93)

Name of Village	No. of farmers	No. of bullocks	Area (ha)	% area shown		Crop Intensity (%)	Average use of a pair of bullock in a year (hrs.)	% Utilization operation wise		
				Kharif (%)	Rabi (%)			Tillage (%)	Sowing (%)	Transport (%)
Nabibagh	0	0	0	0	0	0	0	0	0	0
Palassi	9	9	38.6	16	30	118	265	65	26	12
Islamnagar	14	15	48.7	26	46	150	310	62	20	10
							286	64	23	11

4.1.1 Assessment of draft developed by animals

When the animals are used for a farm operation or for haulage, the work is done through over come through training force offered by the implement or the bullock cart. The restraining force is overcome through 'pull'. The mechanical power developed is the product of horizontal component of pull i.e. draft and forward speed. The Draftability of animals is their ability to exert different magnitudes of pull (or draft) for various durations and various speed. Draftability assessment of animals, therefore, becomes the measurement of draft speed, time and physiological changes taking place in animals to determine the extent to which they can be loaded with various combination of pull, speed and duration without over fatigue. Loading device is used to make the test animals experience desired level of pull. The pull is measured by using the dynamometer. The first dynamometer was design to measure the pulling capacity of two horses by Collins and Caine (1926) (Fig. 4.1).Traditionally spring type dynamometer are used to determine the pull. Such dynamometer is suitable for rough estimation of pull because the rapid fluctuation of needle on the dial.

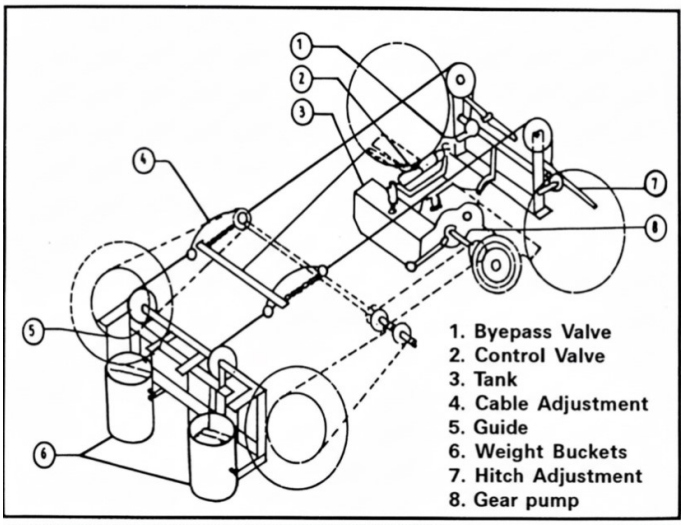

Fig. 4.1 Diagram of Iowa horse testing dynamometer

Later hydraulic type dynamometer was developed in which oil was used to transmit the pull. The pressure valve gave the dial readings calibrated in load (kg). Fluctuations in gauge needle are comparatively less than spring dynamometer due to dumping effect of oil. Presently strain gauge mounted load with indicator are used to determine the accurate pull value (Fig. 4.2).Strain gauges are connected to a wheat stone bridge circuit or a potentiometric circuit. The strain gauges are more popular because the gauges could be adopted to measure the small to very high forces. Also, static as well as dynamic forces could be measured very conveniently.

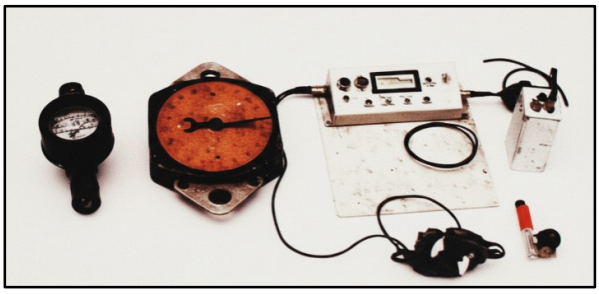

Fig. 4.2Spring type, hydraulic and strain gauge type dynamometers

The performance of draught judged by their draught force, endurance, and power output which are functions of body weight and muscle/bone arrangement. The power output of the draught animals is varied as per the draught force, speed and environment. Although numerous changes have taken place in crop production system in India but much research studies have not been done related to proper and increased utilization of draught animal power in farm and transport-operations Again due to launching the programme for cross breeding of cows to increased milk production, cross bred bullocks are coming up, These cross bred bullocks are healthy, strong muscled , broad deep shoulder, vigorous and powerful It is expected that these bullocks have better pulling capacity in comparison to local breeds. In view of above It is necessary to understand the loading devices and instrumentation system to measure the draftability and fatigue of animals scientifically.

The pull, values of the animals measured by using the dynamometer were rapidly changed due to the friction between the implement and surface. Therefore, it was very difficult to maintain a desire load on the animal in sustained working. Earlier the output of the animal was determined as horse power developed. This was based on draft (horizontal component of pull) and speed of operation without considering the fatigue parameters of working animal. For assessment of accurate power and work output of an animal it is necessary to load it at desired load. For this purpose, the loading devices were developed (Fig. 4.3).Also, the study of behavior of animal fatigue is necessary because over fatigue would reduce the work performance and life span of the animal too. Therefore, there was a need to improve the traditional technology used for determination of power output of the working animals. Presently we are not able to make optimum use of available draft power of animals due to lack of proper understanding and measurement technique for quantifying fatigue. In absence of this the animals can neither properly be loaded nor proper scheduling of their work and rest be worked out.

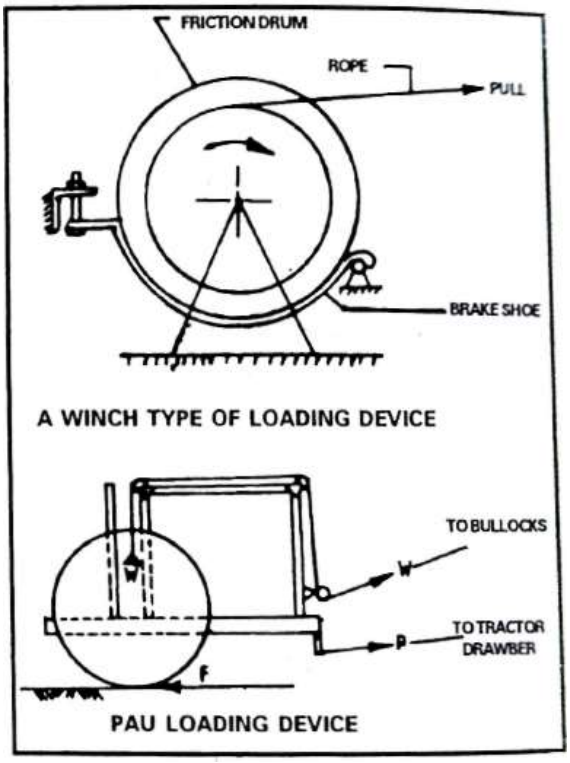

Fig. 4.3Loading devices

Based on the principle of horse power measurement suggested by James Watt, Kibler and Brody (1945) developed an ergometer taller without hydraulic system for motion control. The load mounted was connected with a rope to a horse through 3 pulleys. These weight when raised acted as constant resistance force against the test animal's pull regardless of the surface over which toiler passed. The simplest of loading devices are sledge and winch types, Devadattam (1977) and Panday et.al (1985) developed loading devices based on recirculating oil through a gear pump the use of single stage pressure relief valve affected the load control. Devnani (1981) reported a design of Iowa horse testing car which also used gear pump and relief valve. The drawback of this design was its heavy weight which was

more than 4500 kg. Gupta et.al. (1986) developed a suspended weight type loading car but the limitation of the device was that the animal had to travel between the tractor and the loading device.

4.1.2Constraints of the technology and research gap

The earlier developed animal loading cars/devicesby various organizations had limitations of sturdiness, maneuverability under field and road conditions, ease of load settings, preciseness and reliability of load setting and low capacity. The controls and operations were not very convenient. They had another limitation that they could be used up to draft load of about 200-300 kgf. So, a reliable animal loading car which could be used on the tar road with more precise and reliable load settings and having loading capacity between 30-500 kgf so that even more than one pair of animals could also be used at a time was felt necessary. Treadmills used for draftability and fatigue studies of horses under laboratory conditions is not suitable for cattle as there is a gap between the two rollers which caused strain in hooves of bullock and buffalo. Also, Indian design based on endless chain and wooden rafters caused high noise and it was difficult to change the angle of inclination in these designs.

4.2CIAE animal loading car

Considering the limitations of earlier designs an improved loading car of 300-5000 N draft capacity was designed and developed (Fig. 4.4& Fig. 4.5).The braking effect on the loading car is achieved through control of outlet pressure of two gear pumps run by traction wheel of car. The constructional details (Table 4.3) and testing of loading car as described in the following equation.

Fig.4.4 CIAE animal loading car with cab

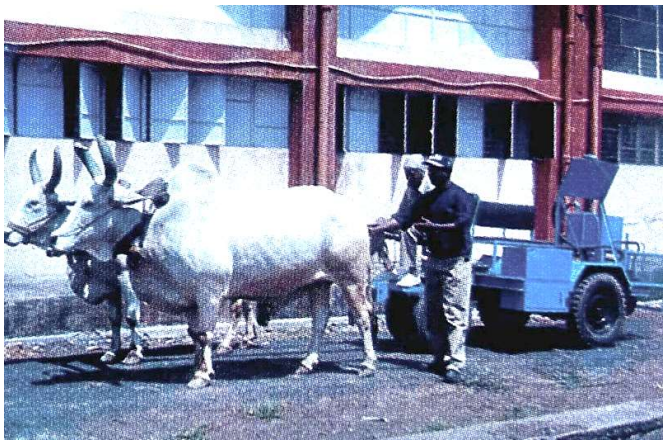

Fig. 4.5 CIAE animal loading car data recording

$$\frac{q^2 e}{2g} = \frac{[k(x_0 + x) - P_2 A_1]\pi^2 d^2 x^2 A_1]}{2A_1 - \pi^2 d^2 x^2} \quad \ldots(4.1)$$

Where,

q = discharge (cc)
e = density of liquid
k = spring constant
x_0 = displacement of spring corresponding to zero value opening (cm)
x = displacement of spring corresponding to discharge q (cm)
A_1 = Inlet sectional area (cm^2)
P_1 = Pump outlet pressure (kg/cm^2)
d = valve diameter (cm)

From equation 20, we see that P1 i.e. pump outlet pressure is linearly related with valve displacement, x which is related to pump discharge q. Considering the pump discharge q is linearly proportional to the forward speed of loading device, we find that the pump outlet pressure and in turn the braking torque is dependent on the forward speed also.

Table 4.3: Constructional details of the loading car

Particulars	Description
Structure	Three-wheeled carrier with rectangular frame (125×65 mm, 100×50 mm channels); MS sheet flooring; front pivot (80 mm tube, bronze bushes, 6×16 tyres); rear on Mahindra Jeep assembly with leaf springs; two seats and tool box provided.
Transmission	Two hydraulic pumps driven by ground wheels (speed 0.28–1.39 m/s, 7–35 rpm). Pump speed 180–900 rpm via jeep differential and chain drives. Clutch at two stages for disengagement. Drive ratios: Rear tyre: 6.00×16; Jeep differential: 1:4.27; 1st chain: 1:1.9; 2nd chain: 1:25.7.
Hydraulic System	Two pumps with two-stage relief valves (5–140 kg/cm^2); load controlled by regulating outlet pressure to vary tractive effort.
Testing of loading car	Conducted on tar road, farm road, unploughed and ploughed fields. Parameters: pull, angle of pull, speed, and skid.
Pull Measurement	Pull was measured using Novatech load cell (0–2500 N, 0–5000 N) and mounted on hitch beam.

Angle of Pull	Measured using Abney level on hitch beam.
Speed	Calculated from distance travelled per unit time.
Skid	Computed from theoretical (Nt) and actual (Na) wheel revolutions over 50 m using, Skid (%) = (Nt–Na)×100/Nt.
Performance	No-load draft: 295 N; skid <15% on road, up to 20% in field (3900–4900 N draft). Speed variation had no effect.
Cost	₹2,00,000/-

4.3CIAE Animal Treadmill

One of the limitations of the loading cars is that according to load and tiredness, the animal adjusts his speed and therefore onset of full fatigue condition get delayed and assessment of draftability of animal at particular load and speed under sustained working condition becomes difficult. animal treadmill is good device for laboratory studies of draftability and fatigue of animals under varying loads, speeds, slopes and environmental conditions. The CIAE animal treadmill basically consists of, a frame, an endless conveyor belt supported on rollers and arrangements for tightening the belt,railings, transport cum inclination changing wheels, mounting platforms,harnessing and loading device and Drive system.Constructional details of CIAE animal treadmill and testing are shown in the Table4.4 and specifications are given in Table4.5.

Table: 4.4: Constructional details of the animal treadmill

Part	Description
Frame	M.S. channel (125×62 mm) frame; ends bent 130 mm for 300 mm rollers; angle iron frame (1500×1000 mm) with 1 mm MS sheet; 3 rollers (35 mm ID) to reduce friction; sliding bearing for belt tightening.
Conveyor Belt	3-ply endless rubber belt (7.5 m × 1 m) supported on MS sheet; 3 rollers (350 mm dia) for flat movement.
Railings	Fixed side railings and hinged front/rear railings; height 1200 mm.
Transport Wheels	Four telescopic wheels; height adjustable up to 500 mm; slope adjustable 0–10°.
Platforms	Slanting removable platforms on both sides for animal movement.
Harness & Loading	Single padded harness with hanging weight device (Fig. 4.6); loading via known weights and pulley.
Drive System	5 kW variable speed (3-phase) motor with reduction unit; speed 0–3 km/h.

Fig. 4.6 Loading of Animal on CIAE Animal Treadmill

Table4.5: Specifications of CIAE animal treadmill

Particulars	Specification
Length	7.5 m
Width	1 m
Conveyor Belt	Heavy-duty endless rubber conveyor belt
Height	Adjustable
Slope	Adjustable from 0° to 10°
Drive	5 kW heavy-duty variable speed, 3-phase electric motor
Loading	By applying dead loads to the animal
Speed	Variable, 0–3 km/h
Cost	Approximately ₹2,00,000/-

During draftability studies on treadmill, 4 bullocks were allowed to walk at 1.25, 1.75 and 2.10 km/h speed on load and no-load condition, observation on physiological parameters and visual distress symptoms were taken at hourly intervals to assess the fatigue score of the bullocks (Fig. 4.7). Sample observation taken at no load and draft load equivalent to 6.0 % of body weight of bullock at 1.25 and 2.10 km/h speed are given in Table 4.6.In the trials the treadmill has been found working very satisfactorily and speed and loading was very reliable. The bullock walked on treadmill very comfortably and recording of physiological parameters on chart recorder was easy and accurate.

Fig.4.7 CIAE Animal Tread Mill Data Recording

Table 4.6: Variation in physiological responses of Malvi breed of bullock (body weight, 514.00 kg) working on treadmill

Time, hours	Average Resp. rate (Breaths/min) at speed		Average Heart rate Beats/min) at speed		Average Rect. temp (°C) at speed		Fatigue score at speed	
	1.25 km/h	2.10 km/h	1.25 km/h	2.10 km/h	1.25 km/h	2.10 km/h	1.25 km/h	2.10 km/h
09.00	16	20	48	50	37.5	37.7	00	00
10.00	18	24	53	56	37.7	3/.9	01	01
1100	21	28	57	61	37.8	38.1	02	03

12.00	23	31	61	66	38.0	38.3	03	05
13.00	26	35	64	70	38.2	38.4	04	08
			Rest					
14.00	20	22	55	58	38.0	38.2	00	00
15.00	22	27	60	63	38.1	38.3	01	02
16.00	24	32	62	70	38.2	38.4	02	05
17.00	28	36	66	75	38.3	39.5	04	08
B. On load (Draft load equivalent to 6% of body weight of bullock)								
09.00	16	20	48	50	37.5	37.7	00	00
10.00	22	29	52	60	37.8	38.0	02	03
11.00	26	37	63	76	38.0	38.3	05	07
12.00	30	44	70	76	38.2	38.5	08	10
13.00	35	50	74	82	38.5	38.7	10	14
			Rest					
14.00	20	26	55	62	38.2	38.4	01	02
15.00	26	36	62	72	38.4	38.6	04	06
16.00	30	44	70	80	38.6	38.9	08	11
17.00	36	52	74	86	38.8	39.2	10	15

Note: The animal is fatigued at 15 points of fatigue score

4.4. Utilisation of Animal Energy

4.4.1 Assessment of Draft Capacity of Animals in Sustained Working

Draftability studies on bullocks were conducted under sustained working conditions on whole day basis of 6-8 hours, in two shifts with a break of about 1 hour in between the two shifts. The study was conducted at draft loads equivalent to 8-20% of body weight. Studies wereconducted for 7 hours/day in two shifts. The results are summarized in Table 4.7.

Table 4.7: Draft Capacity of Animals in Sustained Working

Yoke/ harness	Breed	Summer			Winter		
		Load range studied	Max. Load Negotiated	Load at Max. Output	Load at Max. Output	Max. Load Negotiated	Load at Max. Output
With improved yoke	Malvi	8-14	13	12	8-18	17	15
	Local	8-15	13	12	8-18	17	15
With local yoke	Malvi	8-12	12	10	8-16	14	12
	Local	8-12	12	10	8-16	14	12

Studies on draftability on bullocks under sustained working have shown that:

- The performance of different breeds of animals differed from eachother. Themaximum draft load negotiated under sustained working was varied between 8-20% for different breedsofbullocks.
- The maximum output of Malvi and local breeds of bullocks were at draft loads equivalent to 12 and 10% of the body weight during winter and summer seasons, respectively with local yoke. The Malviand local breeds of bullocks worked upto draft load equivalent to 17% & 13% of body

weight during winter and summer respectively. The maximum work output increase of Malvi and local bullocks were at draft loads of 15 and 12% during winter and summer seasons, respectively.

- Depending upon the weight and breed of the bullocks, the power developed ranged from about 600 watts (local breed) to 1 kW (MaIvi breed).

4.4.2 DraftabilityRelationship of Animals on Test Track and Under Field Conditions

Studies on 2 pairs of bullocks, one Malvi and another local non-descript breed were conducted on test track and under field conditions for ploughing, harrowing and puddling operations to find out correlation between draftabilityon the test track and under field conditions.The performance of bullocks on the test track and under field conditions were given in Table 4.8.

Table 4.8: Performance of bullocks on test track and under field conditions

Condition	Draftability (% of body weight)	
	Malvi Breed	Local Breed
Tar road test track	12	11
Field conditions		
i. Ploughing	10.6	10.0
ii. Harrowing (Sweep Cultivator)	10.1	10.1
iii. Puddling	5.1	6.3

The correlation of draftabilityon the test track and that of field conditions for ploughing, harrowing and puddling operations in case of Malvi breed bullocks was 1:0.88:0.84:0.42 and in case of local breed of bullocks it was 1:0.9:0.91:0.57 respectively.

4.4.3 Development of Instrumentation for Measuring Physiological Parameters and Power of Draught Animals

An animal performance logger was developed in collaboration with NIAE, UK to measure the physiological responses of draft animals during field work. It recorded heart rate, respiration rate, body temperature, stepping rate, walking speed, pull, and angle of pull using suitable sensors. All sensors were connected to a junction box on the yoke, linked to a battery-operated signal conditioning unit and data logger, which transferred data to a microcomputer.

Weather parameters such as ambient temperature, wind speed, solar intensity, and humidity were also recorded using portable units. The range of different sensors and their places of mounting are given below in Table 4.9.Extensive trails of these instrumentations were done jointly by CIAE, Bhopal and NIAE UK on 11 pair of animals belonging toCIAE farm and to farmers. The instrumentation was found working very satisfactory.

Table 4.9: Animal implement performance variables monitored by the animal performance logger.

Sensors Fitted on	Variables	Range
Animal	Heart rate	40-160 beats/min.
	Breathing rate	0-140 breats/min.
	Temperature	25-45°
	Stepping	0-100 steps/min
Implement	Draught load	0-5 kN
	Draught angle	0-45°C
	Forward speed	0-2 m/s

4.4.4 Studies on Physiological Responses of Bullocks in Rest andunder Shed and Other Environmental Conditions

This study was conducted on 4 pairs of bullocks. The study showed that due to heat load itself the fatigue score was increased by 4 points even when the animal was either in rest or walking condition. The study revealed that to avoid heat load the animals should be worked under cooler period of the day.

4.4.5 Assessment of Draft Capacity of Animals in Sustained Working

Draftabilitystudies on bullocks were conducted under sustained working conditions on whole day basis of 6-8 hours, in two shifts with a break of about 1 hour in between the two shifts. The study was conducted at draft loads equivalent to 8-20% of body weight. Studies were conducted for 7 hours/day in two shifts. The results are summarized inTable 4.10.

Table 4.10: Draft Capacity of Animals in Sustained Working

Yoke / harness	Breed	Summer			Winter		
		Load range studied	Max. Load Negotiated	Load at Max. Output	Load range studied	Max. Load Negotiated	Load at Max. Output
With improved yoke	a. Malvi	8-14	13	12	8-18	17	15
	b. Local	8-15	13	12	8-18	17	15
With local yoke	a. Malvi	8-12	12	10	8-16	14	12
	b. Local	8-12	12	10	8-16	14	12

Studies on draftability on bullocks under sustained working have shown that:

- The performance of different breeds of animals differed from each other. The maximum draft load negotiated under sustained working was varied between 8-20% for different breeds of bullocks.
- The maximum output of Malvi and local breeds of bullocks were at draft loads equivalent to 12 and 10% of the body weight during winter and summer seasons, respectively with local yoke. The Malvi and local breeds of bullocks worked upto draft load equivalent to 17% & 13% of body weight during winter and summer respectively. The maximum work output increase of Malvi and local bullocks were at draft loads of 15 and 12% during winter and summer seasons respectively.

- Depending upon the weight and breed of the bullocks, the power developed ranged from about 600 watts (local breed) to 1 kW (Malvi breed).

4.4.6 DraftabilityRelationship of Animals on Test Track and Under Field Conditions

Studies on 2 pairs of bullocks, one Malvi and another local non-descript breed were conducted on test track and under field conditions for ploughing, harrowing and puddling operations to find out correlation between draftabilityon the test track and under field conditions.The performance of bullocks on the test track and under field Conditions were given in Table 4.11.

Table 4.11: Performance of bullocks on test track and under field conditions

S. No	Condition	Draftabilityexpressed as % of body weight	
		Malvi Breed	Local Breed
1	Tar road test track	12	11
2	Field conditions		
	Ploughing	10.6	10.0
	Harrowing (Sweep Cultivator)	10.1	10.1
	Puddling	5.1	6.3

The correlation of draftabilityon the test track and that of field conditions for ploughing, harrowing and puddling operations in case of Malvi breed bullocks was 1:0.88:0.84:0.42 and in case of local breed of bullocks it was 1:0.9:0.91:0.57 respectively.

4.4.7 Draftability of Animals in Team Work

Studies were conducted on the performance of animals in team work. Two and three pairs of bullocks were used in team and contribution of each pair in the total draft was assessed (Fig. 4.8).

Fig. 4.8 Study on Draftability of Animals in Team Work

Team of 2 pairs of bullocks were subjected to draft load equivalent to 4.8 to 12.3% of their combined body weight while the team of 3 pairs of bullocks were subjected to draft load equivalent to 5.6% to 8.7% of combined body weight of 3 pairs of animals. The findings of this study were as under:

a) *When 2 pairs of bullocks were used in a team*
When the two pairs used one after the other, the front pair always contributed more draft ranging from 0.6 to 3.5% of body weight. Minimum deviation in contribution of draft load was found as 0.76 where the rear bullock pair was goaded, as compared to goading of front pairs of bullocks.

b) *When 3 pairs of bullocks were used in a team*

When three pairs were used one after the other the results were as under in Table4.12. The loading was done in the range of 5.6% to 8.7% of combined body weight.

Table4.12: Contribution of Different Bullock Pairs When Various Pairs Were Goaded

Goaded Pair(s)	Rear Pair Contribution (%)	Middle Pair Contribution (%)	Front Pair Contribution (%)
When rear pair was goaded	5.2–8.3	5.97–8.8	5.5–8.7
When middle pair was goaded	4.0–6.8	6.6–10.9	5.86–8.48
When front pair was goaded	2.2–6.7	5.3–8.8	8.3–11.0
When front and middle pairs were goaded together	2.1–4.7	6.3–10.4	7.6–10.5
When front and rear pairs were goaded together	3.9–7.0	5.0–8.7	7.3–10.1
When middle and rear pairs were goaded together	3.7–8.1	6.4–9.5	6.3–8.7
When all the three pairs were goaded	2.2–5.3	5.5–9.9	8.2–10.4

All the goadings were analyzed. Minimum deviation of 0.80 was found in rear pair goading and it was significant at 5% level. Rear pair goading was found best.

4.4.8 Testing and Evaluation of Improved Yokes and Harnesses

Evaluation of five different types of yokes and harnesses were done on bullocks. The yokes selected for the study were;

- Allahabad single animal harness (3 padded collar type),
- CIAE single animal harness (3 padded collar type),
- Allahabad double animal harness (3 padded collar type),
- Nagpur wooden yoke, and
- Local wooden yoke (most popular design of the area).

The details of yokes are shown in Fig. 4.9&Fig. 4.10.

Fig. 4.9 View of Yokes for Single Animal Harness

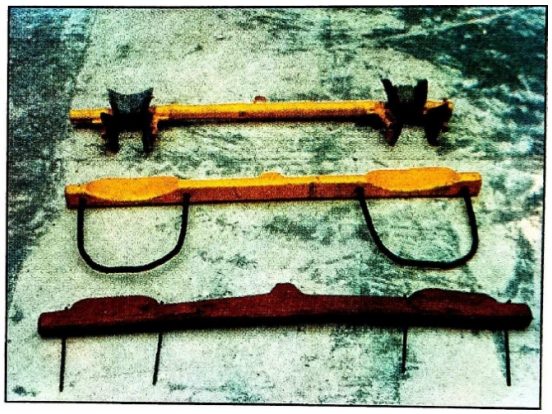

Fig. 4.10 View of Yokes for Double Animal Harness

The draught animals were subjected to draft loads equivalent to 8-20% of animal's body weight in the steps of 1% of body weight. The tests were conducted for continuous operation of 4 hours. This study indicated that:

- The improved single and double animal Allahabad type three padded collar harnesses could give 14.4% to 25.4% higher draft output over local wooden yoke. Similarly,Nagpuri wooden yoke gave 8.9% to 15% higher outputs as compared to local yoke in sustained working.
- Local breed gave slightly higher draft output as percentage of body weight over Malvi breed for all the yokes and harnesses evaluated. However, due to higher body weight the Malvi breed gave higher power output per pair.
- Performance of CIAE and Allahabad single animal harnesses were comparable.
- The performance of Allahabad double animal harness and Nagpuri Yoke were better than local yoke. Allahabad type three padded double animal collar harness was found better than “Nagpuri wooden yoke".

4.4.9 ORP Trials on Use of Improved Harnesses and Yokes

Fifteen units of Allahabad type double animal harnesses and Nagpuri yokes were given to farmers to get user's opinion. 7-15% more output with Nagpuri yoke and 15-25% more output with Allahabad double animal harness in tillage operations were observed by farmers. The farmers liked the Nagpuri wooden yokes more than the Allahabad double animal harness, as it was similar to their local yokes. The advantage of improved yokes and harnesses was more pronounced when the draft load was above 12% of body weight and was in discomfort zone.

4.4.10 Identification of Matching Implements Package for the Draft Animals of Bhopal Region for Crop Production

Implement package for most common rotation of Bhopal region for tillage, sowing and interculture operations were identified. Trials of existing equipment have shown that there was good scope of increasing the sizes of implements by 30-70% to match the draught power available from the animals.

The implements identified for matching with the draught power available in the regions were; MB plough (15-20 cm size), Disc harrow (6-8 disc), Blade harrow

(bakhar) (45-50 cm size), 3 and 5 tine cultivator/sweep, 3-4 row seed cum fertilizer drill/planter, Puddler (45-50 cm size) and Groundnut digger (45-50 cm size).

4.4.11 Energetics of Traditional and Improved Animal Drawn Implements System for Crop Production in Bhopal Region

Five combinations of local and improved animal drawn Implements for tillage, sowing and interculture were compared for their energetics an economics. The system using combination of imp was advantageous in roved blade harrow, CIAE seed cum fertilizer drill and sweep cultivator terms of yield and net income over all other treatments. Energy input per unit area and per unit yield was lowest with the combination of the disc harrow, CIAE seed cum fertilizer drill and sweep cultivator because of higher coverage and yields. Seed bed preparation, seeding and fertilization, and weeding and inter-cultivation accounted for 50-60% of the total cost of production and hence use of high-capacity implements could reduce the cost of production to a great extent.

4.4.12 Feasibility Studies on Utilization of Animal Power in Rotary Mode of Operation for Water Lifting and Agro Processing Operations

One of the important ways of increasing the utilization of draught animals was to use them for water lifting and agro processing work during idle periods. The agro processing complex where a number of machines could be installed and operated by animal was developed at the Institute (Fig. 4.11). The equipment operated and their outputs obtained were as follows (Table 4.13)

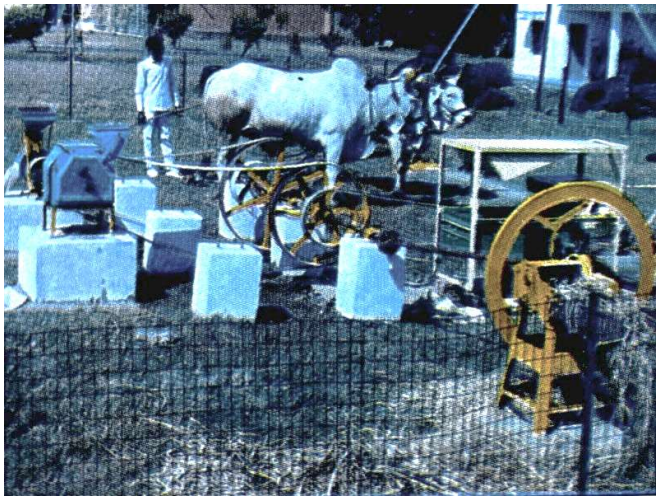

Fig. 4.11Utilizations of Animal Power in Rotary Mode

Table4.13: Outputs of different equipments

Equipment		Output/hour
Grain cleaner	:	120-450 kg
Groundnut decorticator	:	100-150 kg
Soya-flaking machine	:	23-25 kg
Flour mill	:	8-25 kg
Chaff cutter	:	860 kg (green fodder)
Water pump	:	18000 L at 1 m head

The studies have shown that the draft requirement of this equipments were much lower than the draft available from a pair of bullocks.

The economics of operation of some of the machines mentioned above was quite favorable. However, in some cases it would be economical only when cost of hiring the bullocks was not considered. Animal operated agro processing complex would be useful and successful in remote areas where electricity/mechanical power is not easily available.

4.4.13 Study on Feeding Management and Health Care of Few Pairs of Bullocks

The study on feeding management and health care of a few pairs of bullocks was conducted during 1996-97. The study has shown that the bullocks were normally fed dry busha during the year with little bit of concentrates. Daily consumption of feed and concentrates were as under (Table4.14):

Table4.14: Daily consumption of feed and concentrates

Parameters	Slack Period	Peak Working Period
Dry Bhusha	20-25 kg/pair	15-20 kg/pair
Green Fodder	-	10-15 kg/pair
Concentrate	-	1-2 kg/pair
Salt	100-150 gm/pair	100-150 gm/pair
Jaggery	-	1 kg/pair
Cost of feed	Rs. 26.00/day/pair	Rs. 36.00/day/pair
Cost of Management	Rs. 8-10/day/pair	Rs. 8-10/day/pair

CHAPTER - 5

5. Research on Solar Energy

Solar energy has been used for domestic, agricultural, and agro-industrial purposes since ancient times. Due to the rising shortage of conventional energy and environmental concerns, the focus on renewable energy, particularly solar energy, has greatly increased. Solar power is inexhaustible, clean, and abundant, making it vital for future thermal and decentralized power applications. The sun provides about 1.8×10^{11} MW of energy to Earth, making it one of the most promising renewable sources. In India, the average daily solar radiation is around 1800 J/cm^2/day, reaching 2500 J/cm^2/day in parts of Rajasthan and Gujarat during summer, and reducing to 1200–1600 J/cm^2/day in monsoon and winter. Sun drying of agricultural produce is an old practice, and since the 20thcentury, several solar thermal devices for water heating, drying, cooking, and power generation have been developed. Major R&D efforts in India began in the 1960s, supported by government incentives from the 1970s. These led to the adoption of solar water heaters, dryers, cookers, and photovoltaic systems for water pumping, lighting, and small power needs.

To promote renewable energy use in agriculture, ICAR launched the All India Coordinated Research Project on Renewable Sources of Energy in 1983. The key developments in solar energy research and applications at CIAE are summarized below.

5.1 Solar Cookers

Two main types of solar cookers, direct and indirect focusing, have been developed in India. The box-type solar cooker, made of insulated double-walled wood with a glass window and mirror reflector, can reach up to 160°C and cook food within 2–3 hours. PAU, Ludhiana, improved this design with asymmetric double reflectors, achieving higher temperatures but increased weight and cost (Fig. 5.1). CIAE, Bhopal, further refined the cooker using aluminium parts and better insulation, reducing the weight by 40%. The CIAE twin mirror cooker reached 218°C in summer and 168°C in winter, reducing cooking and baking time by 27–45% compared to commercial cookers. The salient features & performance of the solar cookers of three different designs is presented in Table 5.1.

Fig. 5.1 CIAE Twin Mirror Solar Cooker

Table 5.1: Salient features of box type domestic solar cookers of different designs

Parameters		Twin mirror solar		Commercial solar cooker
		CIAE	PAU	
Aperture area, m^2		0.23	0.23	0.25
Approximate weight, kg		19	36	15
Peak stagnation temperature with mirror reflector, °C	Winter	168	165	134
	Summer	218	205	193
Time taken in minute for				
▪ Boiling 3 litre water		135	150	165
▪ Cooking rice 600 g & pulse 300 g		150	170	180
▪ Baking during March				
✓ 300 g biscuits		40	NA	75
✓ 400 g cake		50	NA	45
Approximate cost, Rs		2500	2000	1200

5.2Solar Dryers

Solar dryers are used to enhance drying rates and maintain product quality compared to open sun drying. CIAE, Bhopal, developed a roof-based forced convection solar dryer with a 72 m^2 collector area and 3 hp blower, which raised air temperature from 32°C to 58°C for drying up to one tonne of grain on sunny days.

5.3Solar Water Heaters

Solar water heaters are available in natural (thermosyphon) and forced convection types. A 100 L/day thermosyphon heater developed by PAU, Ludhiana, can heat water up to 75°C. Built-in storage type heaters developed at CIAE, CAZRI, TNAU, and PAU are economical, heating water up to 50–75°C with only a 5–10°C overnight temperature drop, making them suitable for domestic use.

5.4 Solar Photovoltaic Systems

Solar photovoltaic (SPV) technology converts solar radiation directly into electricity using semiconductor devices called solar cells. The first silicon solar cell was developed in 1954 in the USA, and today, many firms in India manufacture these cells. SPV systems are simple, pollution-free, and require little maintenance as they have no moving parts. However, their large-scale use is limited due to the high cost of silicon and complex fabrication processes.

SPV systems are widely used for solar lanterns, domestic and street lighting, rural electrification, water pumping, and small-scale power generation. In agriculture, SPV pumps are ideal for irrigation and drinking water supply as they operate without fuel and pollution. These pumps can handle total dynamic heads up to 12 m and are suitable for boreholes, tanks, and rivers.

To enhance power generation efficiency, CIAE, Bhopal developed an automatic electromagnetic sun-tracking device that keeps SPV panels aligned with the sun (Fig. 5.2). The device, operated by a 12 V rechargeable battery, improves energy output by up to 30% compared to fixed panels. The system costs about Rs. 5000 and has been tested successfully at multiple locations with favourable feedback for its reliable performance.

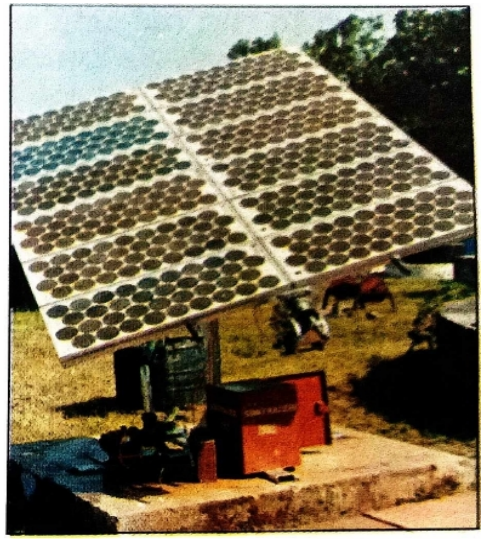

Fig. 5.2 CIAE Electromagnetic Solar Tracking Device

5.5 Step type solar cocoon stifler

The solar cocoon stifler uses solar energy to generate hot air for killing (stifling) the pupae inside the cocoons. A 2 m^2 solar collector was used to heat the water for stifling of the cocoon at Silk Reeling Centre, Hoshangabad (Fig. 5.3). A flat-plate solar collector absorbs sunlight and converts it into heat, which raises the temperature of the air within the stifler chamber. The cocoons placed on layered trays are exposed to this hot air, and as the chamber temperature rises (typically 95–120°C), the larvae inside are effectively stifled. The process depends entirely on solar intensity, with higher sunshine providing faster heating and shorter stifling time. The system functions without electricity, using natural solar heat to achieve stifling quality comparable to conventional electric ovens. The constructional features of solar cocoon stiflerare given in Table 5.2.

Table 5.2 Constructional features of solar cocoon stifler

Component / Parameter	Details
Type of System	Solar cocoon stifler using flat-plate solar collector
Solar Collector Area	2 m^2
Peak Stagnant Temperature (no-load condition),	95°C (Winter), 120°C (Summer)
Tray Design	Specially designed trays arranged in layers for placing cocoons
Loading Capacity	60 kg green cocoons per clear sunny day (6 batches ×10 kg) and 35-40 kg cocoons per day in 3 batches during autumn months
Stifling Time per Batch	45–90 minutes depending on solar intensity
Average Shell Ratio of Green Cocoons	21%
Rendita (Cocoon to Silk Ratio)	7.73

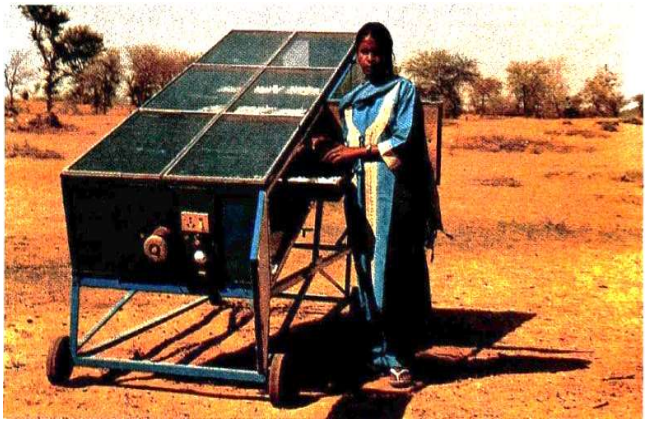

Fig. 5.3Solar cocoon stifling for fresh silk cocoons

5.6 Solar energy for baking

A double-reflector box-type solar baking unit with a 0.6 m^2 aperture area achieved peak stagnant temperatures of about 170°C in winter and 215°C in summer (Fig. 5.4). Under typical sunny conditions, it could bake 2 kg of 2-mm-thick biscuits in winter and 4 kg of 2.5-mm-thick biscuits in summer. The final moisture content of the baked biscuits remained between 3–4%, well within the acceptable limit of 6%.

Fig. 5.4 Solar baking unit for baking biscuits

5.7 Design refinement of CIAE solar tracking device for commercialization

The sun tracker developed earlier at the Institute has undergone several years of field testing, and based on this experience, a series of design improvements have been introduced to enhance reliability and user-friendliness. The earlier timer circuit has been replaced with a fully solid-state IC-based system, and the final worm gear along with its shaft has been integrated into the reduction gearbox to avoid assembly errors. The earlier issue of the SPV panel plane being offset by about 45 mm from the axis of rotation was corrected by modifying the end plates so that the centre of gravity now lies directly on the axis, eliminating the need for any counterweight. The pawl and ratchet mechanism was also simplified, using fewer parts while providing higher torque and smoother operation. In addition to these refinements, the tracker design was upgraded to accommodate a larger 900 Wp solar photovoltaic panel, with modifications in the panel frame and improvements in

the gearbox for better performance and dust protection (Fig. 5.5). The upgraded tracker has already been tested with a 450 W panel, its original design capacity and it successfully maintained accurate tracking.

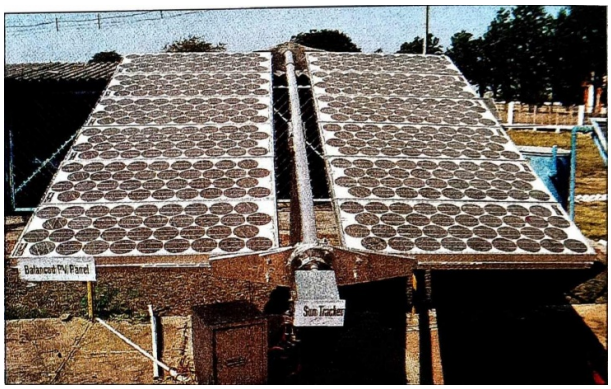

Fig. 5.5 Modified sun tracker fitted with the 450 W SPV panel system

5.8 Development of solar tunnel dryer for horticultural crops/fruits

The solar tunnel dryer consists of a semicircular polycarbonate-covered tunnel with a dedicated solar air-heating section (9 m^2) and a 16 m^2 drying area designed for batch operation (Table 5.3). Warm air generated in the collector moves through the drying chamber, where trays of produce are placed. Inside the tunnel, temperatures naturally rise well above ambient due to the greenhouse effect and controlled airflow, creating a uniform and hygienic drying environment.

Performance evaluation with unripe mango, gooseberry, and red chilli showed that the tunnel maintained drying temperatures between 45 and 71°C depending on the crop requirement (Table 5.4). This led to significantly faster moisture removal than open sun drying, where drying rates dropped sharply once product moisture fell below 15%. Tunnel drying reduced moisture to 2.8–4.2% within 3–5.5 days, compared to 6–10 days in open sun. (Fig. 5.6) The higher and stable temperatures (52–60°C average), along with solar intensities of 605–650 W/m^2, ensured faster drying and improved product hygiene. Microbial counts in tunnel-dried samples were considerably lower, and the dried products exhibited better appearance and overall quality. A larger modular solar tunnel dryer of 250 kg/batch capacity was later developed with a 48 m^2 collector area, 24 m length, 16 drying beds, six 4 W DC axial fans, and a 36 Wp SPV panel. No-load tests showed stagnant temperatures of 50–75°C. Field installation in Gada village (Raisen district) demonstrated effective drying of amla, where moisture was reduced from 84.5% to 3.1% in 8 days, compared to 20 days in open sun (Fig. 5.7). The dried amla had lower microbial loads and good retention of nutrients, reaffirming the dryer's suitability for hygienic, efficient, and quality drying of horticultural produce.

Similarly, the solar dryer was also evaluated for drying mahua flowers (Madhucaindica). With an initial moisture content of 66.2% (wb), the flowers were dried to 3.3% (wb) in 3.5 days during April, whereas open-sun drying required about 12 days. The tunnel dryer operated at an average temperature of 57.2°C, resulting in cleaner, better-appearing dried flowers with significantly lower microbial counts. Although total sugar content was slightly lower (44.39%) than

open-sun drying (47.35%), the overall quality was superior due to faster, hygienic drying and reduced contamination.

Table 5.3: Salient features of the dryer

Total collector area, m^2	:	48
Length of dryer, m	:	24
Drying beds, nos	:	16
Axial fans, 4 W, 12 V, DC	:	6 nos
SPV panel, 36Wp	:	1

Fig. 5.6 Demonstration of solar tunnel dryer in the village Gada

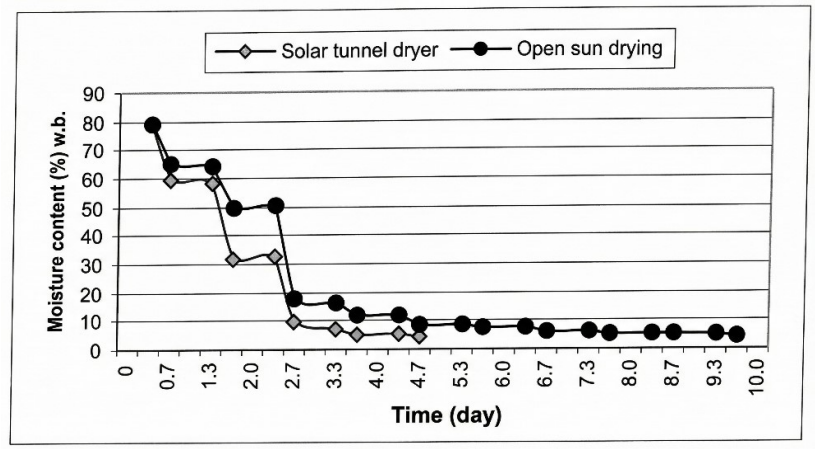

Fig. 5.7 Moisture content reduction of unripe mango in solar tunnel dryer and in open sun

Table 5.4 Performance of solar tunnel dryer for drying of horticultural crops

Parameters		**Product dried**		
		Unripe mango	**Goose berry**	**Red chilli**
Raw product (kg)	(Peeled split mango, blanched pieces of goose berry, whole chilli)	**60**	**65**	**70**
Moisture content, (%) w.b.	Raw product	78.5	85.1	74.5
	Product tunnel dried	4.2	3.2	2.8
	Product open sun dried	4.6	3.9	3.8
Drying (*Average values)	Drying time in tunnel (day)	4.5	5.5	3.0
	Drying time in open sun (day)	10	10	6.0
	*Tunnel drying temp. (°C)	59.5	52.3	56.5

	*Ambient temp. (°C)	37	29.2	36.0
	*Relative humidity (%)	36	40.3	37.0
	*Solar intensity (W/m^2)	620	605.0	650.0
Dried product quality	Tunnel dried, microbial count (cfu/g)	3×10^4	2611.0	20×10^4
	Sun dried, microbial count (cfu/g)	44×10^4	6092.0	34×10^4
	Tunnel dried, ascorbic acid content (mg/100 g)	43.4	358.6	-
	Sun dried, ascorbic acid content (mg/100 g)	49.0	370.3	-
	Tunnel dried, acidity (% as citric acid)	1.03	15.26	1.15
	Sun dried, acidity (% as citric acid)	0.89	10.24	0.70

5.9 Natural convection solar dryers

A comparative performance of two solar dryers, PAU farm dryer and CIAE aspirator dryer, (Fig. 5.8), was evaluated under no-load condition and on load condition for drying cauliflower (Table 5.5). Trays in both dryers were with wire mesh at bottom. Both dryers were loaded on same day.

Fig. 5.8 PAU farm dryer and CIAE aspirator dryer

Under no-load condition, the average stagnant temperature in the CIAE aspirator dryer was 48.1°C, 3.3°C higher than the PAU dryer, on typical sunny day in the month of January. Average ambient temperature and solar insolation during the experiment were 23.1°C and 495 W/m^2, respectively.

During on-load tests, the average drying air temperature in CIAE aspirator dryer was 45°C, 4°C higher than the PAU dryer. The CIAE dryer required one day less than the PAU dryer for drying of the product, mainly due to higher drying temperature. Open sun drying required 13 days to dry the product to 6.2% (w.b.) as compared to 10 days in the PAU Farm dryer and 9 days in the CIAE aspirator dryer. The average ambient temperature, relative humidity and solar intensity during the experiment were 21°C, 41 % and 440 W/m^2.

Table 5.5 Comparative performance of the natural convection solar dryers

Parameters	PAU Farm dryer	CIAE Aspirator dryer
Specifications		
Aperture area	3.34 m^2	2.53 m^2
No. of trays	7	4
Total Tray area	3.15 (0.45 × 7)	2.42 (0.60 × 4)
Glazing cover	Polyethylene film (UV stabilized)	Plane glass
Material of construction for bottom and side covers	Canvas cloth, thermos-coal, MS angels	GI sheet, wood, MS angle
Test at no-load		
*Stagnant temp. in the dryer (^oC)	44.8	48.1
*Ambient temp. (^oC)	23.1	23.12
*Solar insolation (W/m^2)	495	495
Drying test of cauliflower		
Quantity loaded (kg)	15	15
Initial moisture content (%), wb	90.3	90.3
Moisture content of dried product (%), wb	6.03	5.9
*Drying temp. (^oC)	41	45
Drying time (days0	10	9

*Indicate average values

5.10 Solar dryer for silk cocoons

The solar cocoon dryer, previously developed with a 50 kg/batch capacity, was installed at the Silk Reeling Centre in Hoshangabad (Fig. 5.9) and utilizes a collector area of 16 m^2. The drying chamber is equipped with multiple trays for cocoon loading, and since hot air is forced through the system, the cocoons are protected from direct sunlight and UV radiation. Performance was evaluated using about 50 kg of raw silk cocoons at a tray loading rate of approximately 4.0 kg/m, starting with an initial moisture content of 60.7% (wb). The drying process was completed in about 18 sunshine hours during March, with the air entering the drying chamber maintained at 55-65°C. This reduced the final moisture content of the dried cocoons to 11.8% (wb), successfully meeting the recommended moisture content of below 12% (wb). During the drying period, solar intensity ranged from 700-900 W/m^2, the air flow rate was about 480 m^3/h, and ambient temperature and relative humidity were 32-37°C and 40-55%, respectively.

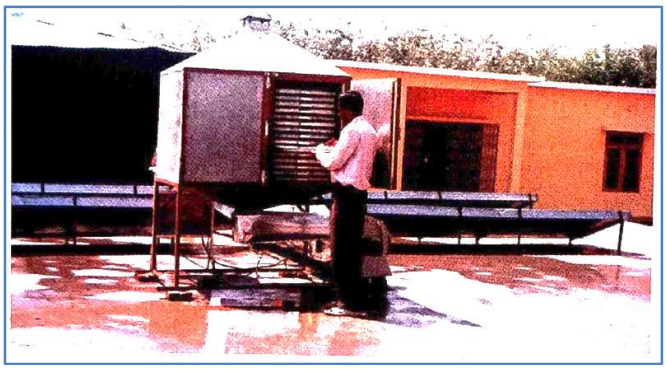

Fig. 5.9Solar cocoon dryer installed at Silk Reeling Centre,Hoshangabad

5.11 Solar assisted heat pump dryer for high value crops

A solar assisted heat pump dryer (20 kg/batch capacity) was fabricated and installed (Fig.5.10). The dryer mainly consisted of a drying chamber, dehumidifier, solar collector panel and heating back up. The heat pump dryer was evaluated by drying Amla fruit (blanched, deseeded and cut into 5-6 pieces) and eucalyptus leaves. The drying time of the Amla in the heat pump dryer was 50 h and 18 h at 35°C and 50°C respectively as compared to 8-10 days in the open sun drying. The ascorbic acid (vitamin-C) content of the Amla dried at 35°C and 50°C were about 490 mg/100 g and 320 mg/100 g as compared to 260 mg/100 g dry Amla in the open sun-dried Attila. The drying time of the eucalyptus leaves in the heat pump dryer was 22, 15 and 10 h at 35, 45 and 50°C respectively as compared to about 3 days in the open sun drying. The eucalyptus oil content in the dried leaves at 35, 45 and 50°C were 18.9, 18.3 and 17.8 ml/kg as compared to 17.1 ml/kg in the open sun-dried leaves. The total (heating and cooling) coefficient of performance (COP) of the heat pump was 4.8. Augmentation of the pump with solar heating system improved the COP to 6.6. Thermal efficiency of the solar assisted heat pump dryer was 24-30%.

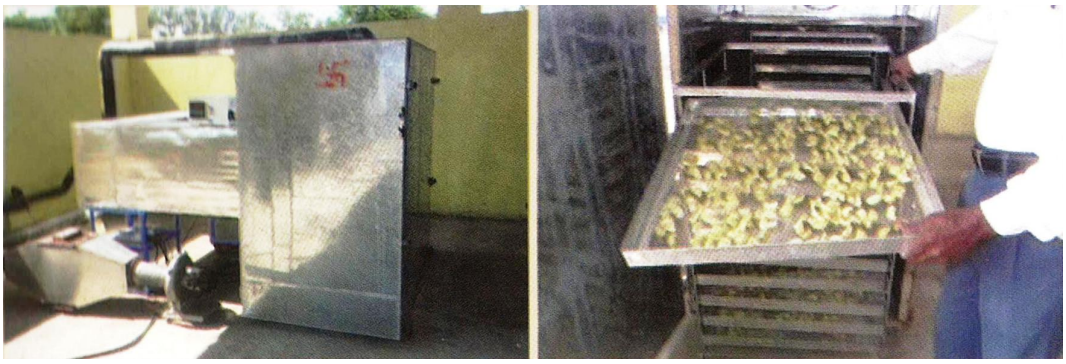

Fig. 5.10A view of the solar assisted heat pump dryer (left), and loading with Amla pieces in the dryer (right)

5.12 Packed bed solar heat storage system for solar dryer

A packed bed heat storage system integrated with a 100 kg/batch solar dryer was developed with key constructional features to enable efficient charging and post-sunset heat supply (Fig. 5.11). The unit consisted of a packed bed storage box filled with 8.5 tonnes of 50 mm stone pebbles serving as the thermal storage medium. Four solar air heating collectors with a total area of 9.2 m^2 were connected to the storage chamber to heat the pebbles during the daytime. The storage box was provided with a double-glass top for effective solar radiation entry and insulated with glass wool to minimize heat losses. A centrifugal blower and ducting system were incorporated to circulate hot air from the collectors to the packed bed during charging and to deliver heated air from the storage box to the dryer during heat retrieval.

Performance evaluation showed that during charging in March, the packed bed temperature increased from 34°C to 45°C between 9:30 AM and 5:30 PM, when solar intensity ranged from 550–920 W/m^2 at an ambient temperature of 27.8°C. The solar collection efficiency of the system was 34–36%. During an eight-hour post-sunset retrieval test, the hot air temperature at the exit of the storage box ranged

from 45.3 to 32.5°C (mean 37.5°C), while the temperature at the dryer inlet varied from 45 to 30.2°C (mean 36.4°C), at an airflow rate of 500 m^3/h. The heat retrieval efficiency of the system ranged from 60 to 62%. The integrated system successfully dried 75 kg of blanched potato chips in a single stretch, reducing moisture content from 89.5% to 7% (wb) within 14 hours at a drying temperature range of 30–60°C. The solar dried chips showed improved colour, texture, and sensory quality compared to open sun drying, with solar intensity and relative humidity during drying ranging from 200–950 W/m^2 and 38–57%, respectively.

Fig.5.11A view of packed bed solar heat storage system coupled with solar tunnel dryer

5.13 Evaluation of PAU natural convection solar dryer

The natural convection PAU solar dryer (Fig. 5.12) consisted a flat plate solar collector and drying box with trays. The collector was tilted at 45° and attached with the drying box. The solar dryer was tested by drying green chilli. Seventeen kg green chilli was dried from initial moisture content of 86.2% (wb) to 10% (wb). Drying time in the solar dryer was 7 days as compared to 13-14 days in the open sun drying in the month of December. The average drying temperature in the box was 45°C (30-56°C). The ambient temperature and solar intensity during drying ranged from 19-23°C and 300-850 W/m^2 respectively.

Fig. 5.12 Views of chill being loaded in the trays (at left) and PAU natural convection solar dryer (at right) PAU natural convection solar dryer (at right)

5.14 Cabinet Solar Dryer Integrated with Gravel Bed Heat Storage System

A cabinet-type solar dryer of 15 kg/batch capacity, integrated with a gravel bed heat storage system, was developed and evaluated for drying different agricultural products (Fig. 5.13 & Fig. 5.14). The system consists of a 2 m^2 solar air heater filled with 600 kg of 50 mm stone gravel, which serves both as a heat absorber and a storage medium. During operation, gravel bed temperature rises significantly during the day and extends dryer operation for about 4 hours after sunset.

The system was first evaluated for drying green chilli, where 15 kg of produce was dried from 88.5% to 7.3% (wb) in 56 hours, compared to 104 hours required in open sun drying. During testing, dryer temperature ranged between 33–60°C, while the gravel bed temperature increased from 31–48°C. Average solar intensity, ambient temperature, and relative humidity were 688 W/m^2 (252–988 W/m^2), 30°C (24–34°C), and 38% (25–65%), respectively. The drying efficiency was found to be 34%.

The same dryer was also evaluated for tomato drying, with tomatoes sliced to 5–6 mm thickness and uniformly loaded in trays at 10 kg/m^2. Moisture content was reduced from 92% to 6.5% (wb). The temperature inside the drying chamber and solar intensity during the operation varied between 40–63°C and 400–1175 W/m^2, respectively. Ambient conditions ranged from 37–44°C temperature and 25–40% relative humidity. The gravel bed temperature increased from 37–53°C, again providing an additional 4 hours of post-sunset drying. The drying efficiency for tomato was 36%, and the drying time reduced to 3 days with the gravel heat storage system compared to 4 days without heat storage.

Fig. 5.13 The cabinet dryer integrated with packed bed heat storage system

Fig. 5.14 Tomato drying solar cabinet dryer

5.15 Micro-controller based single axis sun tracker for SPV panel

To achieve a better precision in tracking of sun, a single axis sun tracker for SPV panel (2.4 kW) has been developed. The sun tracker consists of the SPV panel mounting frame, worm drive stewing ring, gear box with helical gear and pinion set, stepper motor, stepper motor drive and micro-controller (Fig. 5.15). The pinion and worm are powered by a stepper motor. Operation of the stepper motor is controlled with a programmable micro-controller. The controller is programmed to rotate the solar panel at every 7.5 min by 1.875°. The energy output from the tracked SPV panel is found to be 22 per cent higher than the power output of non-tracked panel in the month of November. The total energy output from 2.4 kW SPV panel is estimated to be 12.6 kWh/day and 10.1 kWh/day under tracked and non-tracked condition, respectively. The energy required by the sun tracker to track this panel is estimated as 0.3 kWh/day (about 12 per cent of the increased output due to tracking of panel).

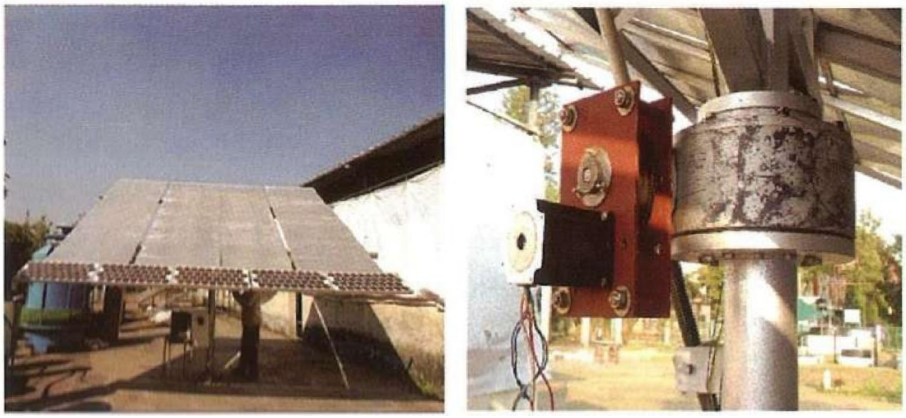

Fig. 5.15 A view of the SPV panel frame assembly with sun tracker (left); and a close view of the stopper motor fitted on gear box and stewing drive worm gear fitted with the frame assembly (right).

5.16 Hybridization of electricity generated from solar and biogas

To hybridize the frequency of the electricity generated from solar power (through inverter, 3.5 kVA) and biogas genset (3 kVA), an electric control system (Fig. 5.16) has been developed. The control system consists of voltmeter, ammeter, frequency meter, energy meter and power factor meter for monitoring voltage, current, frequency, energy and power factor, respectively. A synchroscope is provided to indicate phase lag or lead between the individual power sources. The isolation transformers are connected to both sources to isolate inrush current into the individual source after hybridization. Protection device is also provided against input over voltage, output short circuit, overheat, over/under voltage of genset, over/under frequency of genset. The control system has been tested with inputs of two single phase AC current sources in the laboratory. The frequency of the input power from solar and biogas genset were 50±0.2 Hz and 50±0.5 Hz, respectively. The frequency of the output power was found to be 50±0.5 Hz.

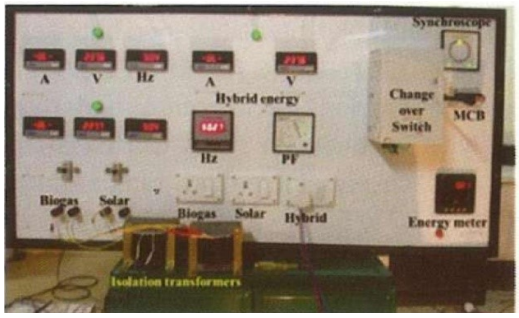

Fig. 5.16AC Electric control system for hybrid electricity generation

5.17 Solar PV based vapour compression refrigeration system

A cold storage facility for storage of fresh horticultural produce, powered by solar photovoltaic (25 kW, capacity) with battery backup (240 V, 900AH capacity) has been developed and installed (Fig. 5.17a & b). The power conditioning unit of the solar power plant converts DC power into three phase, 415-420 V, AC power. The puff insulated walk-in type cold storage chamber (L×B×H, m: 5×4.4×3) was constructed and fitted with a vapour compression refrigeration system (2.5 TR capacity) and a humidifier (Fig. 5.18a & b). The racks were provided in the cold storage chamber to hold fruits/vegetables. Cold storage room was fitted with temperature and relative humidity indicator-cum-controllers to set the room temperature (5-25°C) and relative humidity (65-95%) for storage of the horticultural produce. The energy output from the solar power plant ranged from 80-110 kWh/day during November to March, which was sufficient to operate the cold storage unit.

(a)

(b)

Fig. 5.17 Solar PV power plant (a) Panels (b) Power conditioning unit and battery bank

(a)

(b)

Fig. 5.18 Walk-in-type cold storage room (a) Outside view (b) Inside view

5.18 Pre-cooler for fruits and vegetables

The hydro pre-cooler (100 kg/batch) was developed for cooling fruits and vegetables (Fig. 5.19). It consists of an insulated water tank (L×B×H, m: 0.82×1.6×1.0), evaporative cooling tower with 0.37 kW motor and 0.45 m diameter axial fan, inclined trough for holding products submerged in the tank, belt conveyer and surface moisture drying unit. A pump (0.37 kW motor) was used to recirculate the cold water from evaporative cooling tower to the water tank. Surface moisture drying unit is fitted with an axial fan (0.45 m diameter) below the perforated tray (2 m^2) to blow the fresh air into the produce.

Fig. 5.19 Hydro pre-cooler for fruits and vegetables

5.19 Solar powered bird scarer

Birds are serious threat to standing crop. It has been reported that 20-22% of sorghum and pearl millet (bajra) get damaged due to birds. The extent of damage is normally higher in isolated fields. A gadget to scare away the birds has been developed. The solar powered bird scarer comprised a solar panel (20 Wp), battery (12 V, 7Ah), motor (5W), a steel pan, a watch movement unit and two speakers (Fig. 5.20). The unit produces both mechanical and musical sounds for 20 seconds at interval of 3 minutes to restrict birds entry in the crop field. Noise produced by the unit is 98.5 and 109 dB by mechanical and musical means, respectively at source. However, the noise produced at a distance of 100 meter distance has been observed as 45 and 58 dB, respectively for mechanical and musical means, respectively. The device has been tested in maize crop for 45 days without any damage to crop on account of birds.

Fig. 5.20 Solar powered bird scrarer

5.20 Solar lighting system with centralized DC battery charger in a tribal village of MP

Rural and tribal communities often face severe challenges in accessing reliable electricity, resulting in inadequate lighting in their homes. To address this issue, a centralized solar-powered battery charging system was developed to enable simultaneous charging of multiple batteries using a single solar panel setup (Fig. 5.21). A 1 kWp solar photovoltaic module, along with a suitable mounting structure, centralized bulk battery charging unit and portable battery banks equipped with low-voltage cut-off protection, was designed and tested in the tribal village of Gaildubba, Block Tamia, Madhya Pradesh. During field testing, the system successfully charged 50 batteries (12 V, 7 Ah) at a time. Each fully charged battery provided continuous lighting for up to 6 hours. The measured light intensity at the center of the room and near the 5 W LED lamp was approximately 20 lux and 40 lux, respectively, ensuring adequate illumination for household activities. The centralized solar battery charging station and home lighting units were installed and demonstrated to the villagers. This decentralized, community-managed energy solution has enabled households to access independent and reliable lighting, significantly improving quality of life in remote tribal areas. The system is currently being maintained by trained local residents, promoting community ownership and long-term sustainability.

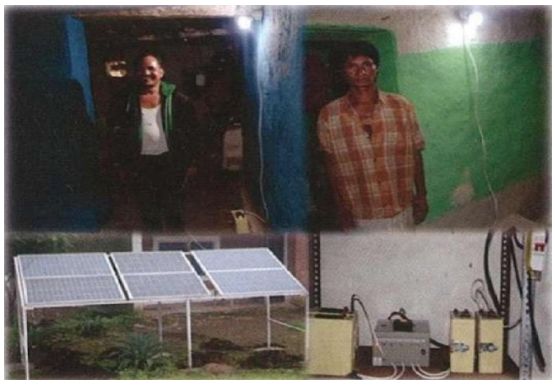

Fig. 5.21Solar-powered battery charging system

5.21 Solar powered e-prime mover for spraying and weeding operations

A solar-powered e-prime mover has been developed for efficient spraying and mechanical weeding operations (Fig. 5.22). The system offers a complete modular solar solution with a smart battery charging setup to enhance manoeuvrability during field activities. It is equipped with semi-flexible solar panels mounted on the roof and a 48V, 100Ah battery pack to power the implements. The spraying unit uses a 14V DC diaphragm pump capable of delivering 10 bar (150 psi) pressure at 7.5 L/min, while a 350 W DC motor drives the mechanical weeder. The operator can easily switch between solar and battery power as needed. The prime mover is ergonomically designed with essential safety features, keeping the total weight including the 70 kg operator, under 450 kg. A chemical storage tank is mounted behind the driver seat at a height of 455 mm. The steering system incorporates a 5° kingpin inclination and a 3° camber angle. Workplace design follows 5th to 95th percentile ergonomics, ensuring optimal placement of controls within the operator's reach. The workstation dimensions (1060×950×1300 mm) and a seat adjustment of 100 mm accommodate operators of varying statures.

Performance evaluation showed that the operational speeds for the horizontal rotary weeder and sprayer were 1.3 km/h and 2.6 km/h, respectively. For weeding, the prime mover achieved 82% field efficiency, 70% weeding efficiency, a field capacity of 0.06 ha/h, and required 550 W of power. For boom spraying, field efficiency was 83%, field capacity 0.52 ha/h, and power requirement 50 W. The prime mover's power consumption ranged from 932–1648 W during field movement and 229–593 W during spraying and weeding operations.

Fig. 5.22 Solar powered e-prime mover for spraying and weeding operations

CHAPTER-6

6.Briquetting and Pelleting of Biomass

Studies indicate that India's forest cover is declining by over 1.5 million hectares annually, particularly in rural areas where much of the wood is used as cooking fuel. Despite large-scale afforestation efforts, the demand for fuelwood continues to exceed supply. To reduce deforestation, surplus crop residues can serve as an alternative energy source. About 1.5 tonnes of residue are generated per tonne of crop, with additional residue produced during processing of crops like sugarcane, rice, groundnut, and coconut. While some is used domestically, much remains underutilized and is often burned, causing environmental pollution and loss of organic matter. Since crop residues have similar composition to wood but are scattered and seasonal, technologies like charring and briquetting help overcome storage and handling issues. Briquetting has proven cost-effective and is increasingly replacing firewood in many regions of the country.

6.1 Biomass Availability and Utilization Pattern

India generated about 544.5 million tonnes of agro-residues in 1996–97 from major crops such as rice, wheat, maize, sugarcane, groundnut, cotton, and several others. With the expected rise in agricultural production, crop residue generation may increase by over 250 million tonnes in the next two decades. Residues produced during primary processing, particularly from sugarcane, rice, groundnut, and coconut, are concentrated in specific locations and can be effectively utilized for energy conversion. Soft residues from cereals and millets are generally used as cattle feed, while woody residues from crops like cotton and pigeon pea serve as household fuel in rural areas. However, the use of crop residues as cattle feed and fuel is declining due to the reduction in draught animals, greater availability of green fodder, and increased access to modern fuels such as LPG and kerosene. In 1996–97, around 3.14 million tonnes of surplus residue with a power potential of 307 MW were identified (**Table 6.1**). With agricultural energy demand growing at about 4% annually, it is estimated that by 2010 nearly 120 million tonnes of crop residue would remain surplus and could be used as a renewable energy source.

Table 6.1 Estimates of biomass production and its surpluses in typical talukas*

S. No.	Name of Taluka	Biomass (tonnes $\times 10^3$)		Types of surplus biomass	Power potential (MW)
		Produced	Surplus		
(A) North India					
1.	Mansa (Punjab)	450	320	Cotton straw, paddy & wheat	32
2.	Bamala (Punjab)	1350	950	Paddy & wheat straw	95
3.	Patti (Punjab)	750	600	Paddy straw, wheat straw	60

4.	Baghpat (UP)	540	250	Sugarcane trash	25
(B) Western India					
5.	Walwa (MS)	2000	120	Sugarcane trash	10
6.	Pusad (MS)	200	80	Cotton stalk, pulses straw	8
7.	Raver (MS)	230	100	Cotton & pulses straw	10
8.	Kharasiya (MP)	450	20	Paddy straw	2
9.	Katangi (MP)	750	10	Paddy & oilseed straws	1
10.	Gotegaon (MP)	170	75	Soybean & pulses straws	7
(C) Southern India					
11.	Pungamuru (AP)	200	116	Groundnut waste &canetrash	10
12.	Bodhan (AP)	180	70	Paddy straw, sugarcane trash	7
13.	Ramachandrapuram (AP)	250	150	Paddy straw	15
14.	Tirupattur (TN)	270	75	Groundnut & millet straws	7
15.	Nilakottai (TN)	160	51	Sorghum waste, pulses waste	5
16.	CN Halli (KK)	200	66	Coconut & millet waste	6
17.	Sindgi (KK)	260	55	Oilseed straw, jowat straw	5
(D) Eastern India					
18.	Mal (WB)	90	23	Paddy straw	2
TOTAL		**7825**	**3141**		**307**

6.2 Technology for biomass Briquetting

The density of most of the agro-residues available either on the farm or from agro industries is low. For efficient utilization and easy handling storage densification of the biomass is an essential requirement. The density of char produced through pyrolysis of biomass is also very low. Densification of biomass to produce small solid blocks for use in domestic and industrial combustion devices is normally referred to as biomass briquetting. Densification processes are basically of 2 types- binderless technique where no external binders are added, with binder where molasses, clay, soil, sodium bentonite, tar or any other material is added. In binderless process the cellulose bonding collapses due to the high temperature (200°C) and very high pressure (1490.5 kg/cm^2) conditions and the lignin get fluidized flowing evenly through the granular mass. The process is used with unhydrolyzed biomass.

6.2.1 Briquetting Equipment

Several institutions have developed small plunger-type and screw-type briquetting machines for compacting biomass char. The char is typically mixed with cattle dung or soil in a 10:1 ratio (by weight), and water is added to maintain 30–35% moisture content before briquetting. At JNKVV, Jabalpur, a hand-operated worm-type extruder with a capacity of 20 kg/h was developed. The Society for Development Alternatives, New Delhi, designed a hand-operated ram press capable of producing 500–800 kg/h, while IIT Delhi developed a simple press to make beehive-shaped briquettes (10–15 cm diameter) suitable for domestic stoves. At CIAE, Bhopal, a power-operated extruder-type briquetting machine (Fig. 6.1) was developed, powered by a 3.7 kW, 3-phase motor, producing five briquettes of 25 mm diameter simultaneously with a rated capacity of 80 kg/h. Tests conducted using a mixture of soybean residue char and biogas slurry (15:1 dry mass ratio) with 30–35% moisture showed an output of 30–50 kg/h of wet briquettes. Common raw materials suitable for briquetting include coffee husk, groundnut shell, mustard stalk, and sawdust, while coir pith, bagasse, and tobacco stems are also used. Ram-type machines, operating on the piston pump principle, compress raw material (10–12% moisture) into high-density briquettes (1000–1400 kg/m^3) compared to loose biomass (60–80 kg/m^3). The calorific value of briquetted fuel is around 16.7 MJ/kg, higher than fuelwood's 14.2 MJ/kg.

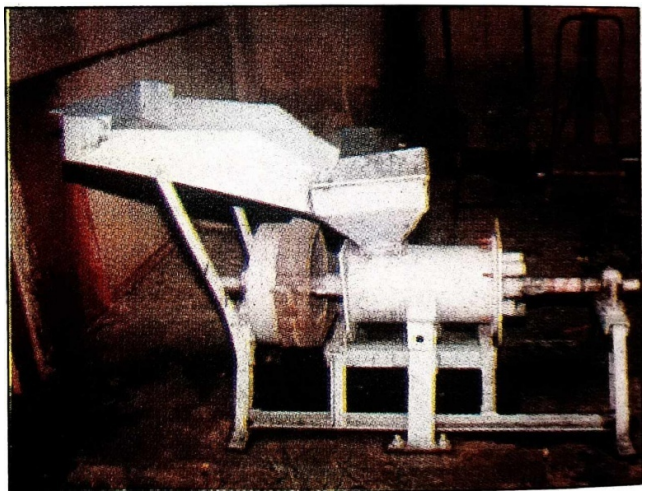

Fig. 6.1 CIAE Charcoal Briquetting Machine

Commercial briquetting units consisting of a hammer mill, dryer, press, and handling systems operate in states like Tamil Nadu, Gujarat, and Punjab, producing 65 mm briquettes used as fuelwood substitutes in boilers. These briquettes sell for about ₹1200 per tonne, with energy consumption reported as 54–75 kWh/t for ram-type presses and 64–75 kWh/t for screw-type presses. Around 150 ram-type presses (capacity 500–750 kg/h) have been installed in the country, with approximately 60 currently in operation.

6.2.2 Testing of briquetting machines with crop residues (soybean and pigeonpea stalk)

The briquetting machine (Fig. 6.2) was tested for production of briquettes from soybean stalk and pigeonpea stalk. The output of the machine with soybean and pigeonpea stalks was in the range of 350-370 kg/h. The briquettes of 30 and 60 mm diameter were prepared by the machine. Except for initial smoke formation no other operational problems were noticed. Briquettes were characterized and tested in CIAE cook stove and local sigri (Fig. 6.3) to assess their suitability for domestic applications. Only 30 mm diameter briquettes could be used with improved cook stove. The briquettes (1.5 tonnes) were supplied to an entrepreneur for assessing the feasibility of briquettes for thermal applications in commercial boilers in Dewas. The feedback received from entrepreneur on use of briquettes indicated that 60 mm diameter briquettes were more suitable for use in boilers.

Fig. 6.2 Briquetting of agro-residues

Fig. 6.3 Burning of briquettes

6.2.3 Evaluation of 20 kW power plant

Biomass (wood chips) based 20 kW power plant for electricity generation (Fig. 6.4) was procured from Vita's Ankur Scientific, Vadodara, Gujarat. The power plant consists of a downdraft gasifier having rotating grate, ventury scrubber to cool and clean the gases, three filters (one coarse and two fine) connected in series and one security filter and gas engine generating set. The gas engine has been specially developed for producer gas. The biomass consumption of gasifier is 40 kWh and capacity of alternator (Fig. 6.5) is 35 kVA. The system was initially operated on wood chips and electricity produced was used to run the 11 kW electric motor of hammer mill of briquetting plant.

Fig. 6.4 View of power plant

Fig. 6.5 View of gas engine genset

6.2.4 Briquetting of jute sticks

Jute stick contains higher lignin (18.2%) and lower ash (1.7%), making it suitable for briquetting. The jute sticks were ground below 2 mm particle size to produce the briquettes (Fig. 6.6) using die and press type briquetting machine (500 kg/h) with tapered die of 60 mm diameter. The true density and moisture content of the briquettes were 900-950 kg/m^3 and 6.2% (wb), respectively. The calorific value of the briquette was 18.6 MJ/kg.

Fig. 6.6 Briquette produced from jute stick

6.2.5 Portable briquetting machine for paddy straw

The machine comprises of feeding hopper, barrel, screw auger, die and power unit (Fig. 6.7). Feedstock for briquetting machine has been prepared by mixing ground paddy straw and other crop residues in 70:30 ratio, binder (cow dung slurry at 20 per cent of total biomass) and moisture content is maintained in the range of 50-60 per cent by adding water. During feeding the speed of screw auger of briquetting machine is maintained at 350 rpm. The briquettes exhibit excellent resistance to shattering and durable as well. The calorific value is 3600 kcal/kg at a thermal efficiency of 35 per cent for paddy straw briquettes.

Fig. 6.7 Portable briquetting machine for paddy straw

6.3 Development of pellets using digested biogas slurry and soybean stalks

This study investigates the utilization of digested biogas slurry (DBS), a byproduct of anaerobic digestion, in combination with soybean stalks to form biomass pellets as an alternative energy source. The research systematically assesses the physicochemical properties of both substrates and evaluates optimally blending ratios (1:1, 2:1, and 3:1) and moisture content (10,15 and 20%) for pellet production. Results indicate that blending (1:1, MC 15%) of soybean stalks with DBS yields pellets which has superior calorific values (17 MJ/kg). Maximum mechanical strength was achieved as 17.28MPa with bending ratio of 1:1, and significant bulk density of 1962 kg/m3was observed with bending ratio of 1:1 (MC 20%). As compared to conventional fuels, developed DBS pellets have reduced emissions and maximum 79.9% water resistance index (3:1). These findings offer a promising approach to managing agricultural waste while promoting circular bioeconomy practices and sustainable energy systems.

6.4 Paddy Straw–Based Insulating Blocks and Boxes

India generates more than 150 million tonnes of paddy straw annually, a large portion of which remains underutilized or is burned, causing environmental concerns. Beyond its conventional use in biochar, gasification, and biogas production, paddy straw offers strong potential as a sustainable thermal insulation material for construction, cold storage, and temperature-controlled applications. In this context, eco-friendly insulating blocks and boxes were developed using paddy straw to provide thermal comfort and low-temperature storage solutions.

Insulating composite blocks of size 300 × 300 × 25 mm were fabricated using treated and untreated paddy straw through cold and hot-press techniques (Fig. 6.8). The optimized composition consisted of about 83% paddy straw, 12% clay, and 5%

seed lac, processed at 10–12 MPa pressure, 110–120 °C temperature, and 45 min pressing time. The developed blocks exhibited low thermal conductivity of 0.08 W m^{-1} K^{-1}, bonding strength of about 0.03 MPa, and compressive strength around 1.14–1.19 MPa. Blocks made from untreated straw showed better insulating performance than treated straw.

For practical application, the blocks were laminated with FRP sheets and coated with a heat-reflective white emulsion to enhance durability, cooling efficiency, and service life. Using these blocks, a paddy-straw-based insulating box was developed for low-temperature storage of vegetables (Fig. 6.9). The cost of insulation was estimated at about ₹980 per m^2, with total energy consumption of 123.83 MJ kg^{-1} and CO_2 emissions of 14.65 kg CO_2-eq per kg of material produced. The developed paddy straw insulation system is suitable for chilled storage, cold rooms, refrigeration units, and can be used in combination with conventional insulation materials such as PUF and polystyrene.

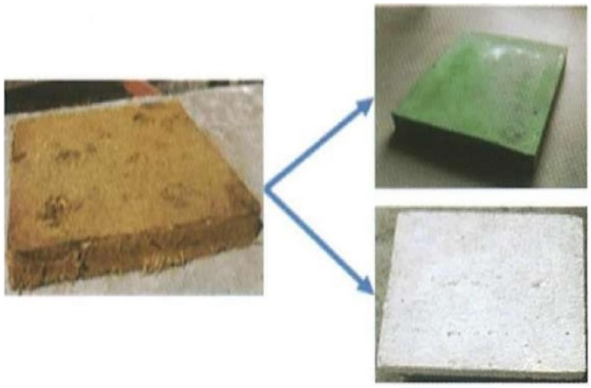

Fig. 6.8 Paddy Straw–Based Insulating Blocks

Fig. 6.9 Paddy straw based insulating box

6.5 Development of plastering material using paddy/soybean straw for small dwellings

Thermally treated straw (paddy and soybean) based mortar cubes (50 × 50 × 50) mm and prismatic samples (40 × 40 × 160) mm were prepared and mixed with cement: sand ratio of 1:3 in different combinations by the replacement of sand with thermally treated straw i.e. 1:2:1, 1:1:2 and 1:0:3 **(Fig. 6.10).** Soybean and paddy straw was selected for thermal treatment at three temperatures i.e. 350,450 and 550°C. The thermally treated paddy and soybean straw was mixed in different proportion with sand at constant proportion of cement. The cement to sand ratio for mortar preparation was kept as 1:3 (volume basis). The water to cement ratio of a 0.6 (weight basis) was used as it is suitable to produce conventional mortar. The sand was replaced by the raw biomass and thermally treated biomass (25%, 50% & 75%) for mortar preparation while the portion of cement was kept same (25%). Similarly for flexural strength test the prismatic bars of 160 × 40 × 40 were prepared for different combinations (25, 50 and 75%) of cement sand and thermally treated

biomass. Samples for compressive and flexural strength testing were prepared in molds and cured in water for 28 days.

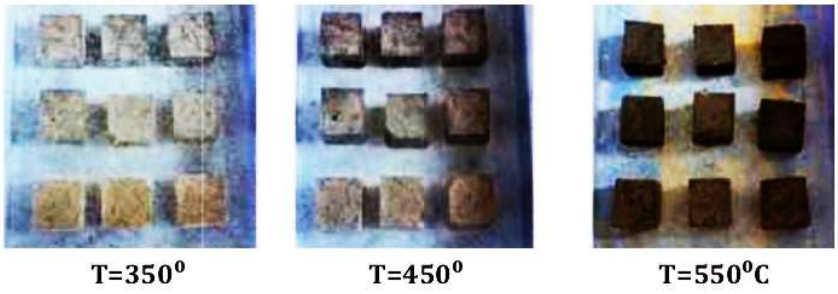

Fig. 6.10 Mortar cubes prepared by mixing of thermally treated biomass at different temperature

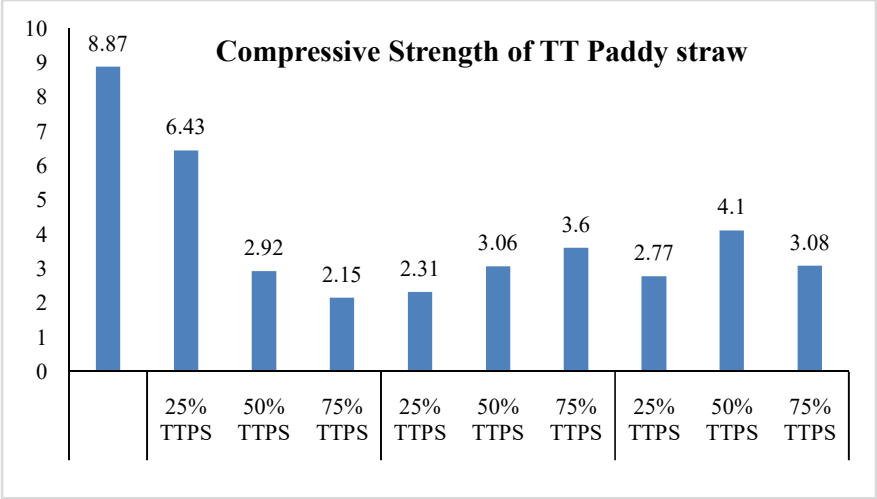

Fig. 6.11 Compressive strength of Thermally treated paddy straw after 28 days of curing

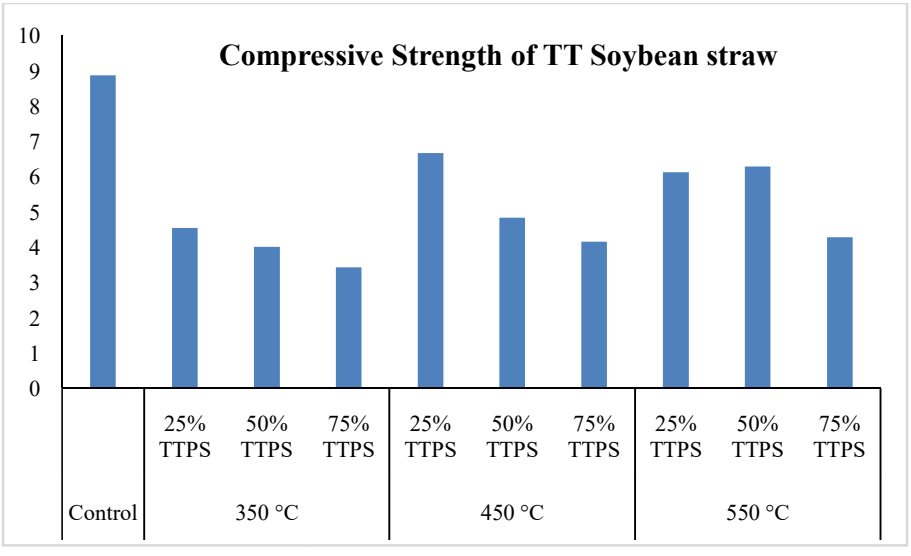

Fig. 6.12 Compressive strength of Thermally treated soybean straw after 28 days of curing

It was observed that replacement of sand with thermally treated soybean straw found better in terms of compressive strength as compared to thermally treated paddy straw. Replacement of sand to the tune of 25% and 50% with thermally treated soybean straw (treatment imparted at temperature of 350 and 550^0C) gives better and stable results as compared to paddy straw (Fig. 6.11 & 6.12).

CHAPTER –7

7. Biochemical Conversion of Biomass

Domestic biogas plants installed in our country use cattle dung mixed with an equal quantity of water to maintain 8-9% total solids concentration (TSC) in the influent slurry. The effluent discharged from the plants is, in general, collected into the slurry pits or spread on to the ground for drying before transportation to fields for use as organic manure. Solid-state anaerobic fermentation requires much smaller quantity of water, makes handling of the digested slurry easier, can utilize a variety of agro-residues as substrate and conserves plant nutrients in the final product. The site also looks much cleaner which may help overcome the farmers' reluctance to locate the plant near their houses.

In view of the above advantages several studies have been carried out on various aspects of solid-state anaerobic digestion of agro-residues and a few designs of solid-state biogas plant have been evolved. Anaerobic digestion of cattle dung and many other agro-residues at initial TSC varying from 16 to 25% in small, batch type and plug flow type digesters under laboratory and field conditions have been demonstrated satisfactorily by many investigators in the country and abroad. However, technically sound design of a family size solid-state anaerobic digester for use with diversified agro-residues is not so far available for wide-spread adoption even with financial support from the Government. Status of research and development work carried out on application of solid-state fermentation technology is presented in the next section.

7.1 Laboratory Scale Studies on Solid-State Anaerobic Digestion

Several researchers have conducted laboratory and pilot-scale studies to evaluate the feasibility and performance of solid-state anaerobic digestion (SSAD) using various organic substrates such as manure, crop residues and industrial wastes. Early investigations demonstrated that SSAD is biologically feasible and can yield significant quantities of biogas with good methane content.

Wong-Chong (1975) reported the successful digestion of undiluted fresh manure, while subsequent studies by Wujcik and Jewell (1979) highlighted the influence of total solids concentration (TSC) on fermentation kinetics. Hills (1980) demonstrated the feasibility of high-solids digesters with mechanical mixing, and Jewell (1982) extended this work to a pilot plant level using wheat straw. Pathak et al. (1985) and Balasubramanya et al. (1986) further explored SSAD with cattle dung, rice straw and willow dust, respectively, emphasizing the effect of TSC and substrate pretreatment. Later studies by Molnar and Bartha (1989), Richards et al. (1991), and Singh et al. (1991) focused on reactor design, temperature effects, inoculum levels, and substrate combinations to improve biogas yield and stability.The summary of these laboratory-scale SSAD studies is presented in Table 7.1.

Table 7.1 Laboratory-scale SSAD studies

Researcher(s)	Year	Substrate/ Feedstock	Reactor Details	Operating Conditions	Key Findings / Results
Wong-Chong(1975)	1975	Fresh manure (20.8% solids)	80 L batch-fed reactor	140 days retention	Solids reduced to 16.5%; 0.71 m^3 gas/kg VS destroyed; 60–65% methane; SSAD biologically feasible.
Wujcik and Jewell (1979)	1979	Cattle dung + wheat straw / newsprint	Laboratory setup	35°C; TSC 10–70%	At ≤40% TSC, fermentation complete as in liquid reactors; methane formers slowed above 30% TSC.
Hills (1980)	1980	Undiluted dairy manure	4 L flask & 70 L plastic digester (mixed at 30 rpm)	35±1°C; 100 days	40.8% VS converted to biogas; 85% conversion within 45 days; 51.3% methane.
Jewell (1982)	1982	Wheat straw	110 m^3 RCC batch digester	25–33°C; TSC 25.9%; 100 days	303 L gas/kg TS; 250 $L \cdot d^{-1} \cdot m^{-3}$ digester volume; leachate recycling improved efficiency.
Pathak et al. (1985)	1985	Cattle dung & dung–rice straw mix (1:2)	Batch laboratory digester	26–32°C; TSC 15.2%	Higher TSC improved solids conversion and gas yield; dung–straw mix outperformed dung alone.
Balasubramanya et al. (1986)	1986	Willow dust	10 L lab & 700 L pilot digesters	Anaerobic; pretreatment with NaOH + lime + slurry inoculum	Best gas yield at 1:1.5 solid–water ratio; 52 m^3 gas in 45 days (pilot); lime replacement improved bio-manure.

Molnar and Bartha (1989)	1989	25% cattle manure + 75% corn stalks	Two 80 m^3 solid-state batch reactors	TSC ≈27%; 55→35°C; 30 days	30% higher gas yield with winter insulation; temperature decline affected performance.
Richards et al. (1991)	1991	Sorghum & sorghum/cellulose mix	Laboratory reactors	55°C; >25% TSC	Stable digestion at OLR 18–24 g VS·kg^{-1}·d^{-1}; methane 5.7–7.5 L·kg^{-1}·d^{-1}; sorghum alone led to NH_3 accumulation.
Singh et al. (1991)	1991	Cattle dung	Batch laboratory digester	35±1°C; TSC 7.6–16%; 85 days	Gas yield 0.21–0.25 L·g^{-1} TS; 80% yield in 55 days; inoculum level had little effect on yield.

7.2 Studies on solid-state anaerobic digestion of agro-residues and development of digester at CIAE

Laboratory experiments were conducted at CIAE to assess the effect of air dried mango leaves as partial and complete replacement of cattle dung, method of pre-treatment of leaves concentration of solids in the slurry and seasons of the Year independent variables and quantity and quality of biogas production as dependent variables. The study was conducted using 3L capacity batch digesters at room temperature. Each digester contained approximately 225 g of dry solid matter. 170 ml fresh digested slurry was added to each digester as inoculum. Air drier mango leaves were used as supplementary feed material maintaining 9 & 16% TSC. The minimum and maximum room temperatures during the period of trials varied from 24 to 35 °C and 26 to 43˚C, respectively. Following conclusions were drawn from the study;

a) There was no reduction in gas yield for 25% dung replacement and only slight reduction in gas yield for 50% dung replacement by leaves for normal slurry concentration.
b) Gas yield at 16% slurry concentration was observed to be higher for the digester containing 25% and 50% of mango leaves as compared to the digester containing dung alone.
c) Aerobic digestion of leaves for 2 days in plain water improved the gas yield, particularly at higher slurry concentration of 16%.

Performance evaluation of HAU design dry fermenter for digestion of cattle dung was also undertaken. Initially, 339 kg fresh undiluted cattle dung and 51 kg digested slurry was charged into digester. After one week time, about 10-11 kg undiluted cattle dung was daily fed into the digester. The gas monitoring indicated that the gas production was 91 L/kg of dry matter fed for a retention period of 31 days. The flowability of digested sludge was observed as most difficult problem while removal of the digested sludge from the digester.

Anaerobic digestion of cattle dung and mixture of cattle dung and paddy straw/ parthenium foliage/air dry mango leaves at initial TSC varying between 12.1 to 26.1% in small capacity out door digesters. Two batch-type digesters of 1.17 1.18 m^3 volume, one of cylindrical shape and the other cuboid, were designed and constructed using reinforced concrete (Fig. 7.1).A steel drum formed the top and floated in the water jacket around the digester to form the gas holder. The internal dimensions of the cylindrical digester were diameter 100 cm, depth 150 cm, and of the cuboid digester were length 125 cm, width 62.5 cm and depth 150 cm. A vertical pipe was provided in the centre of each digester to guide the movement of the gas holder. Both the digesters were buried in the ground to a depth of about 125 cm from the bottom. The gas holder was a loose fit over the digester tank and was 42 cm deep in each case. The retention period varied from 49 days to 110 days mainly depending upon the ambient temperature. At initial TSC of 16-19% the digester was found performing satisfactorily. The details of various trials conducted in cylindrical and cuboid digesters are presented in Table 7.2 and the cumulative gas yield in litres/kg total solids added and average gas yield in litres/day/m^3 of the digester volume obtained for different retention periods of the trials are presented in Table 7.3. The gas yield on a unit digester volume basis varied from 202.2 to 499.3 L $d^{-1}m^{-3}$ for 7 weeks retention period and 196.2-404.7 L $d^{-1}m^{-3}$ for 10 weeks retention period as compared to 204 - 273 L $d^{-1}m^{-3}$ in the case of semi-continuous type conventional digesters that used water-diluted cattle dung and 8-9% TS concentration at 7 weeks retention time. The digestion process in general, was severely affected at TS concentrations in excess of 19%. The gas yield was also affected by season of the year and pretreatment of the agro-residues used However, young tender parthenium foliage slashed and fed without aerobic pre-digestion gave highest gas yield.

Fig. 7.1 View of Solid State Anaerobic Digesters (Underground)

Table 7.2 Details of various trials conducted in cylindrical and cuboid digesters

Trial No.	Date of charging	Retention period (days)	Feed composition (ratio of total solids)	Total solids in digester substrate (%)	(%)
(A)	Cylinder digester				
1a	17.09.91	79	CD + PF (4.0:1)	166.0	15.5
2a	07.12.91	75	CD + PS	174.7	16.4
3a	21.02.92	81	CD + PS	134.0	17.4
4a	12.05.92	98	CD + ML	201.2	18.8
5a	20.08.92	71	CD + PF	84.9	12.1
6a	04.11.92	93	CD + PF	186.6	19.6/18.2a
(B)	Cuboid digester				
1b	04.10.91	110	CD	179.8	17.8
2b	23.01.92	72	CD + PS (2.0:1)	140.0	16.7
3b	06.04.92	22	CD + ML (4.5:1)	215.6	26.1
4b	29.04.92	49	CD + ML (5.7:1)	196.8	19.3
5b	17.06.92	91	CD + ML (3.3:1)	203.6	22.9/20.3a
6b	16.09.92	104	CD + PF (3.1:1)	147.7	19.2/17.5a

CD – cattle dung; PF – parthenium foliage; PS – paddy straw; ML – mango leaves
a – Values computed after addition of water into the working digester

Table 7.3 Cumulative gas yield in litres/kg total solids added and average gas yield in litres/day/m³ of digester volume obtained for different retention periods of the trials

Trial No.	Cumulative gas yield for			Average gas yield for		
	49 days	79 days	Full duration	49 days	79 days	Full duration
(A)	Cylindrical digester					
1a	154.1	176.9	152.1 (79)*	442.4	355.5	324.3
2a	72.2	100.3	106.1 (75)	218.2	212.1	209.4
3a	104.0	153.6	174.7 (81)	241.5	249.2	244.9
4a	123.1	151.3	172.7 (98)	428.4	368.5	300.5
5a	191.0	249.1	251.2 (71)	280.5	256.0	254.6
6a	43.0	58.0	70.8 (93)	138.8	131.0	120.4
(B)	Cuboid digester					
1b	83.5	102.9	125.2 (110)	261.9	225.9	174.9
2b	82.8	114.8	117.8 (72)	202.2	196.2	195.8
3b	85.8	-	85.8 (49)	294.5	-	294.5
4b	140.6	164.0	183.2 (91)	499.3	407.7	350.3
5b	106.4	141.1	168.9 (104)	274.1	254.5	205.0

A cylindrical shaped underground batch type solid-state in-situ bio-digester of 1180 L volume was designed in CIAE. Air dried mango leaves parthenium weed and paddy straw mixed with cattle dung were successfully digested. The internal diameter and depth of the digester were 100 cm and 150 cm, respectively. A vertical pipe was provided in the centre of the digester to guide the movement of gas holder. It has a steel gas holder inverted over the digester floating in the water jacket provided around the periphery of the digester. Mixture of cattle dung and plucked subabool leaves in 1:1 and 1.37:1 on dry weight basis were fed into HDPE digester, whereas mixture of cattle dung and subabool leaves in 2:1 and 0.6:1 ratio on dry weight basis were fed into CIAE design solid-state digester. The effluent from the functional biogas plant was collected and used as inoculum at the uniform rate of 12% of the wet weight of the substrates in all the cases. The total solids concentration of the digester contents were maintained between 16-19% by addition of the required quantity of tap water. The charging details and gas production patternof HDPE and CIAE cylindrical digester are presented in Table 7.4 & Table 7.5 respectively.

Table 7.4 Performance of 240 I HDPE solid-state digester

1.	Date of charging	October 29, 1994	March 16, 1995
2.	Substrate	Cattle dung + subabool leaves	Cattle dung + subabool leaves
3.	Substrate ratio on dry weight basis	1:1	1:37:1
4.	Total solids charged	9.3 kg	18.83 kg
5.	Total solids concentration	17.47 %	17.19 %

Weeks	Gas yield (L/kg dm)		Average weekly ambient temperature (°C)	Gas yield (L/kg dm)		Average weekly ambient temperature (°C)
	Weekly	Cumulative		Weekly	Cumulative	
1	8.82	8.82	21.00-26.75	6.27	6.27	24.00-24.80
2	13.76	22.58	19.50-21.75	11.52	17.81	21.90-27.10
3	12.15	34.73	18.15-21.50	16.20	33.99	24.30-25.50
4	9.78	44.51	16.75-18.35	23.15	57.14	25.0-27.95
5	10.53	55.05	18.00-19.50	22.57	79.71	25.35-29.85
6	10.11	65.16	17.50-20.65	20.98	100.70	27.60-30.65
7	8.17	73.33	13.25-17.50	28.52	129.20	31.10-34.00
8	7.74	81.08	13.10-15.00	24.53	153.74	31.45-34.75
9	7.85	88.92	12.00-17.90	17.91	171.64	30.75-35.90
10	7.31	96.24	12.00-17.00	16.30	187.94	30.80-32.70
11	7.52	103.76	9.50-15.60	16.62	204.57	32.50-35.60
12	6.13	109.90	10.80-17.35	12.37	216.94	34.75-37.85
13	5.16	115.05	12.70-16.30	11.10	228.04	34.00-37.05

Table 7.5 Performance of 1180 L CIAE solid-state bio-digester

1.	Date of charging	January 19, 1995	March 02, 1995
2.	Substrate	Cattle dung + subabool leaves	Cattle dung + subabool leaves
3.	Substrate ratio on dry weight basis	2:1	0.6:1
4.	Total solids charged	130.59 kg	142.09 kg
5.	Total solids concentration	16.78 %	18.52 %

Weeks	Gas yield (L/kg dm)		Average weekly ambient temperature (°C)	Gas yield (L/kg dm)		Average weekly ambient temperature (°C)
	Weekly	Cumulative		Weekly	Cumulative	
1	4.15	4.15	12.70-16.30	15.72	15.72	30.75-34.75
2	6.32	10.47	13.65-16.25	18.04	33.76	33.10-35.90
3	9.66	20.13	15.15-19.00	18.42	52.19	30.75-32.00
4	16.44	36.57	15.80-23.50	19.88	72.07	31.80-34.85
5	14.05	50.62	16.70-18.40	22.87	94.94	34.75-37.85
6	12.99	63.61	14.25-20.20	20.88	115.82	33.50-37.05
7	14.30	77.91	16.80-20.60	19.07	134.90	31.50-36.75
8	13.16	91.07	18.95-24.75	16.38	151.28	30.20-34.00

9	15.57	106.63	24.00-24.80	14.75	166.03	29.70-32.15
10	14.76	121.40	21.90-27.10	15.08	181.11	29.00-33.00
11	10.92	132.32	23.60-25.50	14.55	195.66	24.50-27.90
12	9.13	141.45	25.90-27.95	10.05	205.71	23.70-26.50
13	7.03	148.48	25.35-29.85	9.13	214.84	24.60-27.80

The gas production began with a slower rate of 4.15 L/kg of dry matter fed during the first week after feeding. There was further increase in gas production in next week with increase of ambient temperature. The maximum gas production rate of 16.44 L/kg of dry matter fed could be achieved during the fourth week after feeding. Thereafter the gas production was reduced with slower rate up to sixth week after feeding. Then it increased during seventh week and decreased during eighth week and again increased at the level of 15.57 L/kg of dm and 148.48 L/kg of dry matter fed gas could be achieved during 9.3 nineth and thirteenth week of digestion period. The total gas production in nine weeks was about 53% of the expected gas production. It is evident from the Table 7.5, that almost stable gas production was obtained from the fifth week to tenth week period. The reasons for low gas production may be lower ambient temperature in the beginning affecting the microbial activity adversely.

The gas production from the digester fed with 0.6:1 dung to subabool leaves ratio was 15.72 L/kg dm observed during the first week after feeding as ambient temperature was the optimum for mesophilic range. The gas production further increased and reached to maximum (22.87 L/kg of dry matter) in the fifth week after feeding. Later the gas production declined with the slower rate. The production rate of 166.03 and 214 L/kg of dry matter fed was achieved during ninth and thirteenth weeks, respectively. The total gas production in nine weeks was about 83% of the expected gas production. It was voted that the HDPE digester was more susceptible to the changes in the ambient condition than the CIAE design. However, charging and emptying of the HDPE digester was found easier as compared to the CIAE digester obviously because of the size of the individual digester units.

Similar studies on solid-state anaerobic digestion were also undertaken at various research centres of AICRP on RES using dry leaves, tomato processing waste, kitchen waste, Lantana camara, rice husk and straw, water hyacinth and subabool leaves and encouraging results were observed as far gas production was concerned.

7.3 Slurry handling by filtration

Eight different expanded wire mesh sizes were selected to study the filtration behaviuor of bio-gas plant spent slurry. Slurry was fed to these sieves and the water drained was collected for 24 h to ascertain the daily maximum water removal. The pH of the slurry varied between 6.5 to 7. There was no significant loss of N:P:K content keeping slurry for 2 h (ratio of NPK before was 1.4:0.6:0.6 and after 1.37:0.34:0.50). The maximum average moisture removal was found to be 14.9% with 85 mesh size. Studies were also conducted for slurry enrichment and better

handling utilizing surplus agro-residues viz. rice straw and soybean straw. Rice straw and soybean straw absorbed 15 and 8 times slurry of their initial weight, respectively. Nutrient enrichment of the biomass after composting is under investigation.

7.4 Family size solid-state anaerobic digester for agro-residues

Studies on the design and development of a 3 m^3 Solid-State Anaerobic Digester system (SAAR) for agro residue continued. A leachate circulation system, gas re-circulation system and provision of hooks to control rise of gas holder for gas pressure generation were incorporated in a 1.18 solid-state digester for testing of feasibility of designed components (Fig. 7.2). A small capacity water pump was fitted for pumping the collected leachate from the bottom of the digester into the leachate re-circulation trough. For easier emptying of the digested mass, a perforated cylindrical sieved structure was incorporated. Suitable chain pulley system supported with two side supports was also incorporated in the system for lowering and lifting of the perforated cylinder (Fig. 7.3).

Fig. 7.2 Leachate pumping system

Fig. 7.3 View of the digested mass emptying system

During evaluation, the perforated trough under the gas drum did not function properly. The stationing system of the perforated trough was modified to fit in under gas drum and found workable. Based on local availability, water hyacinth, parthenium foliage, rice straw and soybean straw were identified as suitable feed-stocks.

7.5 System and equipment for drying, enrichment and handling of bio gas plant spent slurry

A variable slope slurry filtration system was developed to study the effect of slope on slurry filtration. It was evaluated by providing 2°4', 5°3' and 7°5' slope to the filtration unit (Fig.7.4). The 2°4' slope of filtration unit was found optimum for slurry filtration as slurry moisture could be reduced by more than 10% within two hours of filtration study (Table 7.6).

Fig. 7.4 Variable slope slurry infiltration system

Table 7.6 Cumulative moisture removal from 85 mesh size sieve at different inclinations

Slope of Filtration tray	Initial moisture content of spent slurry (%)	Moisture content of slurry after 2 h filtration (%)	Moisture content of slurry after 24 h filtration (%)	Reduction in moisture content of slurry after 2 h filtration (%)	Reduction in moisture content of slurry after 24 h filtration (%)	Total solids of filtrate after 2 h filtration (%)
7°5'	92.23	84.07	83.27	8.16	8.96	3.56
5°3'	93.37	84,80	83.90	8.57	9.47	3.00
2°4'	92.66	82.57	81,42	10.09	11.24	2.78

7.6 Development of a system for de-watering and handling of spent slurry for 85 m^3 bio gas plant

A slurry filtration unit of 2 m × 1 m size was modified by incorporating scrapers for easier scraping of the semi-solid material retained over the sieve. The slurry filtration unit having the scraper and double chain drive performed better and took only 2.25 h for filtration (Table 7.7). Hence, a module of the slurry handling system comprising of two such units was developed and coupled with a functional 45 m^3 community biogas plant in a residential school premises, on Bhadabhada Road of Bhopal for field evaluation (Fig. 7.5). It was found that the developed module is useful in the separation of semi-solid and liquid material contained in the spent slurry of bigger size biogas plants (Table 7.8).

Fig. 7.5 Slurry filtration unit coupled with biogas plant in a residential school premises

The microbe-enriched filtrate can be re-used for feeding into the biogas plant to enhance biogas production, and the semi-solid residue can be used as manure. The developed system has good potential in water-scarce areas.

Table 7.7 Comparative evaluation of three filtration units

Slurry filtration unit model	Particulars of the filtration unit	Capacity, kg	Moisture content of spent slurry, % (wb)	Solid content of residue, % (wb)	Solid content of filtrate, % (wb)	Time taken in filtration, h
1	2 m × 1 m without scrapping unit	200	90- 94	20 - 21	2 - 3	3.00
2	2 m × 1 m with scrapping unit (single chain device)	200	90 - 93	20 - 25	2 - 3	2.83
3	2 m × 1 m with scrapping unit (double chain device)	200	90 - 93	20 - 25	2 - 3	2.25

Table 7.8 Specifications and test data of slurry handling unit

Particulars	Value
Capacity, kg/ batch	200
Speed of scrapper, m/min	0.95
Weight of the residue retained on upper surface, kg	115-130
Volume collected as filtrate, 1	60-65
Solid content of residue, %	20-25
Solid content of filtrate, %	2-3
Mean mass diameter of particles contained in, mm	
Slurry	3.65
Residue	4.51
Filtrate	1.86

Viscosity, centipoises	
Slurry	312
Residue	3600
Filtrate	48
Labour requirement, man-h	3 for each feed
Cost of the unit, Rs	4,000

7.7 Evaluation of modified Janta bio gas plant at field level

Five modified Janta biogas plants of 2 m^3 capacity were constructed at user's site in villages and monitored. The production of biogas in Janata biogas plant was 29% more as compared to conventional bio gas plant. The methane content in the bio-gas was 5% more from solid state bio gas plant. The study concluded that the incorporation of pile foundation in biogas plants, particularly in vertisols is useful in avoiding cracks and enhancing life of the plant. Based upon the analysis of collected data from the users, it was found that feeding rate of 25 kg/m^3 is adequate for gas production up to 1850 L/day. On an average saving of 2-2.5 kg of fuel wood / family / day could be obtained through use of bio-gas for cooking food.

For the composting study, pits of 2 × 1.5 × 1 m were constructed and lined at the bottom with polyethylene sheets to prevent seepage and moisture loss (Fig. 7.6). Rice straw and soybean straw were placed in separate pits in 10–15 cm layers, and colloidal filtrate obtained from biogas plant spent slurry was poured daily so that each layer fully absorbed the moisture. Additional layers were added in the same manner until the pits were filled, and the composted material was then left undisturbed for 60 days. There was significant increase in NPK content of the composted mass as compared to the spent slurry (Table 7.9). The physical state of the composted mass resembled with organic matter and non-sticky compost could be achieved after 60 days of composting.

The results showed that rice straw could absorb filtrate up to 11 times its initial weight, while soybean straw absorbed up to 8 times. The total solids of the filtrate–straw mixtures remained between 8–11% for rice straw and 12–14% for soybean straw. During composting, pit temperature rose after the 12th day, peaked around the 25th day, and then gradually returned to ambient levels. Soybean straw decomposed faster than rice straw, and the resulting compost was 22–27% more nutrient-rich, with a significantly reduced C:N ratio. Further investigations are ongoing.

Fig. 7.6 Pouring of slurry into composting pit

Table 7.9 Characteristics of biogas plant spent slurry and selected absorbents

Characteristics	Substrates			
	BSS	**F_{BSS}**	**Ab_{RS}**	**Ab_{ss}**
Density (kg/m^3)	1046	1013	144	156
Moisture content (%)	92 - 93	96 - 98	6 - 8	10 -11
Total solids (%)	7 - 8	2 - 4	92 - 94	89 - 90
Volatile solids (%)	74.1	79.3	72.6	76.8
pH	6.8 - 7.3	6.8 - 7.4	7.6 - 7.8	7.2 - 7.5
C (%)	23.7	12.8	37.3	59.6
N (%)	1.4	1.44	0.58	1.88
P (%)	0.36	0.38	0.09	0.16
K (%)	0.6	0.64	1.14	1.23
CNR	17	9	64	32

BSS : Biogas plant spent slurry
F_{oss} : Filtrate of biogas plant slurry
Ab_{RS} : Absorbent - rice straw
Ab_{ss}: Absorbent - soybean straw

7.8 Adoption and performance evaluation of available gas engine-genset with biogas for power generation for rural applications

A 3.7 kW Kirloskar diesel engine (Model AV1), originally designed with an 80 mm bore, 110 mm stroke, and 1500 rpm rated speed, was modified to operate on 100% biogas using a suitable conversion kit (Fig. 7.7). The compression ratio was reduced from 20:1 to 12:1, and the engine was coupled with a 3.5 kVA alternator for power generation. Performance evaluation was carried out by applying loads through 1000 W heaters. Short-term tests showed stable operation on pure biogas. At a 2 kVA load, the engine speed remained between 1511–1525 rpm, with an output voltage of 230–233 V, current of 8.51–8.71 A, and biogas consumption of 0.90–1.08 m^3/kWh. Overall test results (Table 7.10) indicated reliable voltage, frequency, and power output across no-load, 1 kW and 2 kW conditions, with no operational issues encountered during evaluation. No operational problem was

faced during the short-term feasibility and performance evaluation of the engine-genset system.

Table 7.10 Performance results of modified engine - genset system.

S. No.	Observed engine speed, rpm	Applied load, kW	Observed load, kW	Observed voltage, V	Observed current, A	Observed frequency, Hz	Gas consumption, m^3/kWh
1	1500-1525	No Load	0.001	218-226	0.10	50.9	1.34-1.56
2	1525-1547	1.0	0.99-1.01	225-234	4.25-4.38	50.9-51.3	1.80-1.90
3	1511-1525	2.0	1.99-2.02	230-233	8.51-8.71	50.3-50.9	0.90-1.08

Fig. 7.7 View of modified engine genset system.

7.9 RCC modular biogas plant at ITC-CIAE guest house

A biogas plant composed of a concrete digester and a glass fibre reinforced gasholder has been constructed under vertisol condition at CIAE Guest House with a view to utilize kitchen and dining table waste (Fig. 7.8). The digester has a capacity of 10 m^3 while the gasholder is 1.6 m in diameter with 1.2 m^3 capacity.

Fig. 7.8 A view of biogas plant

The plant was initially commissioned with cow dung and water in 1:1 ratio along with inoculum. Later on, kitchen and dining table wastes have been added to maintain total solid content up to 16% along with cow dung. The biogas is being utilized in the Guest House kitchen.

7.10 25 m^3 biogas plant at village Bamulia in Raisen district of Madhya Pradesh in PPP mode

One fixed dome biogas plant (25 m^3) has been constructed and commissioned under vertisol condition at village Bamulia in the nearby district Raisen under Public Private Partnership (PPP) mode. The beneficiary contributed land for installation and 1.15 lakh, whereas CIAE shared0.7 lakh of expenditure. This was to assist the self help group to enhance the utility of biogas (besides cooking) by generating electricity (Fig. 7.9) for running a briquetting machine of 60-65 kg/day capacity.

Fig. 7.9 Dual Fuel (Biogas + Diesel) Engine based electricity generation for running briquetting machine and lighting

7.11 Biogas purification and storage for engine application

A water scrubber for removal of CO_2 and H_2S present in the biogas was developed (Fig. 7.10). It consisted of four absorbing columns connected in series (2.0 m height and 0.10 m diameter). The absorbing columns arc filled with ranching rings up to 500 mm height. A provision for spraying water at the top of scrubber with help of positive displacement pump was also made. The gas passing through the column comes in contact with water droplets, resulting in absorbtion of CO_2 in the water. The travelling length of the biogas (through the columns) has been provided up to 8 m. The scrubber has been installed near a biogas plant (6 m^3/day capacity) for its evaluation.

Fig. 7.10 Water scrubber for biogas

7.12 Self-sustainable energy management for medium size dairy farm through biogas generation from dairy waste

A dairy farm having 50 animals was planned to make it energy self-reliant by producing power from biogas. Presently, the dairy consumed 3.46 kWh of electricity and 95 man-hour/day to complete unit operations like; water pumping, chaff cutting, lighting, feed preparation, dung management, milking. A fixed dome type biogas plant of 25 m^3/day capacity was constructed at the dairy site in village Jamunia (Sehore district) for power generation to meet the energy requirement of dairy (Fig. 7.11). The biogas produced from the plant is enough to generate 12-14 kWh electricity per day to meet the present power requirement of the dairy farm and provide the surplus energy for other economic activities.

Fig. 7.11 A view of 25 m^3/day capacity fixed dome type biogas plant installed at dairy site in village Jamunia, Sehore district

7.13 Biogas Purification and Storage System for Engine Applications

A biogas purification and storage system was developed and evaluated for use in engine applications (Fig.7.12 & Fig. 7.13). The purification unit consisted of a water scrubber equipped with four absorbing columns connected in series, each 2.0 m in height and 0.10 m in diameter, packed with Raschig rings up to 500 mm height. Water was sprayed at the top using a positive-displacement pump to enhance

absorption of CO_2 and H_2S as the biogas passed through an effective 8 m contact path. The system was installed near a 6 m^3/day biogas plant for field evaluation.

A portable version of the scrubber, consisting of scrubbing towers, water storage tanks, a piston pump, and a compressor, was also developed (Fig. 7.13). This system enriched methane concentration up to 85% under optimum operating conditions of 9 bar pressure, 40°C water temperature, 0.3 m^3/h water flow rate, and 0.8 m^3/h gas flow rate. The energy consumption for scrubbing 6 m^3 of biogas was 7.61 kWh, resulting in a net energy gain of 32 kWh for producing 4.8 m^3 methane-enriched biogas (85%) from biogas containing 65% methane.

For storage, the purified gas was first passed through a moisture adsorption chamber filled with 3A molecular sieves to remove residual moisture. The dried biogas was then compressed into a CNG cylinder. In the fixed system, the biogas was compressed to 9 bar, allowing approximately 1 kg of biogas to be filled within 20 minutes. In the portable system, methane-enriched biogas could be stored at 5 bar, accommodating 0.5 kg in a CNG cylinder. The stored gas remained compositionally stable over two months under ambient conditions, with methane concentration consistently maintained at around 80–85%.

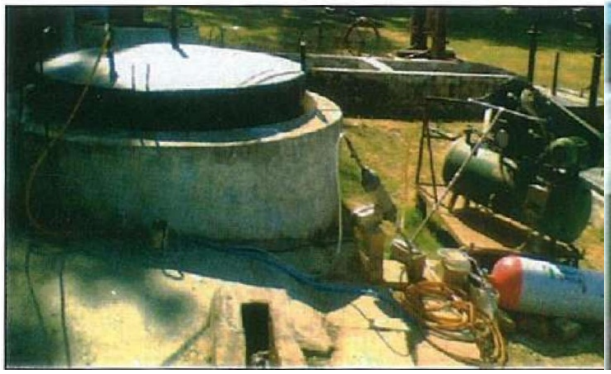

Fig. 7.12 Biogas compression and storage system

Fig. 7.13 Biogas scrubbing and storage system

7.14 Bioreactor for accelerated composting

A rotating drum type bio-reactor of 1.25 m diameter and 1.5 m length has been developed for accelerated composting of agro-residues (Fig. 7.14). The reactor is provided with water jacket and heaters (four numbers strip heating element) of capacity 1 kW each outside of the water jacket. Further, 50 mm thick glass wool insulation is also provided in the reactor to maintain required temperature inside the reactor. The temperature of substrates inside the reactor is controlled by providing a temperature indicator cum controller. The reactor is mounted on a three wheeled structure for easy transport. The arrangement is also made to rotate and moisturize the substrate manually to maintain proper moisture, aeration and better environment for growth of microorganisms. The accelerated composting of soybean straw mixed with biogas slurry of 1percent is tried in the reactor. The micro-

organisms are found to be most active during 6-9 days of composting. There is decomposition of cellulose, hemicellulose and lignin of soybean straw along with significant mineralization of the soybean straw under thermophilic phase. The water extractable carbon is found to be reduced from 23.25 to 3 per cent, and C/N ratio was reduced from 53.54 per cent to 32.23 per cent.

Fig. 7.14 Bio reactor for accelerated composting

7.15 Scrubbing of biogas for removal of impurities

A water scrubber (Fig. 7.15) was developed to remove impurities present in the biogas such as CO_2 and HS. The water scrubber consists of a scrubbing tower (H×D, m: 1.25×0.50), water/chemical solution collecting tank (H×D, m: 0.60×0.79), spraying nozzle and piston pump (2.2 kW and 720 L/h capacity). An aqueous solution of NaOH at different molarities (0.1 to 0.5 M) was sprayed into the scrubbing tower. Biogas was supplied into the scrubber from the bottom using a compressor. For every cubic meter of biogas 14 of chemical solution was used. The chemical scrubbing was found more effective in increasing methane content of biogas from 64.3% to 92.3% (with 0.5 M NaOH solution) as compared to water scrubbing (85%). Total time required to scrub the 3 m^3 biogas was 18 min.

Fig. 7.15 Biogas purification system

7.16 Biogas production from urea pretreated paddy strawbales

A whole value-chain approach was adopted to utilize paddy straw for biogas production while simultaneously addressing mechanization challenges in collecting straw at the plant site. The biogas generation process followed a co-digestion method, using a 75:25 mixture of urea-treated baled paddy straw and cow dung at 10% total solids, fed into a 1.1 m^3 batch-type bio methanation digester. Biogas production was recorded for 150 days, during which a cumulative yield of 22,450 litres was achieved. The biogas potential of baled paddy straw was estimated to be about 250 L/kg. The digestion process operated within a temperature range of 21–42 °C. The methane content in the produced biogas ranged from 50 to 56%, along with CO_2 and trace gases. Additionally, each batch yielded 60–70 kg of nutrient-rich biofertilizer. Overall, the study demonstrates that anaerobic digestion is an efficient and sustainable technology for converting paddy straw into clean energy and organic fertilizer, offering a viable solution for managing crop residues and enhancing energy recovery.

7.16 Paddy straw hydrolysate cum slurry centrate production unit for microalgae production

Nutrient media is a crucial part in microalgae production, therefore a unit for paddy straw hydrolysate cum slurry centrate production of 1.5 m^3 capacity is developed by ICAR-CIAE, Bhopal. Centrate is the homogeneous liquid extract of slurry produced by washing, filtration and sedimentation. This unit has been designed to have two concentric rectangular containers. Paddy straw will be placed in inner perforated container for 12 to 16 hours. Upper lid has uniform water distribution facility from where water is sprayed on paddy straw. The unit has two outlets and is placed at the designated height so that the hydrolysate or centrate directly can be empty in to race way pond for microalgae production (Fig. 7.16).

Fig. 7.16 Raceway pond

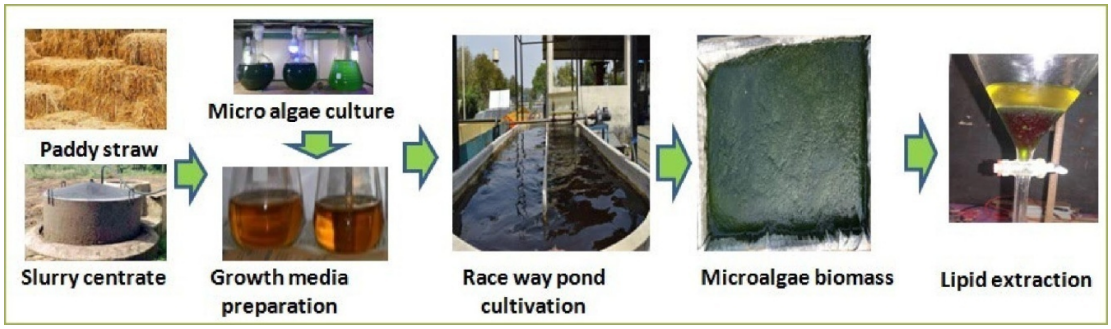

Fig. 7.17 Process to produce paddy straw hydrolysate based microalgae

Upper outlet is for slurry centrate so that the sediment will not be disturbed and fine centrate will be available. The growth media produced utilizing Paddy straw hydrolysate mixed with biogas slurry centrate at 50:50 ratio and Paddy straw – cow dung co-digested slurry centrate diluted with water at 1:7 ratio, could generate microalgae of 1.2 g/L and 1.4 g/L, respectively in the ponds that are 20 and 40% than commercial fertilized based media. Lipid extracted from the produced microalgae biomass is in the range of 17 to 21% (Fig. 7.17).

7.17 Modification of Diesel Engine Tractor for CNG

A comprehensive effort was undertaken to convert a standard three-cylinder diesel tractor engine into a 100% Compressed Natural Gas (CNG), operated spark ignition (SI) engine (Fig. 7.18). The retrofit involved redesigning and modifying key engine components to accommodate CNG combustion characteristics. A mounting frame was fabricated and installed at the front of the tractor to hold a 60-L water-capacity CNG cylinder, and the complete CNG kit was integrated with the system. To suit CNG operation, the original diesel engine's compression ratio was reduced from 17:1 to 10.33:1 by placing a 5.2 mm thick spacer below the engine head. The conventional fuel injection pump was removed and replaced with a spark distributor, aligned precisely with the engine's timing gear mechanism using a modified flange. Spark plugs were installed in all three cylinder heads to enable ignition. A new inlet air manifold was fabricated, and a carburettor was fitted to ensure proper regulation and mixing of the air–CNG charge. Suitable connections were provided between the carburettor and the air cleaner to maintain stable and clean airflow. With these modifications, the tractor engine operated successfully on 100% CNG. Field trials showed that the engine consumed 3.07 kg/h of CNG under no-load operating conditions, while during rotavator operation (1676 mm width), the CNG consumption was 4.2 kg/h, demonstrating the feasibility and operational reliability of the CNG-converted tractor engine.

Fig. 7.18 CNG based system retrofit in the tractor engine

7.18 Development of process protocol for the production of hydrogen with porous C-induced dark fermentation using paddy straw

Bio-hydrogen generation though biochemical conversion pathway was initiated using paddy straw. Paddy straw as lignocellulosic biomass is an attractive resource as it is renewable, cheap and available in large quantities. It has high carbohydrate content that can be converted into bio-hydrogen through dark fermentation process. The paddy straw was treated with 0.5% and 1 % Sulfuric acid and hydrolysate obtained was used for experiment (Fig. 7.19). The solid fraction was washed and dried at 65°C. Biochar was produced from solid fraction at a temperature of 400, 500 and 600°C for 1h. The biochar sample was analyzed for surface area and proximate analysis. Experiments were conducted using hydrolysate with addition of biochar at a rate of 10 g per liter. The surface area of material was analyzed using BET surface area. It was observed that with the increasing pyrolysis temperature the surface area of biochar was increased. It was 18.49, 29.62 and 204.77 m^2 per g at a pyrolysis temperature of 400, 500 and 600°C respectively for 0.5 % treated sample. Similarly for 1 % acid treated sample it was 36.33, 66.67 and 234.27 m^2 per g at a pyrolysis temperature of 400, 500 and 600°C respectively. Maximum recovery of hydrogen gas was 2.47 L per kg of paddy straw obtained at a process condition of 1% treated material and biochar prepared at 600°C. It suggested that more surface area of biochar is favourable for microbial community growth to enhance the hydrogen production.

Fig. 7.19Process for the production of hydrogen

7.19 Process optimization for maximizing the fermentable sugar yields from paddy straw and corn cobs

This study focuses on maximizing the fermentable sugar yields from paddy straw and corn cobs through an integrated acid and enzymatic pretreatment process. Two-step pretreatment process: dilute sulfuric acid pretreatment followed by enzymatic hydrolysis was experimented. A response surface methodology (RSM) with a Box-Behnken design was employed to optimize key process parameters such as acid concentration, temperature, and residence time for the pretreatment.

For paddy straw, the optimal conditions were found to be 1% H2SO4, 80°C, and 20 minutes, which resulted in effective cellulose enrichment (95.4%) and lignin reduction (38.2%), promoting efficient enzymatic hydrolysis. Using cellulase from Trichodermareesei, enzymatic hydrolysis yielded high glucose concentrations of 225.2 mg glucose/ml per gram of paddy straw. Surface modifications of pretreated paddy straw were validated using Brunauer-Emmett-Teller (BET) analysis and morphological studies, revealing a 58.6% decrease in surface area, a 25% decrease in pore volume, and an 87.9% increase in mean pore diameter under optimized conditions (Fig. 7.20). These changes indicate improved accessibility of cellulose for hydrolysis and suggest a more efficient conversion of paddy straw into biofuel.

Similarly, for corn cob, the optimal pretreatment conditions involved a 0.5% sulfuric acid concentration, 120°C reaction temperature, and 40-minute duration. Under these conditions, the cellulose content of the pretreated corn cob increased to 66.10%, while the hemicellulose content decreased significantly. Enzymatic hydrolysis of the pretreated corn cob resulted in a maximum saccharification yield of 41.1%, corresponding to a glucose yield of 185 mg/g of corn cob (Fig. 7.21). The

fermentation experiments using Acetone-Butanol-Ethanol (ABE) are currently under progress to assess the potential for converting the fermentable sugars obtained from the pretreated biomass into biofuels.

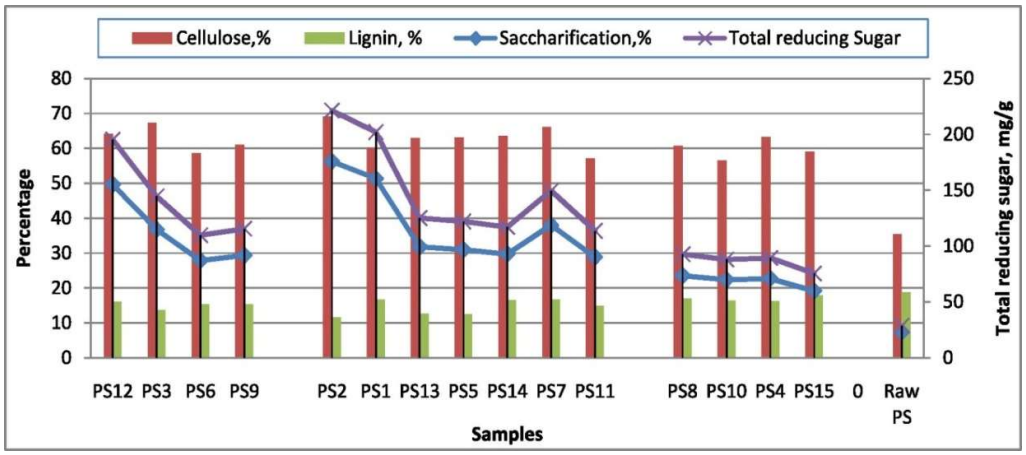

Fig. 7.20 Effects of acid pretreatment, time and temperature on total reducing sugar yield and saccharification efficiency of paddy straw.

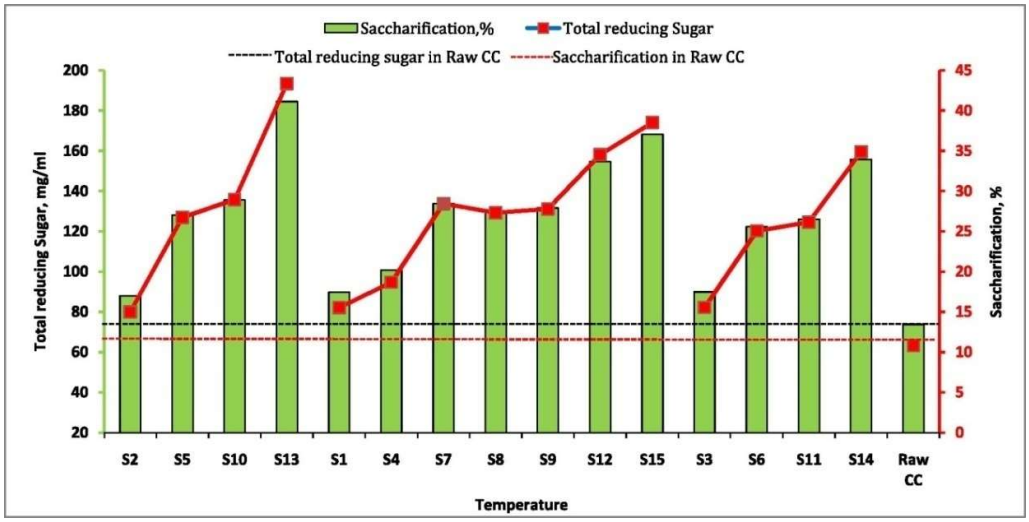

Fig. 7.21 Effects of acid pretreatment, time and temperature on total reducing sugar yield and saccharification efficiency of corn cob.

7.20 Extraction of cellulose from corncob residues

Process technology for extraction of cellulose from corncob residues valorization of corncob residues was done through synthesis of high crystalline cellulose using chemical treatments, which involved alkaline pretreatment and bleaching (Fig. 7.22). The cellulose content was notably increased in the extracted cellulose (88.13%) as compared to corncob biomass (42.30%). The morphological, chemical, and thermal properties of the resulting cellulose were thoroughly examined through various analytical techniques. The fiber diameter of extracted cellulose was reduced compared to corncob biomass. The chemical structure of the cellulose was analysed using the FTIR, confirming the effectiveness of the

treatments. The XRD pattern of extracted cellulose exhibits sharp peaks at 2θ of 16°, 22°, 34° and 45°, respectively. The appearance of sharp peaks attributes the typical crystalline nature of the cellulose. The XRD results showed that crystallinity index of corncob, which was 29.63%, increased to 53.95% in extracted cellulose. Furthermore, thermogravimetric analysis demonstrated that the lower degradation temperature of extracted cellulose would be beneficial for degradation of bio based materials.

Fig. 7.22 Process technology for extraction of cellulose from corncob

CHAPTER - 8

8. Thermo Chemical Conversion of Biomass

Biomass gasification involves converting carbonaceous biomass solids into a combustible gas by partially controlling oxygen or air supply to the fuel bed. The resulting producer gas mainly contains carbon monoxide, hydrogen, and traces of methane, along with non-combustible gases like nitrogen and carbon dioxide. About 10–30% of the fuel's energy is lost during conversion. Biomass sources include charcoal, wood, peat, and agricultural residues such as rice husk, groundnut shells, corn cobs, and bagasse. Air gasification produces a low-energy gas (1000–1300 kcal/N cum) suitable for direct combustion or I.C. engines, while oxygen gasification yields a higher-energy gas (3500–6500 kcal/N cum) used in industries and for synthesizing fuels like methanol, ammonia, and gasoline.

8.1 Technology for Charring of Biomass

Char is produced through pyrolysis of biomass. In general, pyrolysis is defined as destructive distillation of biomass heated to more than 200°C in absence of air/oxygen but in practice, a restricted quantity of air is allowed for partial combustion to achieve the temperature required for pyrolysis. During the process of pyrolysis, the fibre content of the biomass is broken which facilitates briquetting of the char produced.

The process of producing char may be classified in two categories depending upon the method of supply of heat to the feed stock. In the traditional method of charring some of the biomass is burnt to generate the heat required for maintaining the process of pyrolysis. In this method all product of pyrolysis except char are lost to the atmosphere. In the improved methods, the reactor is externally heated in a control way for carrying out the pyrolysis of biomass. The pyrolysis gases produced during the process are normally used as fuel for heating the reactor.

The maximum heating valve of biomass is given within 5% by (Dulon's Formula).

$$Q_M = 338.83C + 1442\left[H - \left(\frac{O}{8}\right)\right] \qquad \ldots (8.1)$$

Where, Q_M is the higher heating value of biomass or fuel in J/g. C, H and O are weight percentages (on a dry and ash free basis) of carbon, hydrogen and oxygen respectively.

8.2 Charring Equipment

Three types of kilns are commonly used for charcoal production earthen, brick, and metallic. The traditional earthen mounds and pits were inefficient and produced poor-quality char due to uncontrolled air supply. Brick kilns, when properly constructed and operated, yield high-quality charcoal. Their size varies with application: large kilns for commercial use and small ones for domestic or

community needs. Metallic kilns, both portable and stationary, have been developed at several institutions. Portable units suit domestic use, while stationary ones cater to community and commercial operations.

The Tropical Products Institute (TPI), UK, developed a metallic kiln with two interlocking cylinders and a conical cover supported on eight radial air channels (Fig. 8.1). Four smoke stacks were fitted during charring, and four steam release ports were provided on the cover. Recommended wood log size was ≤60 cm long and ≤20 cm in diameter. The kiln had a loading time of 2 h, charring time of 19 h, and unloading time of 2 h, with 19–22% efficiency depending on wood moisture content.

Fig. 8.1 TPI Metallic Kiln

PAU, Ludhiana (AICRP on RES) developed a similar kiln using a bitumen drum, achieving 60% conversion efficiency with sunflower stalks. JNKVV, Jabalpur designed a portable pyrolyser from a bitumen drum with 20 mm holes and a funnel-shaped chimney (Fig. 8.3). Using 10 kg of leafy biomass, it produced ~70% charcoal yield.

At IIT Delhi, biomass pyrolysis systems were designed for domestic, community, and commercial use (Fig. 8.2). The domestic unit (200 L oil drum) processed 25–30 kg biomass per batch in 2–3 h, producing 'Paru fuel' briquettes (Baveja& Grover, 1985). Larger systems (up to 6 tonnes/batch) were developed for community and industrial applications, capable of producing 4 tonnes of Paru fuel/day with 25 kW power, covering 1000 m^2 area and operated by 15 workers. Feedstocks included rice husk, straw, sawdust, pine needles, groundnut shells, Lantana camara, and forest residues.

At CIAE, Bhopal, both stationary brick kilns and portable metallic kilns were developed and tested. The char yield ranged from 25–60%, depending on biomass

type and operating variables. Studies using rice husk, sawdust, maize, and sorghum stalks showed higher char yield at lower heating rates and moderate temperatures. Optimal conditions were 150°C for 6 h (rice husk) and 200–250°C for 2–2.5 h (maize/sorghum stalks). Lower yields from maize/sorghum were due to low lignin content (Table 8.1).

Table 8.1 Result of studies for Charring of biomass in different kilns

Biomass kiln	Qty of biomass charged (Kg)	Duration of charring (h)	Temp. of charring (°C)	Yield of charcoal (kg)	Charcoal analysis		
					Volatile matter, (%)	Ash, (%)	Fixed carbon, (%)
		4	150	8.0	50	20	30
Rice husk,		6	150	5.0	20	20	60
stationary	10	8	150	3.0	50	30	20
brick kiln		10	100	5.0	40	20	40
		12	100	2.5	30	20	50
		1.5	200	15.0	40	10	50
Maize and		2.0	250	10.0	49	17	34
sorghum		2.5	200	6.5	11.6	20	68.4
stalk,	25	3.0	250	11.0	20	30	50
Stationary		3.5	250	8.0	35	35	30
brick kiln		4.0	250	5.0	36	30	34
		4.0	200	10.0	17	34	49
		1.5	250	14.0	30	20	50
Maize &		2.0	250	8.75	20	15	65
sorghum		2.5	160	3.50	56	20	24
stalk,	35	3.0	150	15.0	60	15	25
Portable		3.5	150	3.5	40	50	10
metallic in		2.5	200	10.0	34	17	49
		3.0	250	3.0	25	40	35

Source: Srivastava&Mahewari (1986)

A CIAE survey of commercial units (8 out of 15 firms) reported annual capacities of 250–300 tonnes, but faced issues like unstable pyrolyser output, frequent breakdowns, high drying fuel needs, and short briquette burning duration compared to coal, indicating a need for further R&D.

Fig. 8.2 View of IIT, Delhi Charring Kiln

Comparative evaluation of IIT Delhi (Fig. 8.2), JNKVV Jabalpur (Fig. 8.3), and Tongon kilns (Fig. 8.4) at CIAE Bhopal with soybean waste, pigeon-pea, cotton, and sunflower stalks revealed that the Tongon kiln performed best but had low capacity for economic adoption.

Fig. 8.3 View of JNKVV, Jabalpur Charring Kiln

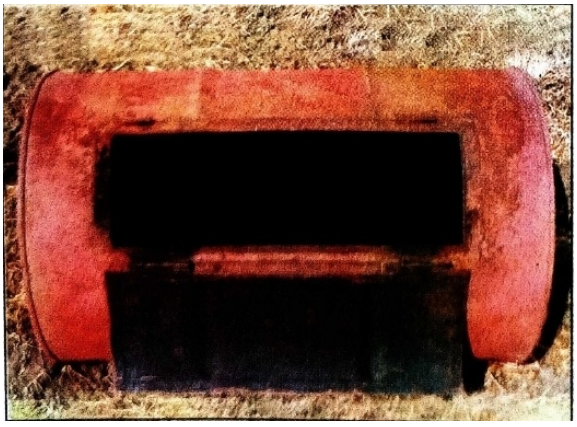

Fig. 8.4 Tongon Charring Kiln

To address this, CIAE Bhopal developed an improved kiln (Fig. 8.5) with three times higher capacity. It consists of a metallic cylinder (800 mm × 1100 mm) with a rectangular lid (550×450 mm) for feeding. 100 kg batches are charred in 2-4 h, yielding 35–40% char with 18–20 MJ/kg calorific value (higher than fuelwood's 15–16 MJ/kg). The char can be easily briquetted for domestic use. Extensive testing with soybean, pigeon-pea, and cotton residues showed 36–40% yield and calorific values of 15.0–17.5 MJ/kg. Long-term operation produced about 80 kg char/day in two batches, demonstrating reliable performance over a year.

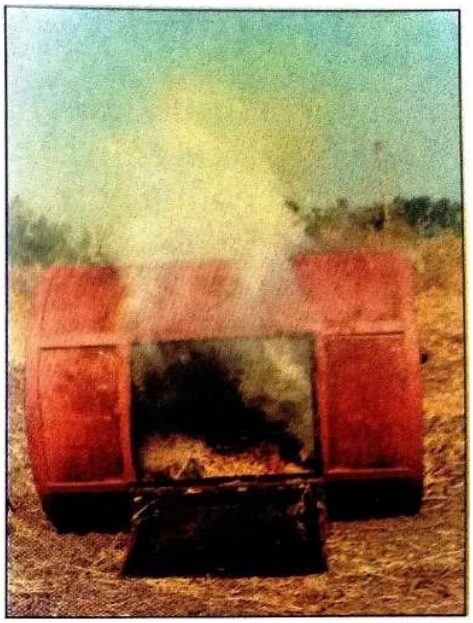

Fig. 8.5 View of High Capacity CIAE Charring Kiln

8.3 R&D Activity in Biomass Gasification and its Commercialization in the Country

- M/s Jyoti Ltd., Baroda began commercial manufacture of gasifiers (5–100 kW) for mechanical and electrical uses. Most systems are downdraft types, ideal for woody biomass and rice husk.
- Commercial systems include power generation units (3–500 kW) and thermal application units, with wood consumption of 1–1.4 kg/kWh and diesel replacement of 65–75%.
- IISc Bangalore developed downdraft gasifiers (5–100 hp) for water pumping and power generation, using a single angled air nozzle. The system achieved 75–85% diesel replacement with 1.4 kg/kWh wood use.
- SPRERI, VV Nagar designed open-core, throatless downdraft gasifiers for rice husk and groundnut shells. A 3.5 kW system saved up to 80% diesel, with 49% conversion efficiency and 16% engine thermal efficiency. The 20 kW version achieved 55–60% diesel replacement using ~30 kg/h rice husk for a 16 kW output.

8.4 Contribution of CIAE

The research work carried at CIAE and their output in the field of Thermochemical Conversion Technology is described below;

8.4.1 Characterization of available surplus agricultural residues

The study was carried out to identify the surplus biomass suitable for producer gas generation the physical properties, volatile matter, fixed carbon and ash content of some of the agricultural residues were determined (Table 8.2).

Volatile matter, fixed carbon and ash content of 33 agro-residues varied between 64.9 to 83.1%, 11.3 to 25.4% and 1.1 to 19.2% respectively. The information on line cellulosic component and ultimate analysis i.e. carbon, hydrogen, oxygen, nitrogen, sodium, potassium, phosphorus, calcium, magnesium, silica and ash properties of various agricultural residues were compiled. Carbon hydrogen and oxygen varied between 36.8 to 53.3, 4.2 to 61 and 39.5 to 51% respectively.

Table 8.2 Physical and thermal characteristics of biomass

Biomass	Density (kg/m^3)	EMC at 80% Rh (%)	Heating value (MJ/kg)		Proximate Analysis		% Ash
			Lower	Higher	Fixed carbon	Volatile matter	
Acacinenutriculiformis	700	29.50	19.56	17.94	16.05	81.77	2.18
Acacinnilotica	820	24.80	19.21	17.79	16.84	80.86	2.30
Albizialebbek	630	-	19.09	17.48	13.64	84.40	1.90
Albiziaprocera	550	-	18.87	17.39	15.20	83.40	1.38
Amaltas	-	-	16.00	-	11.48	86.52	1.15
Arhar Stalks	180	20.58	18.58	17.60	15.12	82.90	1.98
Azadirachtaindica	700	30.70	18.20	16.72	15.90	80.76	3.30
Bagasse	70	34.86	20.00	18.30	15.86	79.20	4.94
Bamboo	-	-	17.50	-	21.17	76.50	2.43
Castor stalks	-	-	16.50	-	18.36	77.87	3.77
Casurinaequisatifolia	-	-	18.50	-	19.17	77.20	3.63
Coconut husk	-	-	15.60	-	14.31	78.74	6.95
Cotton sticks	160	27.05	17.40	16.00	15.30	81.40	3.30
Cow dung	-	-	13.20	-	14.48	57.22	28.30
Maliazadarachu	-	-	17.80	-	17.70	79.80	2.45
Dalberginsissoo	710	24.60	18.70	16.95	15.70	80.40	3.90
Derris indica	590	30.30	18.20	16.52	15.50	81.60	2.92
Eucalyptus hybrid	770	30.40	19.40	17.96	16.60	82.40	0.98
Groundnut shell	100	-	20.01	18.60	11.67	83.90	4.43
Leucenaleucocephala	730	30.40	19.40	17.85	16.60	84.40	1.00
Maize cobs	100	28.00	17.40	15.30	15.16	83.01	1.84
Maize stalks	50	38.08	16.70	16.10	17.10	79.60	3.40
Mulberry (Morus alba)	-	-	17.30	-	17.40	79.50	3.10
Pine needles	-	-	16.00	-	15.80	80.55	3.65
Pithecellobiumdulce	670	28.14	19.40	17.78	16.42	81.50	2.04
Prosopisjuliflora	780	24.20	18.70	17.11	20.96	75.90	3.15
Rice husk	105	29.40	15.50	14.10	12.50	71.00	16.05
Rice straw	30	36.70	15.00	13.50	11.10	69.70	19.02
Sesbaniaacculiata	-	31.03	17.51	16.10	14.32	82.70	2.98
Sesbaniagrandiflora	340	25.89	17.91	16.30	11.70	82.30	6.00
Sorghum stalks	-	-	17.00	-	11.20	85.00	4.80
Sunflower stalks	-	-	15.05	-	8.80	75.40	8.90
Terminaliaarjuna	660	28.40	17.40	15.90	14.40	78.60	7.02
Wheat straw	60	34.00	17.20	15.70	17.93	73.60	8.47

Note: Density, values are for true and bulk densities for the crop residues and firewoop species, respectively.

8.4.2 Energy requirement in biomass preparation for Gasification

The study was conducted to measure the capacity of the machine to cutwood logs in to 25 mm long pieces. The wood cutting machine was equipped with 300 mm diameter circular saw driven by 1.5 kW electric motor. The wood logs were divided into three groups 18 to 25 mm, 25 to 35 mm and 35 to 55 mm. Four members of operators were selected for the study. Energy consumption/power requirement were measured using energy meter. The output of wood pieces varied from 20.2

kg/h to 28.4 kg/h. The average energy consumption to cut 100 kg wood pieces varied from 1.8 kWh to 2.2 kWh.

8.4.3 Development of Natural Draft Gasifier

A natural draft gasifier was developed by analysing the chimney effect of hot gases generated in the gasification process (Fig. 8.6). The developed gasifier had 470 mm dia& 1000 mm height. Two gates were provided one at the top (275 mm dia) for feeding the biomass and another at the bottom (165 mm dia) for removal of ash. The air was sucked through 50 mm dia pipe provided below the grate. The gas outlet was provided 310 mm above the grate at 30° to vertical axis of gasifier. The gasifier was operated with wood chips and Soybean straw. The flame temperature was varied between 827-928°C with wood chips and 791-859°C with soybean straw. The biomass consumption varied from 3.2 to 1.5 kg/h. The temperature at combustion zone was found varying between 1149-1278°C and 1087- 1219°C with wood chps and soybean straw, respectively.

Fig. 8.6 CIAE Natural Draft Gasifier

8.4.4 Development of Portable Gasifier for Thermal Application

A portable updraft gasifier system was developed for thermal application along with two types of burners matching to gasifier (Fig. 8.7). The specifications of gasifier are given in the Table 8.3.

Fig. 8.7 CIAE Portable Updraft Gasifier

Table 8.3 Portable Gasifier for Thermal Application

Particulars	Specifications / Description
Construction Material	Mild steel sheets, bars & flats, angle iron, and GI pipes
Size of Grate (mm)	250
Diameter of Air Inlet Pipe (mm)	25
Gas Outlet	Located 760 mm above the grate with 35 mm dia GI pipe
Fire Port	50 mm dia, positioned 50 mm above the grate
Ash Chamber (mm)	350 × 350 × 40
Overall Dimensions (mm)	350 × 350 × 850
Biomass Feeding Port	200 mm dia with lid fixed by nut and bolt
Burner (Single Port)	120 holes of 5 mm dia arranged in six circles; gas inlet through 25 mm dia pipe tangentially
Burner (Three Port)	90 holes of 5 mm dia arranged in six circles; burner dia 200 mm; gas supplied through 25 mm dia pipe

The gasifier was extensively evaluated on different bio fuels such as, wood chips, soybean straw, pigeon pea stalk, maize cobs, and groundnut shell. The calorific value of the producer gas varied from 948 kcal/m^3 to 1276 kcal/m3. The gasification efficiency varied from 66- 77% **(Fig. 8.8)**. The accumulation of tar on surface of the burner and its chocking was observed when the system was operated for about 3 to 4 h of operation. The flame temperature of the producer gas generated from different bio fuels varied from 785 to 1046°C. The temperature of reduction zone was from 1143 to 1294°C.

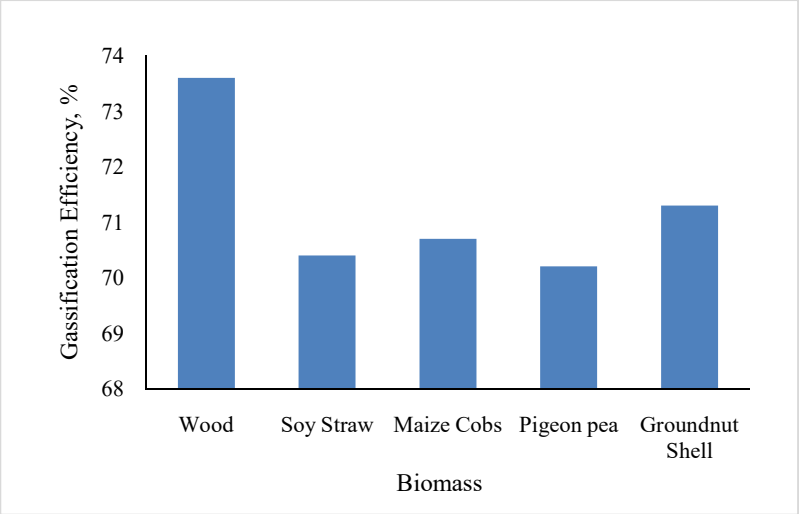

Fig. 8.8 Efficiency of Portable Gasifier with Different Biomass

8.4.5 Development of a Gasifier for Agricultural Waste

A down draft gas producer of 1 m diameter and 2 m height was erected in the Energy Enclave, CIAE with a water seal at the bottom. Uniform and rapid ash removal is achieved with the help of a combined vertical and horizontal rotating grate. The fuel is fed from the top whereas the air is admitted through an opening at the side of the producer-gas plant to ensure proper combustion and subsequent gasification. The batch capacity of the unit is 200 kg of agriculture waste.

8.5 Improved Cookstove (Sigri)

More than half of the world's nearly six billion people rely on traditional biomass fuels such as wood, crop residues, charcoal, and animal dung, for cooking and heating. In rural India, especially among women, the collection and use of these fuels form an essential part of daily life. Since these fuels are part of the natural carbon cycle, their use does not add net carbon dioxide to the atmosphere, making them environmentally friendly.

A newly designed charcoal stove improves efficiency through the proper selection of perforated mild steel (MS) sheets, which regulate air flow and direct hot gases toward the cooking pot for faster heating. The stove consists of two concentric MS grates supported on a 6 mm MS rod grill, with an overall size of 230 mm diameter and 160 mm height. It holds 450–500 g of charcoal or briquettes, sufficient for about one hour of cooking, and can be ignited easily from below using kerosene-soaked rags, becoming ready for use in 10 minutes. To reduce heat loss by radiation and convection, the burning chamber is enclosed by two concentric aluminium reflectors separated by an asbestos insulation layer (3–5 mm thick), riveted securely (Fig. 8.9).

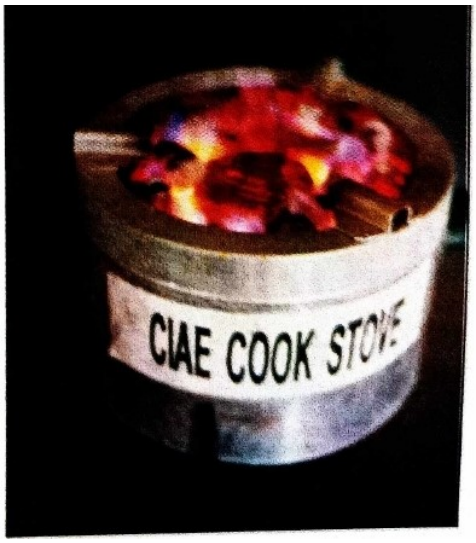

Fig. 8.9 CIAE Cook Stove

It has been found that the stove performs well with charcoal as well as briquettes made of charred agricultural crop residues. The stove has been found to give steady heat output and the tests conducted on are shown in the Table 8.4.

Table 8.4 Test results of CIAE Improved Charcoal Cookstove

Brief Description	Fuel Used	Rate of fuel used (gm/min)	Evaporation rate (gm/min)	Average Efficiency % (PHU)	Remarks
Annular Grate with A1 reflector and asbestos insulation	Briquette	14.50	6.89	24.88	High rate of burning
	Charcoal	11.81	6.87	23.89	
Annular Grate with SS reflector and asbestos insulation	Briquette	7.92	5.35	24.90	Low rate of burning
	Charcoal	4.94	4.85	24.32	

The stove has given consistently high percentage heat utilisation (PHU) of 25%.

8.6 Agro industrial application of gasifier

The performance of modified CIAE portable updraft gasifier (25 kW capacity), installed at a menthol oil extraction plant situated at village Khajuri in Bhopal district during 1999, was monitored. The gasifier was used in batch mode during the period of crops availability for oil extraction. The economical and energy audit analysis of the plant was carried out based on the monitored data. The energy expenditure per hour for gasifier system was 433 MJ/h as compared to 615 MJ/h in case of the conventional system using firewood (Table 8.5). The energy saving was 29.6% over the conventional system. The batch process time increased by 8.9% due to more time required in the initiation of steam generation in the plant. The cost of

operation of the plant was estimated to be 4.3% lower than the conventional system. The study revealed that the gasifier system fitted with the plant was energy efficient and cost competitive.

Table 8.5 Hourly energy expenditure in the oil extraction plant

Item	Gasifier system	Conventional system	Saving in gasifier system
Fuel wood, MJ	427.50	614.70	187.20
Electricity, MJ	5.40	Nil	-5.40
Human energy for wood processing, MJ	0.20	Nil	-0.20
Human, MJ	0.03	0.20	0.17
Total		**433.13**	**614.90**

8.7 Development of natural draft gasifier of 100 kW for wood and crop residues

The scaled-up model of the CIAE natural draft gasifier was redesigned to deliver about 92,000 kcal/h of thermal output, with the gas outlet diameter enlarged from 75 mm to 300 mm to reduce friction losses. The system was tested on wood chips and groundnut shells to assess its performance (Fig. 8.10). Flame temperatures ranged from 850–1090°C with wood chips and 810–1021°C with groundnut shells, while the specific gasification rate varied from 69–78 kg/m^2. Producer gas from wood chips had a calorific value of 980–1276 kcal/m^3. Biomass consumption was 38–43 kg/h for wood and 19–22 kg/h for groundnut shells. Temperature near the grate reached 1238–1348°C for wood and 1080–1232°C for groundnut shells, indicating a lower temperature in the reduction zone. The present gasifier faced the problems of fly ash moving along with the producer gas and falling of partially burnt groundnut shell from the grate.

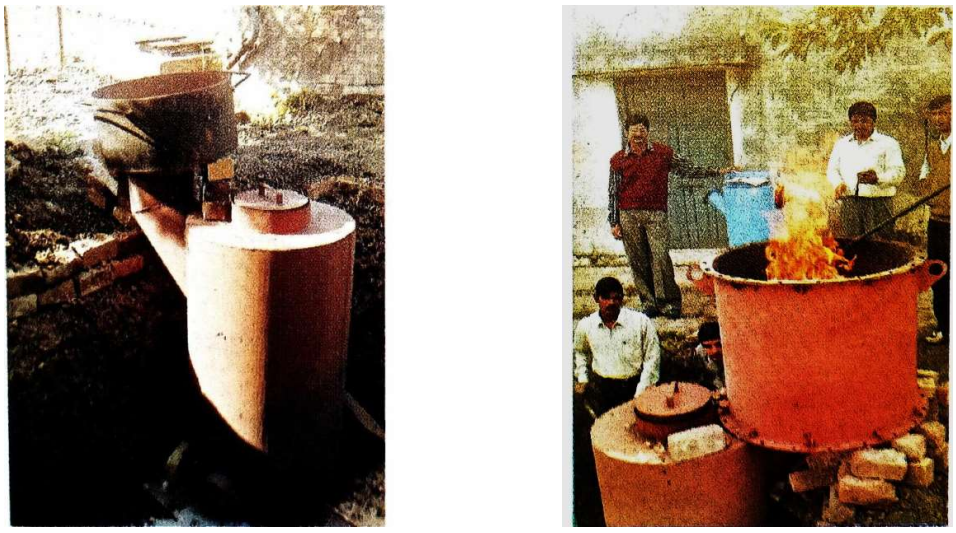

Fig. 8.10 100 kW CIAE natural draft gasifier

8.8 Effect of producer gas on performance of diesel engine

A study was conducted to evaluate the effect of producer gas on the performance and life of a diesel engine using two identical engines. One engine (A) was operated on diesel, while the other (B) ran on dual fuel mode (producer gas + diesel) under constant water-pumping load. The dual-fuel engine performed satisfactorily for 600 hours despite issues like difficult starting and injector sticking, but finally seized after 750 hours (Fig. 8.11 & Fig. 8.12). Both engines were dismantled to compare component wear.

Engine B showed significantly higher wear than engine A. Cylinder bore ovality increased to 0.02 mm in engine B versus 0.005 mm in engine A, and liner taper was 0.03 mm compared to 0.005 mm. Piston skirt wear in engine B was 0.06 mm more, and piston–bore clearance was 2.8 times higher than in the diesel-only engine. Wear on inlet and exhaust valves of the dual-fuel engine was 2.4 and 1.9 times higher, respectively. Bearing clearances were also greater in engine B, likely due to deterioration of lubricating oil when operating on producer gas. Overall, producer gas use increased engine wear and reduced engine life under long-duration operation.

Fig. 8.11 Slicked valves due to excessive tar deposition

Fig. 8.12 Seized compression rings on piston grooved

8.9 Investigations on generation and purification of hydrogen gas from biomass and evaluation with alkaline fuel cell

The study focused on generating hydrogen from biomass-based producer gas and using it in an alkaline fuel cell (Fig. 8.15). A 2.5 kW downdraft gasifier was developed to produce the gas, which showed a calorific value of 930–1120 kcal/m^3, tar content of 10–15 mg/m^3, and flame temperature of 532–766°C (Fig. 8.13). The CO concentration ranged from 21.1–27.4%. By blending producer gas with steam in a 1:18 ratio and passing it through a catalyst setup, CO was converted to hydrogen with an efficiency of 69.4–89.7%. To make the gas suitable for fuel cells, a water-and-charcoal-based filter was developed (Fig. 8.14). It reduced tar by 76.9–82.3%, and the highest removal (84.9%) was achieved using a 20 cm water column and 25 cm charcoal bed (Table 8.6).

For hydrogen enrichment, the gas mixture was passed through a series of reactors, Zinc oxide, HT shift, LT shift, soda-lime bed, and PROX reactor. The iron–chrome oxide catalyst performed best at 315–355°C, achieving CO conversions up to 89.7% and hydrogen levels of 12–15% (Table 8.7). Copper oxide catalyst was effective at lower temperatures (175–215°C), yielding CO conversion of 70–79% (Table 8.8). The purified hydrogen was then supplied to a 460 W alkaline fuel cell stack. When operated with pure hydrogen, the stack delivered 6.2 A at 4.8 V, while a 1:1 H_2–N_2 mixture produced 5.4 A at the same voltage. The system was successfully tested using a custom electrical loading unit.

Table 8.6 Performance of the filter with 10 cm water column and 20 cm charcoal bed

Column and bed height, mm	Tar content (mg/ m^3)		% absorption of tar	Pressure drop (mm H_2O)
	Before filter	After filter		
10 and 20	121.2	28.4	76.9	68
	289.3	31.3	82.3	62
	123.1	24.1	80.5	64
20 and 25	149.4	25.1	83.2	79
	120.1	22.2	81.5	83
	114.5	18.2	84.9	82
25 and 30	152.6	23.1	84.3	89
	131.1	22.8	82.6	92
	104.8	17.6	83.2	84

Table 8.7 Performance of iron chrome oxide catalyst

Temperature (°C)	Steam carbon ratio	Space velocity (L/ L cat.h)	Gas flow (I/ h)	Level of CO (%)		Conversion	Hydrogen (%)
				Initial	Final		
343	1.38	1066	188.2	23.81	7.07	70.3	13.48
346	2.83	1644	290 4	22,41	4.73	78.9	14.61
351	2.75	1593	281.3	18.39	4.12	77.6	12.21
338	2.76	1728	305.2	23,12	5,50	76.2	13.18
343	2.90	1575	278.2	26.04	5.51	79.4	15.12
315	3.85	1009	178.2	21.18	3,43	83.8	14.65
355	4.12	1037	183.2	19.32	4.99	89.7	15.23
338	3.96	1710	302.2	23.30	4.71	79.8	13.73
331	4.15	1765	311.7	18.54	3.67	80.2	13.51

Table 8.8 Performance of copper oxide catalyst

Temperature (°C)	Steam carbon ratio	Space velocity (L/ L cat.h)	Gas flow (L/ h)	Level of CO		Conversion (%)	Hydrogen (%)
				Initial	Final		
190	3.81	1049	185.2	4.81	1.21	73.1	6.21
215	4.14	1016	179.5	5.12	1.54	70.7	5.93
175	3.92	1145	202.2	7.20	1.83	75.2	6.54
182	4.31	920	162.4	6.83	1.49	79.2	5.96

Fig. 8.13 Fuel processor with producer gas generation system

Fig. 8.14 Fuel cell stack in operation for lighting

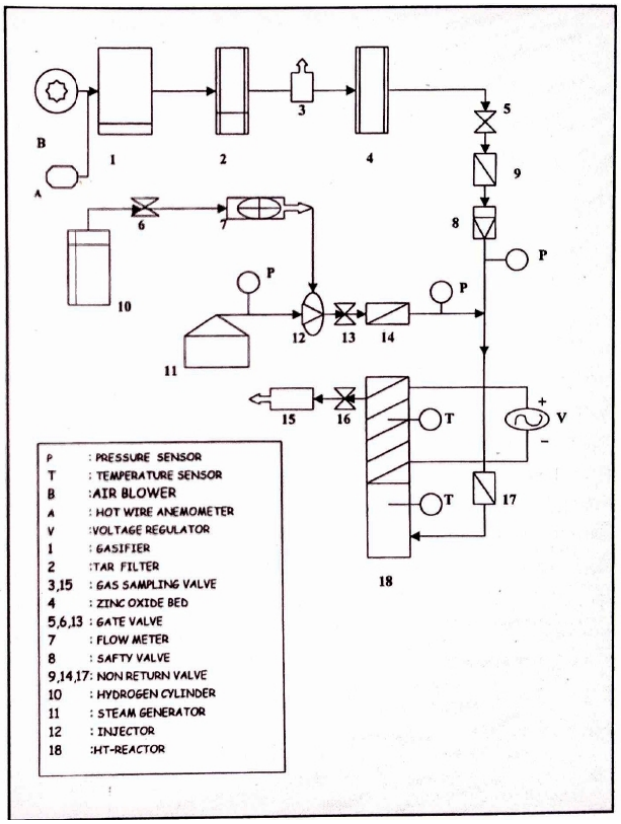

Fig. 8.15 Experimental set-up hydrogen generation from for biomass

8.10 Performance of gasifier with modifications in air supply system

The natural draft gasifier was initially constructed with a central grate and a single 50 mm air inlet pipe, and its performance was evaluated using soybean straw with a moisture content of 10.1–13.2% (Fig. 8.16). During these tests, the biomass consumption rate ranged from 28 to 39 kg/h, the specific gasification rate from 57 to 72 kg/h·m^2, flame temperatures from 845°C to 965°C, and grate temperatures between 1050°C and 1242°C. The starting time varied from 20 to 35 minutes, and the calorific value of the producer gas was 980–1276 kcal/m^3. However, heap formation inside the reactor required frequent poking for smooth fuel flow, and short-circuiting of gases near the air entry was observed. To address this, the air supply system was redesigned by replacing the single 50 mm pipe with four 25 mm diameter pipes positioned at 90° intervals above the grate to ensure uniform air distribution. Additionally, an ash-removal mechanism using combing action was developed, consisting of two sets of six MS pegs (50 mm high, 5 mm thick, 15 mm wide) projecting 25 mm above the grate and moving 120 mm per stroke to clear ash between the grate bars. These modifications significantly improved operation, as initial tests showed that without ash removal the flame height and temperature reduced steadily and flaring stopped after 80–90 minutes, necessitating agitation. With the new ash-removal system, continuous flaring was maintained for over two hours when tested on wood chips, especially when the combing action was applied

within the first hour or when flame height declined. Further evaluation of the modified gasifier using wood chips (8.2–10.5% moisture) demonstrated a 12.5% increase in thermal capacity, a higher specific gasification rate of 94–124 kg/h·m^2, flame temperatures between 845°C and 1065°C, and overall improved operating continuity, confirming the effectiveness of the design enhancements.

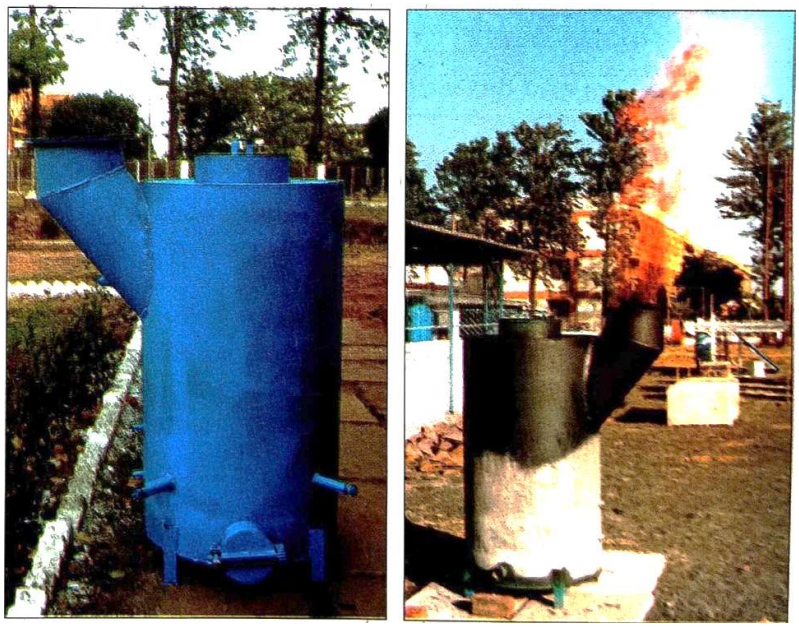

Fig. 8.16 Modified natural draft gasifier and its evaluation

8.11 Design and development of an efficient filter and tar cracking device for engine quality producer gas

The tar cracking unit was put under rigorous thermal testing to ascertain the performance of heating system and to maintain the requisite environment for tar cracking. Heating elements of high thermal capacity and temperature sustaining capability were selected and used in the unit shown in Fig. 8.17. The no load testing was conducted thoroughly for 20 h and it was observed that with better configuration of heating system the tar cracking unit was able to sustain the requisite temperature (900 to 950°C). The system is being provided with the thermal insulation of cera blanket. The critical thermal insulation thickness was computed to be 50 mm considering the thermal conductivity. Two units of wet filter using sand bed were designed considering the gas flow and optimum retention period for removal of tar present in the gas. The system has been designed for 10 kW downdraft gasifier engine system.

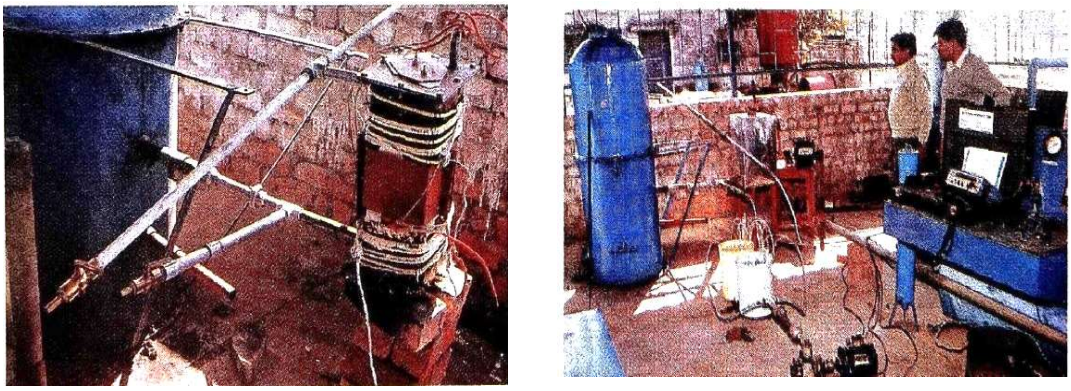

Fig. 8.17 Experimental set up for tar cracking

The energy assessment for tar cracking unit matching to 10 kW gasifier system was conducted and results are given in Table 8.9. The energy loss during cracking of tar present in the producer gas was estimated in the range of 13.4 to 28.2%. The details of energy estimation are presented in Table 8.10 for different biomass. The production of tar per kg of dry biomass is presented in Table 8.11. The tar production from the biomass varied from 4.5 to 7.6 g/kg of biomass.

Table 8.9 Energy assessment of tar cracking unit for 10 kW gasifier system

Feed material	Wood
Biomass consumption, kq/h	10
Moisture content, %	10
Dry biomass consumption, kg/h	9
Calorific value of biomass, MJ/ kg	18
Energy input to the gasifier, MJ/h	162
Energy input for tar cracking, MJ/h	18.71
Energy input for raising catalyst temperature, MJ/h	0.87
Dolomite required, kg	3
Energy output, MJ/h	101.64

Table 8.10 Energy for tar cracking of producer gas from different biomass

Feed material	Calorific value of gas, MJ/m³	Input gas temp, °C	Gas temp during tar cracking, °C	Energy required to raise the gas temp., MJ/m³	System efficiency, %	Gain in calorific value due to tar cracking, MJ/m³	Net energy, MJ/m³	Energy, output, MJ/m³	Net energy loss during the process
Wood chips	4.62 - 5.41	220 - 280	700 - 825	0.592 - 0.853	80	0.1 - 0.12	0.740 - 1.066	4.74 - 5.51	13.4 - 22.48
Soybean stalk	4.18 - 5.16	180 - 260	700 - 825	0.620 - 0.909	80	0.1 - 0.12	0.775 - 1.136	4.30 - 5.28	14.6 - 26.4

Groundnut shell	4.24 - 5.21	180 - 285	700 - 825	0.585 - 0.909	80	0.1 - 0.12	0.73 - 1.136	4.36 - 5.31	13.7 - 26.1
Pigeon pea stalk	4.03 - 5.16	165 - 245	700 - 285	0.642 - 0.931	80	0.1 - 0.12	0.801 - 1.162	4.15 - 5.26	15.2 - 28.2

Table 8.11 Tar production with different biomass (10 kW down draft gasifier)

Feed material	Gas flow, m^3/ h	Biomass consumption, kg/ h	Moisture content, %	Dry biomass consumption, kg/ h	Tar content mg/m^3	Tar production, g/ kg biomass
Wood	14.9	6 1	9.2	5.54	1707	4.5
Soybean	15 4	6 5	10.5	5.82	2306	6.1
Pigeon pea	16 5	6.9	11.2	6.12	2834	7.6

8.12 Improved designs of CIAE updraft gasifiers

Improved designs of CIAE updraft gasifiers focused on enhancing feeding efficiency, thermal performance, and fuel compatibility. In the 10 kW unit, the earlier screw-tight feed port was replaced with a lid and water-seal system, and Insulyte-11 insulation with vertical support pegs was added to reduce heat loss (Fig. 8.18). These refinements allowed smooth feeding and improved performance, with biomass consumption of 10–12 kg/h on wood chips (8.8–10.3% moisture) and an SGR of 105–117 kg/h/m^2, representing a 9.5–12.3% gain due to better insulation.

For the 100 kW, natural draft model, the ash-removal mechanism was upgraded from a reciprocating to a rotary system, reducing draft requirements and improving continuous operation. Five units were fabricated and evaluated on wood chips (50–100 mm), showing biomass consumption of 22–24 kg/h and flame temperatures of 780–965°C. These gasifiers were deployed for operational demonstrations, including hot water and cooking applications at ShardaVihar Residential School (Bhopal). Additional units supplied to TNAU, Coimbatore, and PAU, Ludhiana performed satisfactorily during multi-locational testing.

Fig. 8.18 Operation updraft CIAE gasifier with briquettes

Parallel studies were conducted to develop suitable briquetted fuels for gasification. Thermogravimetric analysis of soybean stalk at heating rates of 10–50°C/min showed that moderate heating (10–20°C/min up to ~300°C) supports production of lower-density briquettes (600–700 kg/m^3), which are more suitable for gasifiers compared to high-pressure binderless briquettes (1000–1200 kg/m^3). Briquettes prepared from charred soybean stalk with cattle dung binder were tested in the CIAE portable gasifier, with biomass consumption of 6.5–8.2 kg/h and flame temperatures of 845–937°C; however, gas sustainability beyond one hour was poor due to high ash content.

The SPRERI 600 kW open-core gasifier was also evaluated with binderless briquettes made from sawdust–sunflower husk mixtures. The unit recorded a briquette consumption rate of 45.6 kg/h, grate temperatures of 780–890°C, a gas calorific value of 3.6–4.7 MJ/m^3, and an average thermal output of 400 MJ/h, demonstrating its potential for large-scale briquette-based gasification. Overall, the improved CIAE gasifier designs and complementary briquette fuel studies contributed to more efficient, field-ready biomass gasification systems suited for rural and agro-industrial applications.

8.13 Integrated bio-fuel cell technology (Asian Swedish Research Partnership Programme)

The Integrated Bio-Fuel Cell project under the Asian–Swedish Research Partnership Programme focuses on developing an intermittent-temperature solid oxide fuel cell (ITSOFC) operating on biomass-based producer gas. Fuel cell development is being carried out at KTH, Sweden, while producer gas generation and cleaning systems are being developed at CIAE, Bhopal.

At KTH, ITSOFCs fabricated using dry-press technology showed superior performance compared to tape-cast cells, delivering a power density of 317

mW/cm^2 at 675 mA/cm^2 with an open-cell voltage of 875 mV to 1 V (Fig. 8.19). Reversibility phenomena in the electrodes were observed during testing, and key parameters, anode support structure, electrode thickness, compaction pressure, and sintering temperature were optimized accordingly.

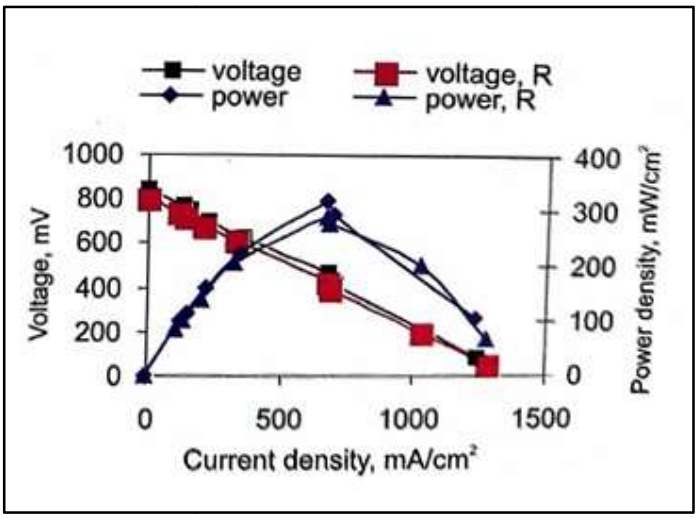

Fig. 8.19 Reversibility phenomena of ITSOF single cell

At CIAE, Bhopal, a laboratory model of 10 kW fixed bed updraft gasifier was designed for high hydrogen concentration with low tar content (Fig. 8.20). The gasifier generated CO levels of 14.6–17.2% and H_2 levels of 11.8–13.5%. Tar content ranged from 1.1–1.7 g/m^3 for wood chips, 2.5–6.5 g/m^3 for soybean stalk/maize cob, and only 0.11–0.17 g/m^3 when charcoal was used. To achieve the required tar level of less than 0.01 g/m^3, a tar-cracking unit operating at 725–800°C and handling gas flows of 1.2–1.9 m^3/h was integrated with the gasifier, reducing tar content to 0.049 g/m^3.

Fabrication and testing facilities for ITSOFC electrodes were also developed at CIAE (Fig. 8.21). Cells were prepared using nickel-based anodes and Ba–Sr–Co–Fe cathode material synthesized through precipitation, followed by sintering at 600°C. Performance evaluation with air at the cathode and hydrogen at the anode across 400–750°C produced an open-cell voltage of 0.7–0.8 V, validating the feasibility of coupling clean producer gas with ITSOFC technology.

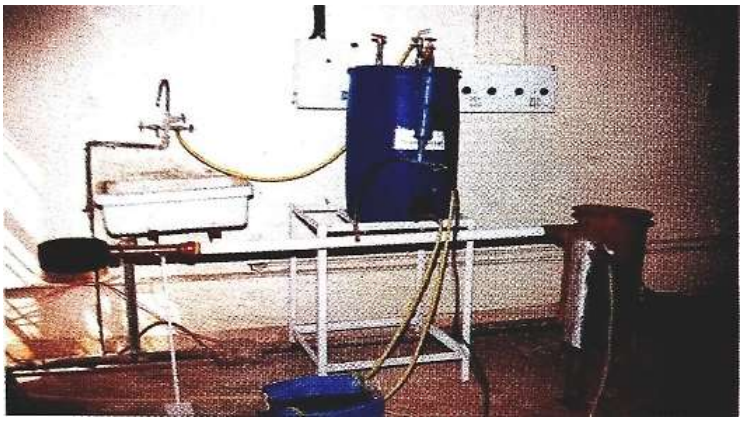

Fig. 8.20 Developed gasifier connected with tar cracking unit

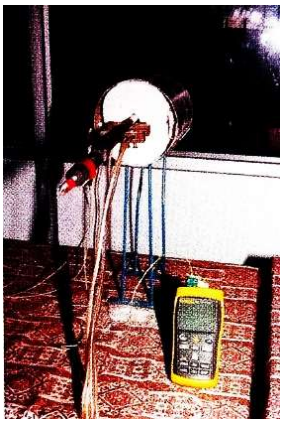

Fig. 8.21 ITSOFC test set up

8.14 Design and development of 20 kW producer gas cooling and cleaning system

A 20 kW producer gas cooling and cleaning system was designed and developed with a focus on optimizing tar removal through different biodegradable filter materials and bed heights (Fig. 8.22). Laboratory evaluation showed that tar absorption increased with bed height: 80.7–95.7% at 0.2 m, 89.3–99.1% at 0.3 m, and 92.5–99.3% at 0.4 m. Among the materials tested, coconut coir consistently showed the highest tar absorption, followed by charcoal and maize cobs. Water requirement for cleaning 100 L of producer gas varied depending on the filter media, 4.3–12.3 L for charcoal, 5.1–14.0 L for maize cobs, and 8.0–19.4 L for coconut fibre. Based on these results, a three-stage filtering system was developed, consisting of a water scrubber, a wet charcoal filter, and a dry coconut-coir filter. The system was designed to achieve a final tar content of 30–50 mg/m^3, with provisions for water drainage and a perforated support plate for holding the filter media. Coconut coir in the dry filter also helped remove residual moisture before the gas entered the engine.

Performance evaluation using wood chips showed a gas flow rate of 20.5–30.1 m^3/h. The system effectively reduced tar concentration to 24–53.5 mg/m^3, achieving 98.49–99.14% tar removal, with a pressure drop of 13–23 mm water column. Dust levels at the outlet ranged from 11 to 18 mg/m^3, confirming that the system produced engine-grade producer gas suitable for 20 kW gasifier applications.

Fig. 8.22 Evaluation of 20 kW cooling and cleaning system

8.15 Evaluation of the CIAE, SPRERI and PAU producer gas filters

SPRERI and CIAE gas filter units (20 kW capacity) were installed with an updraft gasifier for performance evaluation (Fig. 8.23). Both systems were tested for extended operation. The CIAE filter ran smoothly for 50 hours without any choking, while the SPRERI filter experienced blockage after about 15 hours. During operation, the water flow rate in the filtration bed was maintained between 420 and 600 L/h. Tar absorption ranged from 85–89% in the SPRERI unit and 90–93% in the CIAE unit. The inlet gas temperature was 170–190°C and the outlet temperature was 33–35°C. Tar and dust levels in the cleaned gas were 42–57 mg/m^3 for SPRERI and 36–40 mg/m^3 for CIAE. Upon dismantling the SPRERI filter, heavy tar deposits along with gravel and sand accumulation were observed; the unit was cleaned, reassembled, and further tested.

Fig. 8.23 Gas filters (CIAE, SPRERI and PAU)

The performance of filters at optimum water flow rate of 600 L/h are summarized in Table 8.12.

Table 8.12 Performance of gas cleaning unit at optimum water flow rate of 600 L/h

Gas now rate, m^3/l	Gas inlet temp., ˚C	Gas outlet temp., ˚C	Water inlet temp., ˚C	Water outlet temp., ˚C	Tar and dust at inlet, mg/m^3	Tar and dust at outlet, mg/m^3	Tar at gas outlet, mg/m^3	Pressure drop across filter, mm-H_2O
SPRERI gas cleaning unit								
13.5	180	33	19	22.8	1710	92	48	158
15.9	179	35	19.1	22.9	1596	83	46	159
17.2	178	36	19.3	23.4	1950	81	44	160
17.4	179	37	19.4	23.5	1490	78	42	161
CIAE gas cleaning unit								
13.5	180	34	22.5	24.0	2008	83	43	131
15.9	179	33	22.5	24.0	1613	86	47	135
17.4	178	34	23.0	24.5	1998	74	37	138
17.7	181	35	23.5	25.0	1860	72	39	140
PAU gas cleaning unit								
13.8	187	40	34	37	1690	98	48	145
15.6	195	42	33	36.5	1910	94	47	162
16.3	189	39	34	37.5	2025	92	45	154
17.5	193	41	33.5	37.5	1730	94	46	168

(Average ambient temperature and RH of the air were 24.5˚C and 45%, respectively)

8.16 Studies on Thermal Gasification of Cashew Shell and Cashew Shell Cake

Under a collaborative project between CIAE, Bhopal and NRC for Cashew, Puttur (Karnataka), detailed characterization and gasification studies were conducted on cashew shell (CS) and cashew shell cake (CSC). True density measurements using the toluene displacement method showed values of 0.98 and 1.12 g/cm^3, indicating good compactness of CSC. Thermogravimetric analysis (TGA) was performed in an inert environment at heating rates of 10–40 °C/min from 35°C to 1000°C (Fig. 8.24), with the temperature initially held at 35°C for stabilization.

Elemental analysis revealed that CSC contained 0.1% N, 45.8% C, 0.4% S, and 6.3% H, while CS showed 0.5% N, 55.8% C, 1.1% S, and 6.2% H. The lower nitrogen content in CS suggests lower corrosive potential during gasification, whereas its higher carbon content indicates better gas yield and calorific value. CSC had a low ash content of 2.24%, favorable for smooth gasification.

TGA of CSC indicated moisture loss up to 250°C, followed by release of lighter volatiles between 220–380°C, accounting for 44–52% of mass loss and suggesting significant tar formation. Multiple peaks observed between 230–360°C (Fig. 8.25)

corresponded to decomposition of oil, hemicellulose, and cellulose. Oxidation temperature (To) increased with higher heating rates, confirming typical thermal decomposition behavior (Fig. 8.26).

Preliminary gasification trials demonstrated that continuous, smoke-free operation with a blue flame was achievable using the CIAE updraft gasifier (Fig. 27). Extended testing over 70 hours showed biomass consumption rates between 5.0–10.8 kg/h, depending on air inflow. Flame temperatures ranged from 387–718°C (mean: 587°C). However, high tar generation was observed during CSC gasification, with deposition occurring along the gas conduit. The specific gasification rate (SGR) varied from 76 to 167 kg/h-m^2 (mean: 116 kg/h-m^2, SD: 32.3).

Despite tar formation, CSC was successfully gasified in the updraft gasifier, and an operational protocol was developed. The system proved suitable for thermal applications requiring 10–12 kW output. The gasifier achieved reliable ignition within 15–20 minutes at startup, with quick re-ignition (2–3 minutes) after intermittent feeding. Daily startup was rapid, achieving flame within 5 minutes. The optimal feeding interval was 50–55 minutes, supporting stable and consistent operation.

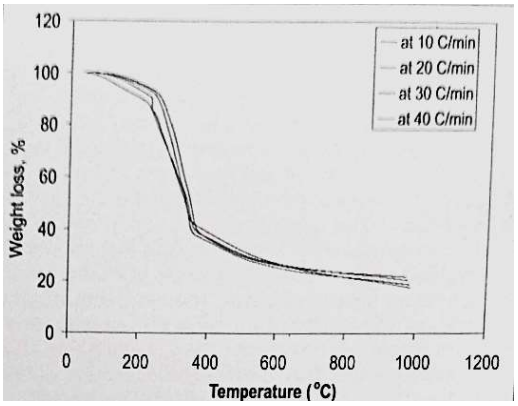

Fig. 8.24 Thermo gravimetric analysis of cashew shell cake

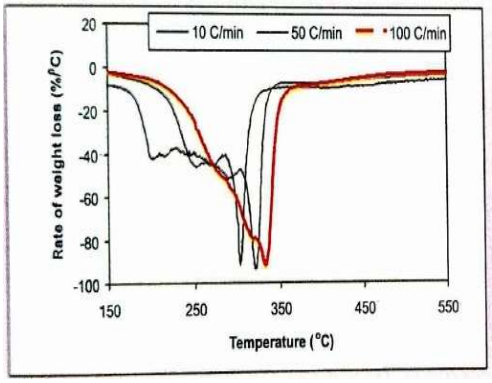

Fig. 8.25 First derivative of thermo gram of cashew shell cake at HR of 10, 50 and 100 °C/min

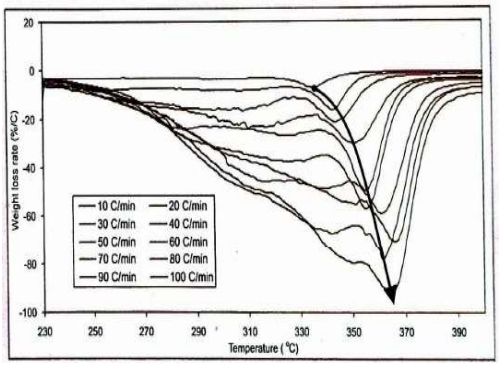

Fig. 8.26 First derivative of CSC-TGA at different heating rates

Fig. 8.27 Gasification of cashew shell in portable gasifier

8.17 Gasification for electricity generation - performance evaluation of 20 kW biomass based power plant installed at CIAE, Bhopal

The 20 kW biomass-based power plant installed at CIAE, Bhopal was evaluated using resistive loading, gradually increasing the load to 20%, 40%, 60%, 80% and 100%. At rated power, biomass consumption varied between 1.1 and 1.4 kg/kWh, and the overall system efficiency ranged from 17.4% to 20.6%. This small-scale power plant also demonstrated employment potential, capable of generating 600–700 man-days for various operational activities. Exhaust emissions from the system were recorded with variations in O_2, CO and NO levels. An energy audit conducted at 18 kW load revealed that only 18% of the total biomass energy was converted into electrical power. While known losses accounted for 31% energy loss, whereas 51% of the energy loss remained unaccounted, indicating scope for efficiency improvement in the system.

8.18 Water quality analysis for gas conditioning system with 10 kW updraft gasifier and optimization for water recycling

Studies on tar contaminated water from gas conditioning system of gasifier were carded out to determine the severity of contamination. The contaminated water was not found to be fit for consumption on BIS standards and needed treatments before disposal. Cleaning water quantities were 14.6, 7.6, 4.8, and 3.61/$m^3$of gas at the 2nd, 4th 6th and 8th h of gasifier operation. The rate of increase in the acidity reduced drastically between Q_{cw} values of 7.6 and 4.81/$m^3$of gas. Change in the increase (relative to its preceding value) in case of BOD and hardness minimized at the Q_{om}, values of 7.61/m^3gas, but in case of COD the minimum increase rate was reached at C), values of 4.81/m^3gas. These trends showed that the water contamination reached to saturation level (Fig. 8.28) within 4 to 6 h of operation of gasifier and during this period, the water must be cleaned or changed. Study revealed that 8-10 l of water is required to clean the producer gas generated from 1 kg of biomass.

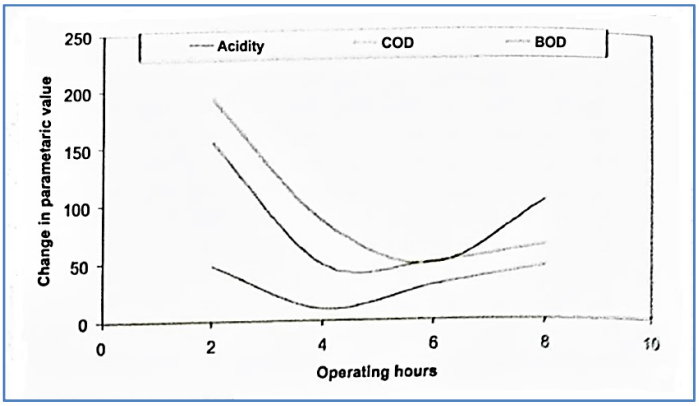

Fig. 8.28 Saturation level of water reaching between 4th to 6th h of gasifier operation

8.19 Quality improvement in charcoal through activation

The activation of char obtained as by- product from gasifier was attempted through thermal oxidation method for enhancing the water cleaning ability of char. Iodine value (IV) could be raised, to 899 (IV of activated charcoal) from 201 (IV of inactivated charcoal). Thus, the target of achieving the charcoal having the iodine value nearer to commercial activated carbon (1137) was achieved by 79 %. Fig.8.29 shows the water cleaned through commercial activated and optimized process activated charcoal.

Fig. 8.29 View of contaminated and treated water through activated charcoal

8.20 Fuel preparation studies for gasification

Techno-economic evaluation of SPRERI design wood cutter for preparation of fuel for gasifier was undertaken. The specific energy consumption during wood cutting varied from 0.013 to 0.022 kW-h/kg while power requirement was 1.25 kW (Fig. 8.30). The output of the machine varied from 57.3 to 87.1 kg/h. The operating cost was estimated to be 26.55/ h and the cost of wood cutting as 0.30/kg of processed wood. Two major contributors in the total cost were labour (57%) and electrical input (34%). Other costs (including depreciation, interest, shelter and repair and maintenance) were only 9%.

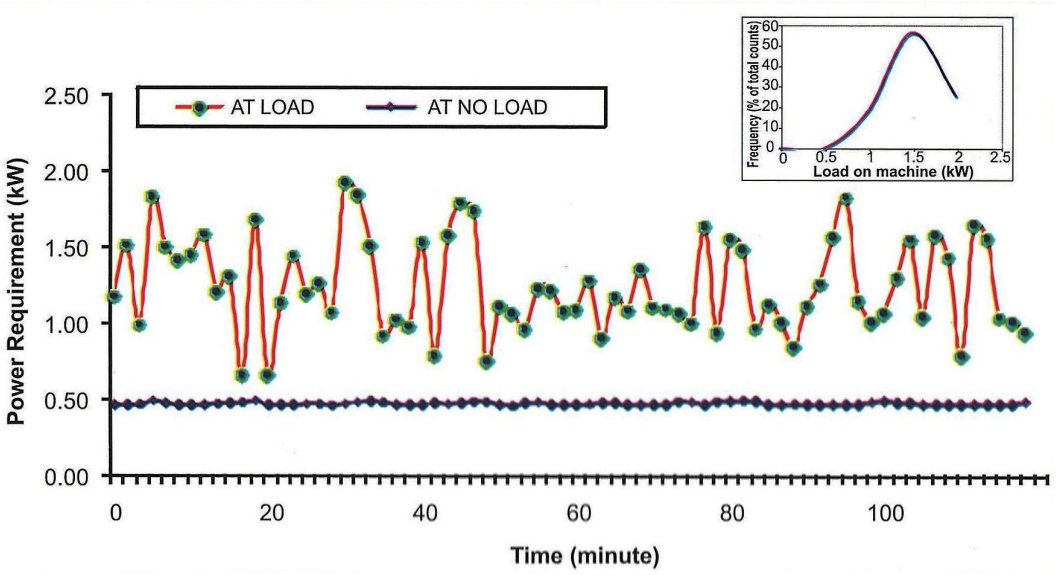

Fig. 8.30 Power requirement of wood processing machine at load mid no load (Figure in inset, shows the frequency distribution of power requirement at load)

8.21 Operation and evaluation of 32 kVA power plant at village Mana

The analysis of operating data for 350 h for power plant at village Mana indicated that briquetted fuel size does not have an effect on biomass consumption whereas the share of briquetted fuel in total fuel (along with wood) has effect on biomass consumption. The biomass consumption increases with increase in briquetted fuel in fuel mix (Fig. 8.31).

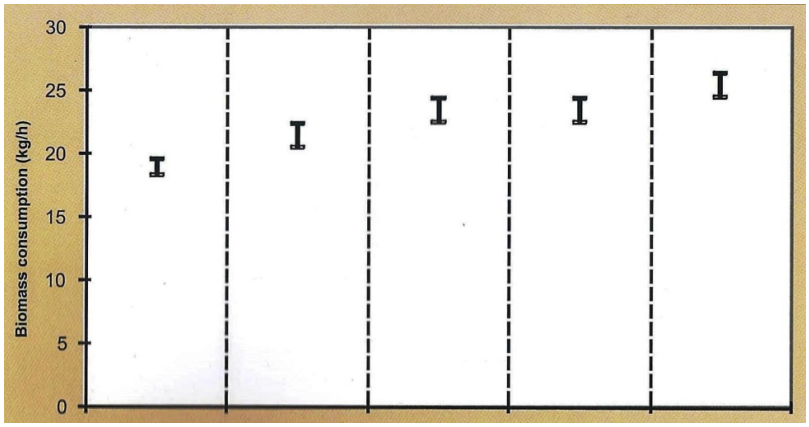

Fig. 8.31 Effect of fuel mix and briquette size on gasifier performance

The problems encountered during long duration evaluation were identified for preparing a maintenance schedule Clinker formation (Fig. 8.32) inside the gasifier, choking of the gas outlet pipe with ash and wetness of active filter media were observed.

Fig. 8.32 Clinker formation

Long duration testing of briquetting plant: Long term evaluation of briquetting plant installed mid contra ss lolled at village Maim, Raisen district produced 25 tonnes of briquettes. The power requirement of briquetting plant and hammer mill was assessed to be 17-22 kW and 14-17 kW, respectively. The specific energy consumption for briquette production was 0.080.1 kW-h/kg at an average briquette production rate of 225 kg/h.

8.22 Studies on transportation of crop residues

Transportation studies for different biomass were conducted. Truck and trolley were employed for this purpose. Using commercial truck (10 wheeled), 8.2 tonnes of pigeon pea stalk (shredded) was transported for 125 km at a cost of8000. For loading the shredded pigeon pea, stalk of 80 man-h was needed, whereas unloading needed 8 man-h.

Studies for transportation of soybean straw at different lead distance for loose, threshed, and bailed biomass were conducted using tractor trolley (3.05 m × 1.83 m × 0.61 m). Trolley accommodated 700-800 kg loose or 1000-1200 threshed or 1500-1600 kg bailed crop residues per trip. Fig. 8.33 and Fig. 8.34 shows the labour engaged for loading and unloading the trolley and the cost of transportation, respectively, for different states of crop residues for a lead distance of 5 km.

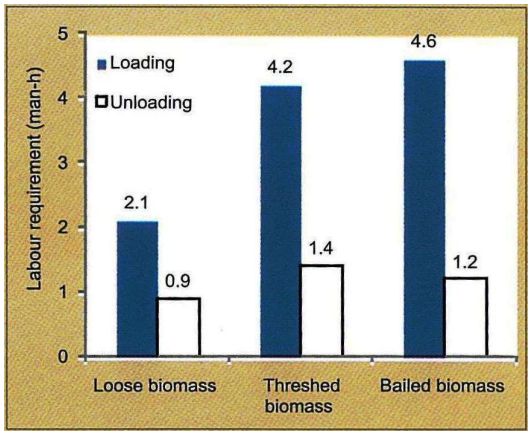

Fig. 8.33 Labor engaged for loading and unloading the tractor trolley

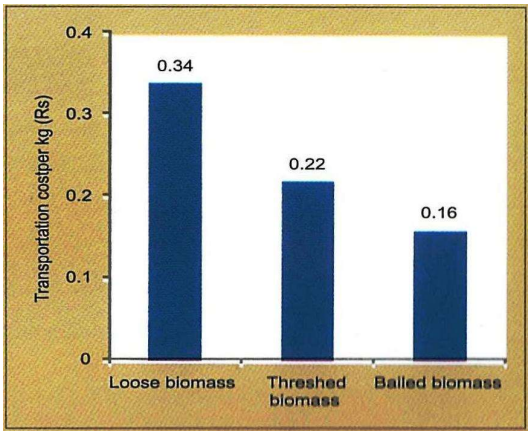

Fig. 8.34 Cost of transportation using tractor trolley

8.23 Establishment of briquetting plant at agro industry in Udaipura, Raisen

A briquetting plant (500 kg/h) was installed and commissioned at Udaipura where pigeon pea is grown as a major crop and pigeon pea stalk is in surplus (Fig. 8.35). The power generation has been planned to use for operation of briquetting plant and supply of electricity to adjoining agro industry complex, dal mill, polishing mill and ware house. This plant is to be energized by green power generated through gasifier based power plant to be supplied by SPRERI, VV Nagar.

Fig. 8.35 View of briquetting plant installed at Udaipura

An analysis to assess the benefits of establishment of a value chain of biomasscollection, briquetting and power generation was done as shown in Fig. 8.36.

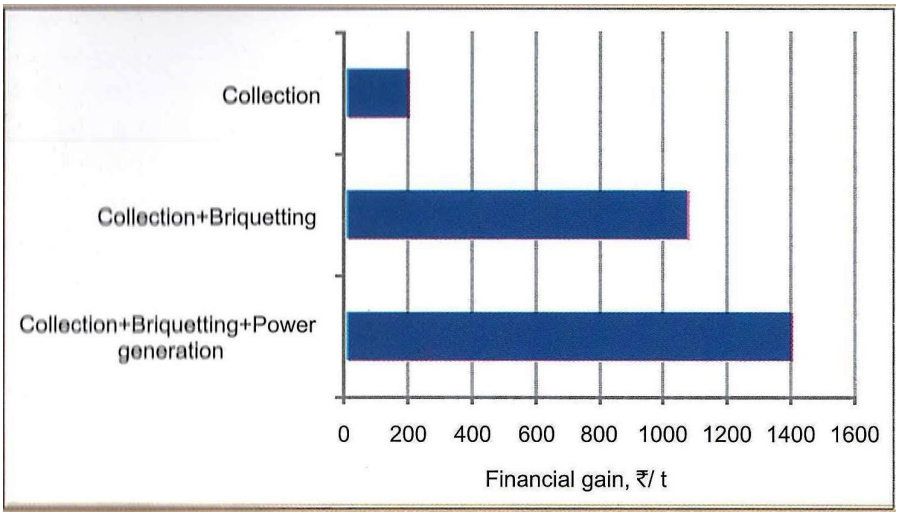

Fig. 8.36 Financial gain obtainable due to establishment of value chain

8.24 Assessment of quality of conditioning water

Updraft gasifier was operated with wood, briquettes and mixture of 50% briquettes + 50% wood. The tar content in water continuously increases with duration of water recirculation and after certain duration the tar content nearly

stagnated. Briquetted fuel was found to give least tar content in water as compared to wood and wood+briquettes in updraft gasification mode. The saturation level of water pollution reached at around 3-5 h of operation, indicating the need for changing or cleaning of water for further use.

8.25 Evaluation of improved cook stoves

Three improved cook stoves namely ClAE, SPRERI and Oorja were evaluated with biomass briquettes (of 25 win diameter) by standard water boiling test. The thermal efficiency of the CIAE cook stove, SPRER cook stove and Oorja cook stove ranged from 22-24%, 25-27% and 29-31%, respectively. The emission level around the cook stove (at 0.5 m height and about 0.5 in radius) varied from 10-45 ppm, which was within the safe limit.

8.26 Generation of bio-char from different crop residues and Estimation of C-Gain and CO, Fixation

Biochar from various crop residues was produced using an externally heated, electrically operated vertical cylinder biochar reactor (Fig. 8.37). The yield ranged from a maximum of 40% at 250 °C to a minimum of 21% at 450 °C, as shown in Fig. 8.38. Among the residues evaluated, pigeon pea stalk produced the lowest iodine value (192), followed by cotton stalk (200) and soybean straw (337), indicating that pigeon pea and cotton residues yield more stable biochar than soybean straw. Stable char was generally obtained at process temperatures between 350 °C and 450 °C. Pigeon pea and cotton stalks were charred for detailed characterization of both raw and processed materials. Thermogravimetric analysis (TGA) of four samples, conducted using a linear heating rate of 10 °C/min up to 1000 °C under an inert atmosphere, showed a higher oxidation temperature for raw cotton stalk (342 °C) compared to pigeon pea stalk (326 °C), with results presented in Fig. 8.39. The oxidation temperatures of their respective chars were similar (~113 °C), although the maximum devolatilization rate was lower for cotton char, indicating better thermal stability.

For estimating carbon gain and CO_2 fixation, soybean straw, pigeon pea, and cotton stalk were pyrolyzed in both externally heated (vertical cylinder) and internally self-heated (CIAE charring kiln) reactors. In the external heating system, char yield and carbon content ranged from 20–40% and 71–77%, respectively, whereas the internal heating system produced 27–30% char yield with 90–94% carbon content. The potential CO_2 fixation through charring of each tonne of crop residue was estimated as 0.89 tonne per year for the external heating reactor and 0.71 tonne per year for the internal heating reactor. Carbon sequestration in soil through biochar application was significantly higher than direct residue incorporation, showing increases of 91%, 80%, and 42% for soybean straw, pigeon pea stalk, and cotton stalk, respectively.

Fig. 8.37 Vertical cylinder bio-char reactor

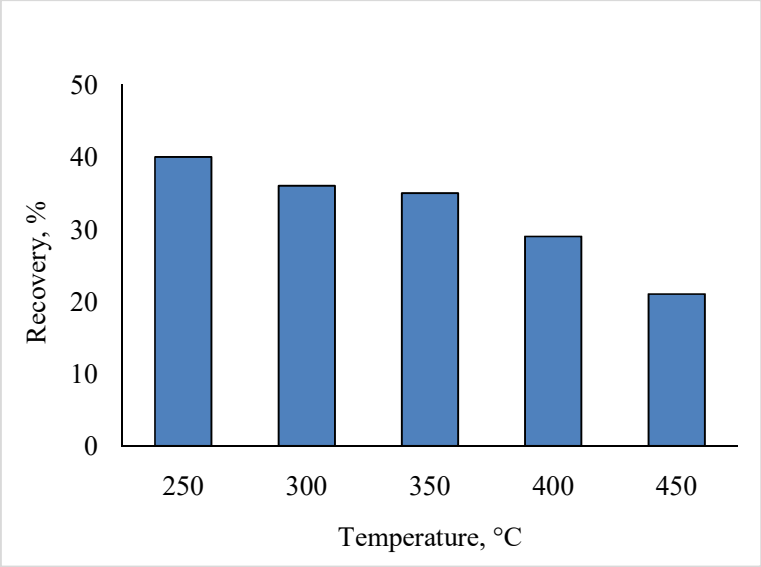

Fig. 8.38 Char recovery from pigeon pea stalk

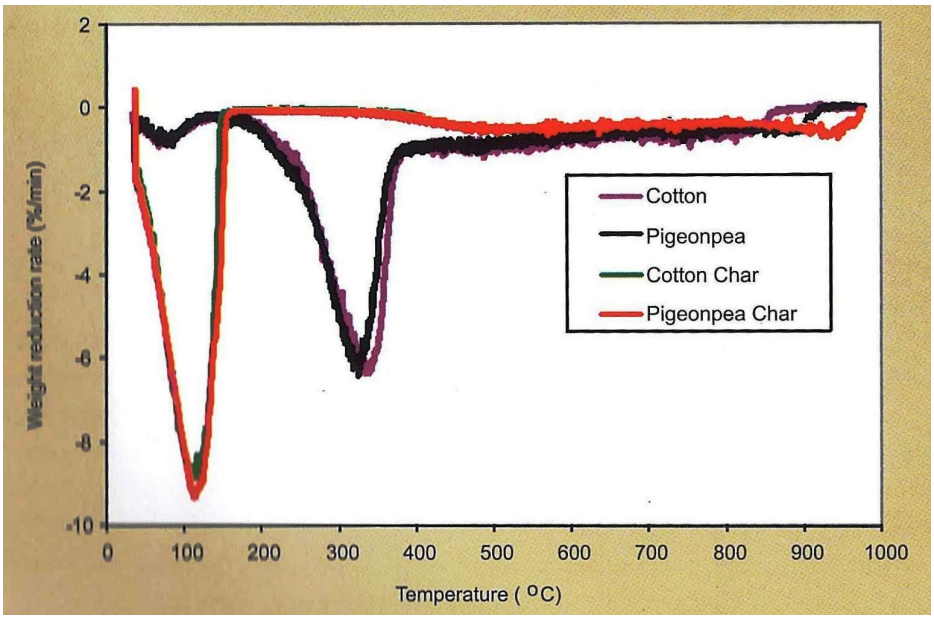

Fig. 8.39 Comparison of first derivative of thermo grams

8.27 Liquefied petroleum gas (LPG) supplementation for efficient governing of producer gas-based power plant

A LPG based supplementation system was developed and integrated with the producer gas based power plant (20 kW) to achieve better governing efficacy and easy starting of the power plant. The time to govern the speed change at different load variations (25%; on and off) was found to vary from 480 s to 720 s when power plant was run on producer gas alone. The time periods with sudden loadings were reduced to 5-10 s by introducing the LPG based system. The blending of 3 % by volume (34 % by energy content) with LPG was found optimum. (Fig. 8.40).

Fig. 8.40 A view of the LPG based supplementation integrated with producer gas based power plant installed at energy enclave

8.28 Characterization of Bio-oil Produced by Fast Pyrolyzer

A fast pyrolyzer was developed for condensing the volatile fraction of agro-residues into bio-oil (Fig. 8.41). The laboratory-scale unit has a production capacity of 1 litre of bio-oil per hour and consists of a 2.0 m long vertical reactor equipped with a 10 kW heating element, an auger-type feeding mechanism, a cyclone separator, and a condenser. Bio-oil yield from soybean straw ranged from 10–15% (Fig. 8.42), and the temperature profile along the reactor is shown in Fig. 8.43. The bio-oil obtained from fast pyrolysis was characterized to evaluate its physical and chemical properties. Its density with moisture, without moisture, and after 20 days of storage was found to be 1.01, 1.10, and 1.19 kg/m^3, respectively, indicating an increase in viscosity during storage. Correspondingly, the viscosities at 45°C were 0.83, 0.86, and 1.60 cSt, respectively (Fig. 8.44). The bio-oil exhibited a flash point of 159°C and contained phenolic compounds, carboxylic groups, aldehydes, and ketones. Other by-products of the fast pyrolysis process included uncondensed gases and char. The gases were found to contain H_2, CO, CH_4, and CO_2, confirming their combustible nature.

Fig. 8.41 Fast pyrolysis setup

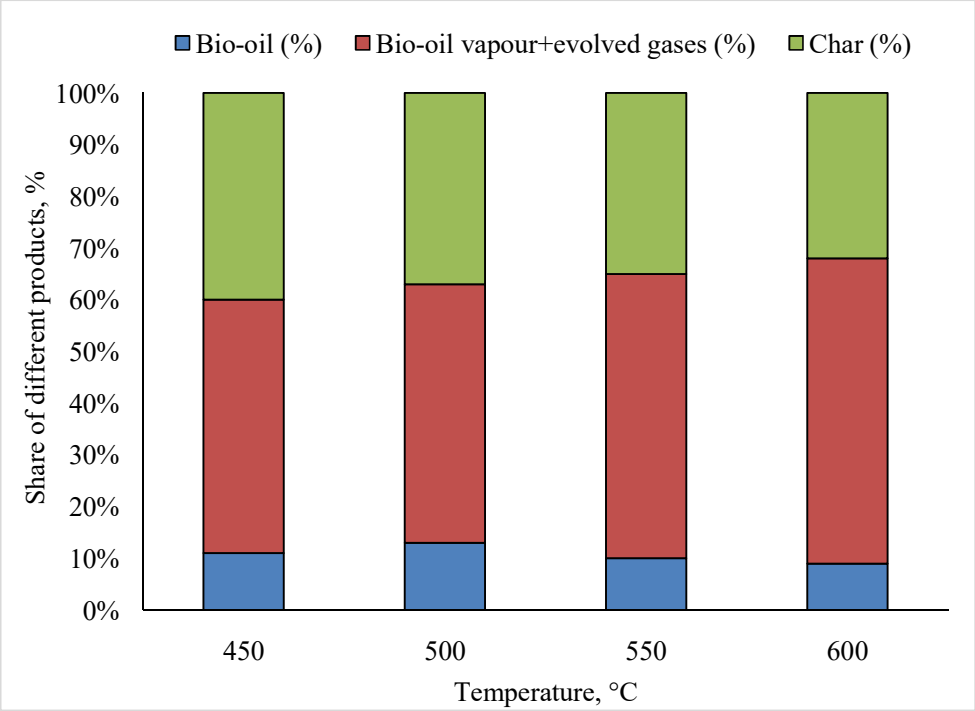

Fig. 8.42 Mass balance of fast pyrolyzed material

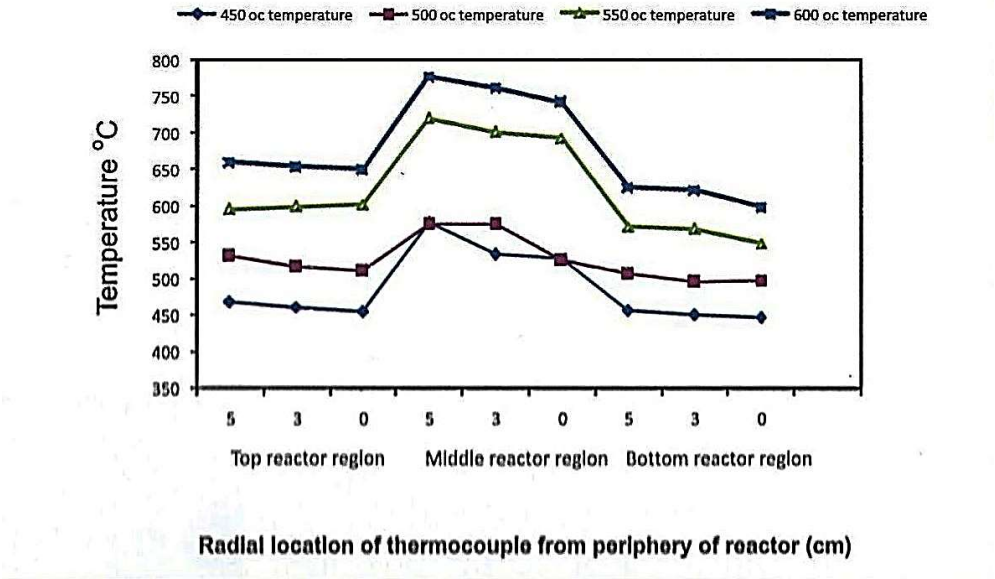

Fig. 8.43 Temperature profile of the fast pyrolyser reactor

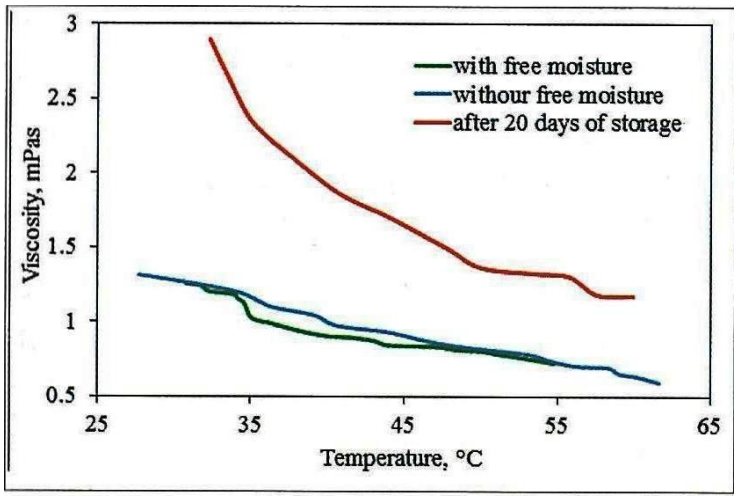

Fig. 8.44 Variation of Bio-oil viscosity with temperature and with storage of 20 days

8.29 Electronic Control Module for Automatic Supplementation of LPG to Producer Gas Based Electricity Generation System

An Electronic Control Module (ECM) was developed for automatic supplementation of liquefied petroleum gas (LPG) to a producer gas–based electricity generation system to improve governing efficiency and ensure stable operation during sudden load variations (Fig. 8.45 and Fig. 8.46). The control module was consisted of speed sensor (rpm), programmable logic controller (PLC), relay and power supply unit. The complete system (ECM + LPGSS) was evaluated with producer gas based electricity generation system of 20 kW. The preliminary results showed a recovery time of 500-668 s was required to govern speed change at different load variations while running the genset with producer gas alone. However, when the genset was regulated by EMC based LPG supplemented system; the recovery time to govern speed change was observed to be 5-7 s as compared to 7-9 s with the manual control LPG supplemented system. The blending of 3% by volume and 34% by energy content was found suitable. The most important aspect of ECM with LPGSS was that intervention of manual control was totally avoided for operation of LPGSS. Transient speed change was within the acceptable limit and there was no permanent speed change when the load on system varied and ECM was used to supplement the LPG blended producer gas at the time of load change.

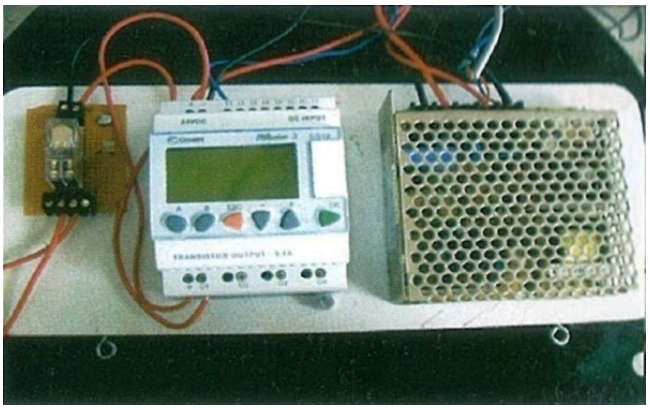

Fig. 8.45 Electronic control Module based LPG supplementation system

Fig. 8.46 A view of the LPG based supplementation integrated with producer gas based power plant installed at energy enclave

8.30 Torrefaction Unit for Processing of Biomass

A torrefaction unit (Fig. 8.47) was developed for thermal treatment of biomass (soybean and pigeon pea) to reduce the energy consumption and increase calorific values for efficient gasification. The developed unit was consisted of a blower and a reactor fitted with electrical heater for raising the temperature of reactor for heating the biomass. A digital temperature controller was fitted to regulate the temperature of reactor. The system was evaluated for treating the biomass at different temperature ranging from 200-250°C. The torrified biomass produced by torrefaction unit has resulted uniform particle size during the grinding and reduction in energy consumption by 20% as compared to untreated biomass. The recovery of biomass after torrefaction varied from 65-80% and calorific value of biomass has increased from 17 MJ/kg to 20 MJ/kg.

Fig. 8.47 Torrefaction unit for thermal treatment of biomass

8.31 Generation and Activation of Charcoal from Pigeon Pea Stalk Using a Chemical-Free Charring Process

Charcoal was produced from pigeon pea stalk through slow pyrolysis in electrically heated reactors. In the horizontal charring unit, pyrolysis temperature (450, 500, and 550 °C), residence time (60, 120, and 180 min), and stalk diameter (≤5, 5–7 and ≥7 mm) were used as independent variables. Under these conditions, char recovery ranged from 33–60%. The total carbon content of the raw material (45 ± 0.5%) increased up to 78% after charring. The produced charcoal exhibited strong adsorptive capacity, achieving iodine numbers >800 mg/g under optimized conditions, compared with 250 mg/g for the raw biomass. The pH of the material also shifted from acidic to basic (pH > 7) due to carbonization.

After generation, the charcoal was further evaluated for activation potential. Char produced in the vertical cylinder bio-charring unit at 250–450 °C showed initial iodine values of 200–320 mg/g (Fig. 8.48), which were lower than commercial activated carbon (1140 ± 10 mg/g). To enhance adsorption performance, thermal activation was carried out at 630 °C for different durations in a muffle furnace. An activation time of 30 minutes proved most effective, increasing the iodine value to approximately 650 mg/g for charcoal produced at 250 °C.

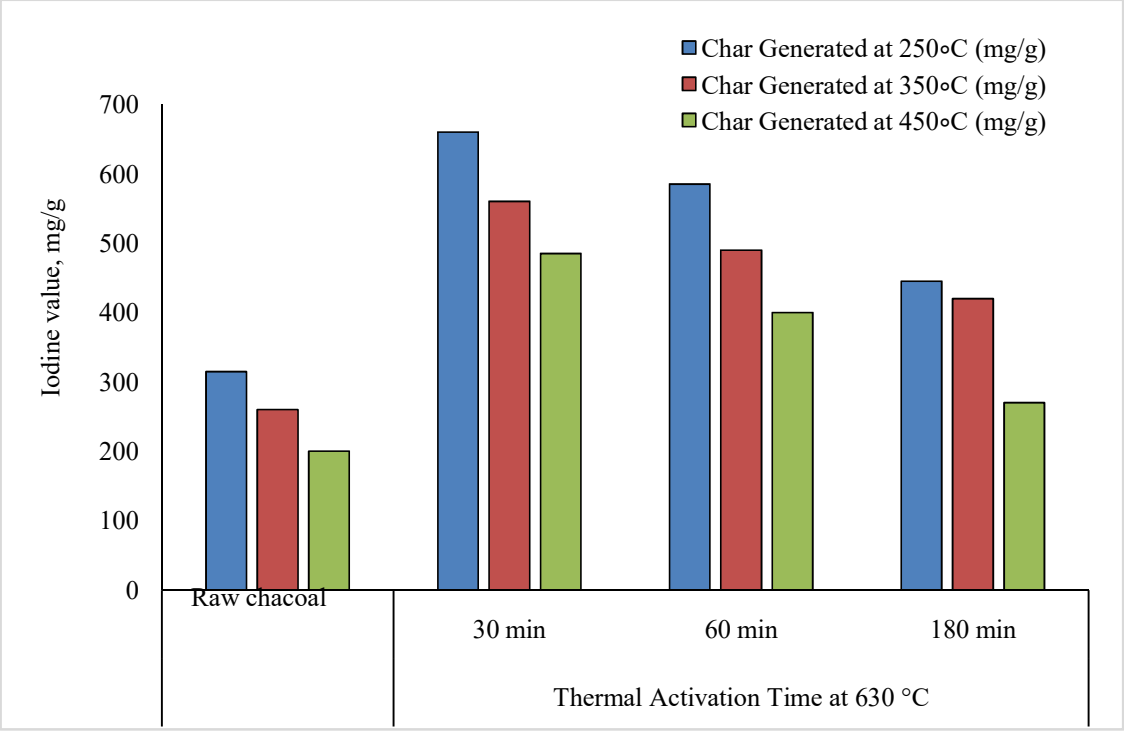

Fig. 8.48 Iodine values of raw and activated charcoal

8.32 Kinetics of pyrolysis process under confined and un-confined conditions

The kinetics of the char generated under confined and unconfined conditions is compared using the thermogravimetric information. The Coats-Redfern method is used to understand the thermal degradation behaviors of the two kinds of char and raw pigeon pea stalk. The char generated from the unconfined system (Fig. 8.49) has a superior activation energy profile as compared to the char generated from confined system (Fig. 8.50). A new method for quantitative evaluation of acceleration and retardation of thermal degradation has been developed. This method is based on the segmental analysis of conversion fraction profile with respect to reaction temperature. The char generated in the confined system has the deposition of the lighter volatiles over its surface and therefore it is thermally less hard compared to char produced in unconfined system.

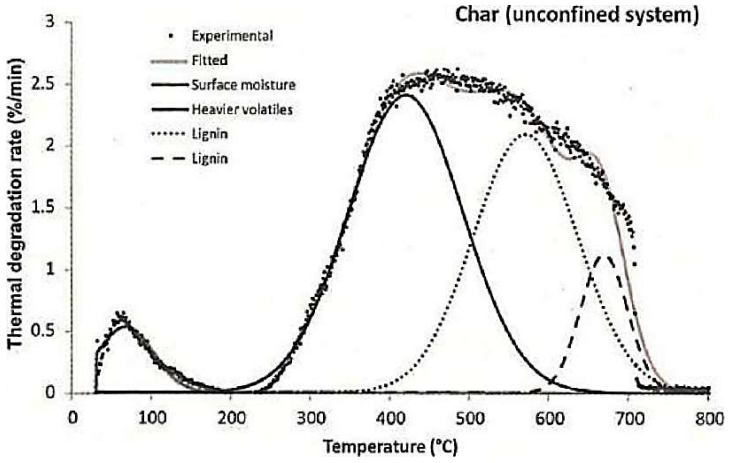

Fig. 8.49 Char generated in unconfined system

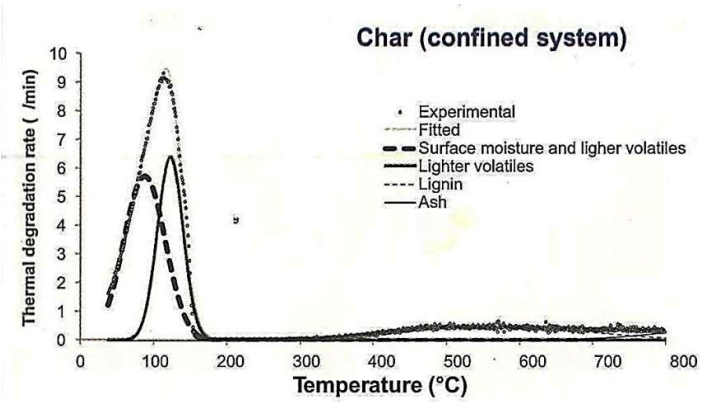

Fig. 8.50 Char generated in confined system

8.33 Kinetics of cashew shell and cashew shell cake

Transitions in the thermogravimetric signals related to the various intrinsic biopolymeric components, such as hemicellulose, cellulose and lignin, in cashew shell and cashew shell cake have been investigated.

The activation energies pertaining to different intrinsic bio-constituents are compared using Kissinger-Akahira-Sunose (KAS) method. The overall kinetics are determined over a complete range of conversion fraction (α = 0.05, 0.15, 0.25, 0.35, 0.45, 0.55, 0.65, 0.75, 0.85, 0.95). KAS points [1/T, In (β/T^2)] are drawn from TGA data at all experimented heating rates (10-100 °C/min) in the α-span of 0.05-0.95 for cashew shell (CS) and cashew shell cake (CSC) [Fig. 8.51]. The activation energy is found to increase until the lignin region and then activation energy reduced for both bio-materials. The activation energy profile (Fig. 8.52) of CS always dominates over the CSC in a-span of 0.05-0.95 indicating that the CS is hard material for thermal degradation. The reduction of activation energy from CS to CSC is highest in lignin related segment (conversion fraction; α-span: 0.70-0.90) Indicating weakening of lignin. The reductions in values of activating energy from CS to CSC

are 61.60, 69.45, 106.61, 50.61 kJ/mole at a-value of 0.7, 0.8, 0.85 and 0.90, respectively.

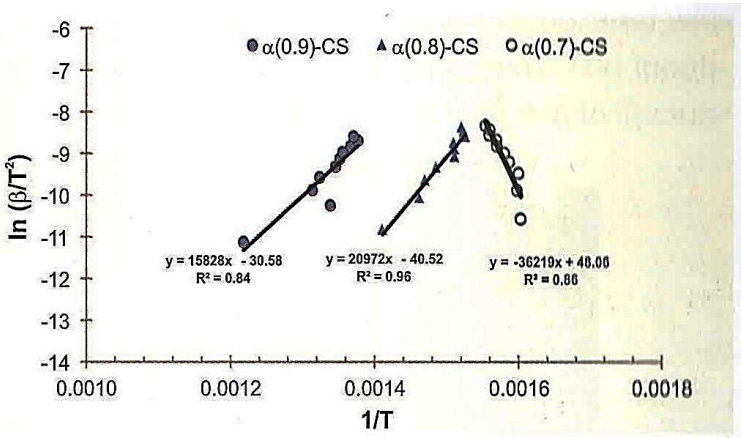

Fig. 8.51 KAS isoconversional kinetic lines for shell at lignin region

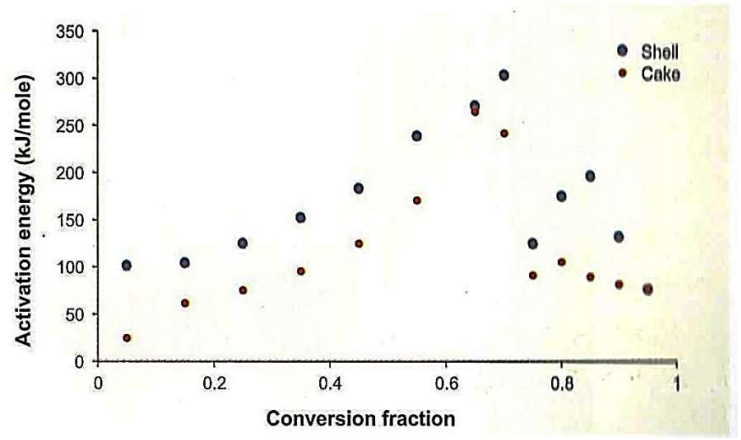

Fig. 8.52 Dominant activation energy profile of cashew shell over cashew shell cake

8.34 Thermal hardness of briquetted bio-oil of pigeon pea stalks

Thermal hardening or softening of the different components of bio-material in briquetted biofuel (pigeon pea stalk) is explained in transitions of thermogravimetric signal end activation energy levels (Fig. 8.53). Lignin signals are shifted towards higher temperature and higher conversion fraction In briquettes indicating thermal hardening. The activation energy profile (Kissinger-Akahira-Sunose method) of briquette is observed dominating over raw residues of pigeon pea crop highlighting the overall hardening in briquetted biofuel (Fig. 8.54).

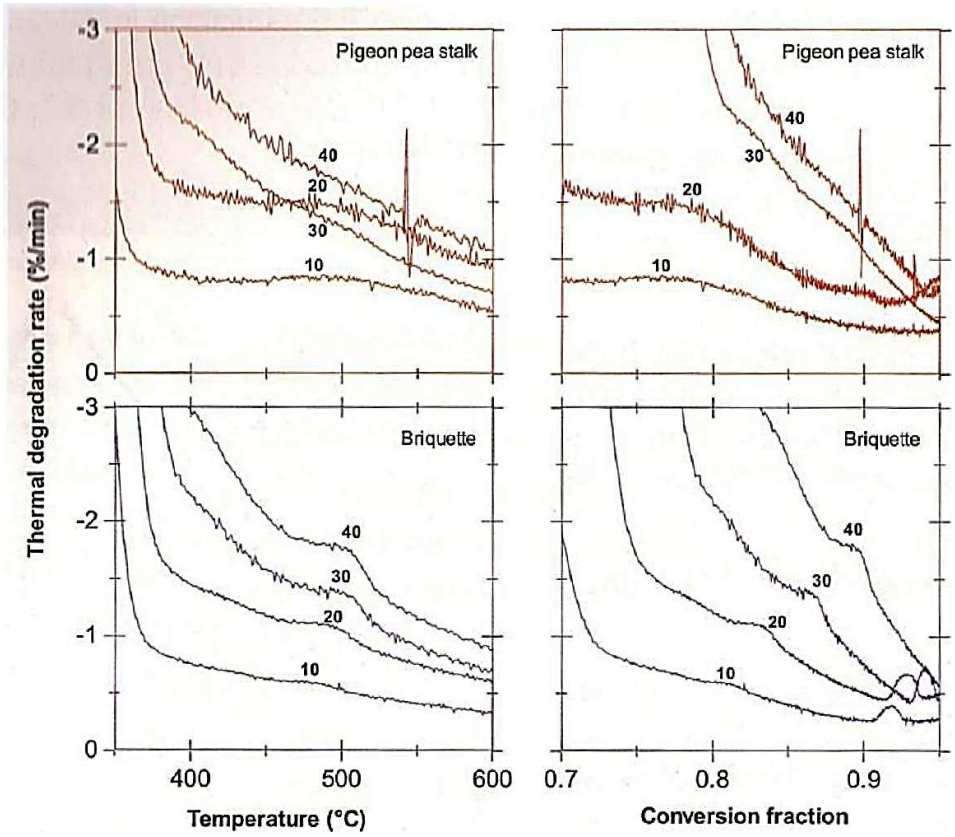

Fig. 8.53 Lignin transitions from raw pigeon pea stalk to briquette (Numbers 10, 20 30 and 40 given near curves are the heating rates (Timin) at which the DTG was obtained

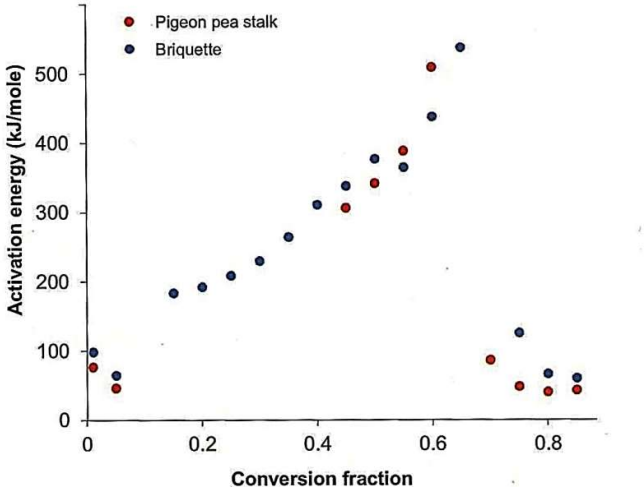

Fig. 8.54 Activation energy profile of pigeon pea stalk and briquette

8.35 Development of entrained gasifier

Under the NICRA program, an entrained gasifier having a height of 1.7m and diameter 300 mm with 50 mm cement insulation on inner side of reactor wall and 50 mm thick ceramic fiber blanket on outer side of reactor has been developed. The gasifier consists of a reactor, an entrained biomass feeding unit, and heating system

to start the gasifier (Fig. 8.55). Biomass feeding unit consists of screw conveyor with pressurized air to mix biomass with air before feeding to the reactor for gasification. The feeding rate during gasification is maintained at 8 to 10 kg per hour through screw conveyor system by rotating the auger at 16 to 18 rpm. The pre heating of biomass to the gasification temperature of 1000-1100°C is achieved by electrical heater fitted in the reactor. The system is operated with particle size between 0.2 to 1.7 mm. The inconsistency in gasification is observed due to fluctuation of temperature inside the gasifier.

Fig. 8.55 Entrained gasifier

8.36 Annular core biochar reactor for generation of char in nitrogen ambient

To achieve oxygen free pyrolysis environment during slow pyrolysis, an annular inner core biochar reactor was developed to accomplish charring under nitrogen environment. The annular inner core biochar reactor was evaluated with pyrolysis of gram stalk under air and nitrogen environment (Fig. 8.56). Annular core biochar reactor was charred at 500°Cin air and in nitrogen, and compared for the adsorbent ability in terms of iodine number (IN). The char must be stable to act as biochar for the purpose of carbon sequestration, i.e., its IN should be low. It was found that the activation level of biochar under nitrogen environment (IN: 250 + 5 mg/g) was comparatively lower than the levels obtained using similar process condition under air environment (IN: 260 + 10 mg/g). Recovery of the biochar was more or less similar in the air and nitrogen environment to the tune of 25-35%. The process conditions for biochar preparation from gram stalk were optimized to be 500°C, 45 min of process time and nitrogen ambience using annular inner core bio-char reactor.

Fig. 8.56 Annular core biochar reactor

8.37 Hybrid dryer for pigeon pea dal

A hybrid (solar biomass) hot air dryer was installed in agro processing centre. The dryer is covered on the outside with UV stabilized solarization sheet (double fold) for intake of solar radiation during day, and is insulated on the inside with polyurethane foam for heat retention. External heating arrangement for operation during the night and under cloudy weather is also provided using two downdraft inverted gasifier above and conduction tubes, placed in plenum chamber. The equipment is equipped with dehydration chamber with six partitioned double-tray racks. During testing, the temperature in solar tunnel area and in the plenum chamber was recorded as 70±10 and 50±10 °C, respectively, when the outside ambient temperature was 34±2 °C. The temperature drop measured inside tunnel during night (evening to morning) was 10±2 °C. Approximate cost of the unit is Rs.1.20 lakh. The dryer was tested with full load (200 kg soaked pigeon pea) at an average ambient temperature of 36±5 °C. Moisture content of wet pigeon pea was found to reduce from 35.8 to 8% (wet basis) in 20 solar hours (8 h/d) compared to 32 solar hours under open sun drying. The dryer also provided dust and contamination free drying environment.

8.38 Biochar production system

This biomass fired biochar production unit of capacity 300-600 kg per batch can produce quality biochar from crop residues in the form of briquettes. This system comprises a cylindrical reactor, combustion chamber, vapour recirculation unit and air supply unit (Fig. 8.57). The reactor is placed inside the insulated combustion chamber lined with refractory bricks for uniform heating. Air is supplied to combustion chamber using an air blower for initiation of burning of fuel. The pyrolyzed gases generated during the production process are recirculated into the

combustion chamber for use as fuel to maintain the reaction temperature. The system has been evaluated with soybean straw and pigeon pea stalks (Fig. 8.58 & Fig. 8.59). The reactor can attain the design temperature of 500°C in 30 minutes. Time required to produce one batch of biochar from crop residues has been found to vary from 1-3 h depending upon type and size of crop residue. The calorific value of biochar produced varies from 24.8 to 26.3 MJ/kg with recovery of bio char in the range of 24 to 27 per cent. The cost of the unit is about 1.25 lakhs.

Fig. 8.57 Biochar production system

Fig. 8.58 Soybean straw and biochar

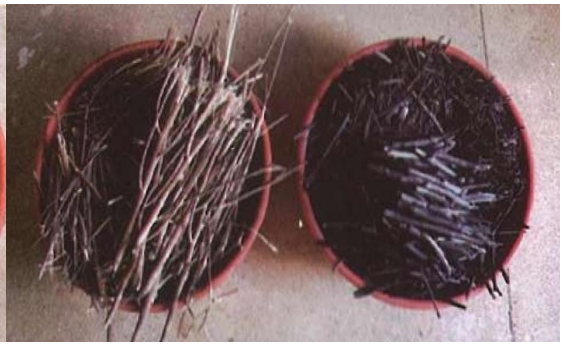

Fig. 8.59 Pigeon pea straw and biochar

- Horizontal drum type reactor with fully biomass based combustion system
- Recirculation of vapour produced to avoid greenhouse gaseous emission
- Calorific value enhancement upto 25%
- Biochar recovery 26-37% with energy efficiency of 33-36%

8.39 Rapid combustion system for thermal application

This forced draft system comprises of a combustion chamber insulated with ceramic fibre blanket, continuous biomass feeding unit with provision for feed control, raiser at the top of the combustion chamber, axial fan for air supply, cladding for thermal safety and sliding ash bin for easy ash collection (Fig. 8.60). The biomass feeding unit and axial fan is operated using a 12V, 7Ah battery. The unit has been tested using 6-8 mm biomass palettes of crop residue (pigeon peas and soybean stalk mixture). The thermal efficiency of combustion system is found to be 35 per cent, which is more than conventional (13 per cent) and CIAE improved (22

per cent) cook stoves of same capacity. The output of the system has been controlled between 5 to 8 kW to suit for various thermal applications such as cooking and steam generation.

Fig. 8.60 Rapid combustion system

8.40 Fluidized bed reactor system for bio-oil production

The developed reactor has a capacity of 20 kg/h of biomass for fast pyrolysis. The system comprises of fluidized bed reactor, free board, cyclone, quencher, recycling unit and feeding unit (Fig. 8.61). Heating coil is wrapped on the outer periphery of main reactor to raise the microcontroller controlled temperature of bed material up to 600°C. Screw type feeding system with variable speed control feeds the ground biomass inside the reactor. A regenerative blower is used to fluidize the bed of alumina and biomass inside the reactor and nitrogen gas used for initial fluidization of bed materials followed by subsequent fluidization using non-condensable pyrolysis vapour. Two stage quencher is used to condense the pyrolysis vapour into bio-oil. The system has been evaluated with ground soybean straw and jute sticks (particle size of 2 mm). The bio-oil recovery is found to be 37 and 41 per cent for soybean straw and jute sticks, respectively. Physical fuel properties of bio-oil obtained from different biomass has been tabulated below. During the four months storage stability study, pH of the bio-oil from soybean straw was found to slightly decrease while the viscosity increased from 1.43 to 1.74 mPas (Table 8.13). Methanol is found to be better solvent in enhancing storage life than ethanol. Bio-oil from the fast pyrolysis has also been synthesized into bio-oil phenol formaldehyde (BPF) resin, a desirable resin for development of phenolic-based material.

Fig. 8.61 Fluidized bed reactor for bio-oil production

Table 8.13 Properties of bio-oil obtained from soybean straw and jute stick

Fuel properties	Soybean	Jute
pH	2.7	5.5
Conductivity, mS	2.6	3.9
TSS, °Brix	28	-
TDS	1.8	-
Viscosity, mPas at 31 °C	1.4	1.3

8.41 Batch type bio-crude production unit

A laboratory level batch type bio-crude production unit capable of converting biomass to bio-crude in slow pyrolysis mode has been developed (Fig. 8.62). The stainless steel reactor has a loading capacity of one kg powdered biomass. Precise temperature control of ambient to 700°C can be achieved. The unit has been tested with recovery of approximately48% biocrude. The condenser has been designed with concept of tube-cell heat exchanger with provision of cleaning in case of excessive tar deposition. There is also provision for injecting nitrogen for maintaining inert atmosphere during pyrolysis process. Pyrolytic behaviour of biomass can be studied in this unit.

Fig. 8.62 Batch type bio-crude production unit

8.42 Portable gasifier with in-built tar cracking system

The portable gasifier has been designed to deliver clean gas with average tar content of 28 mg/Nm^3 (Fig. 8.63). The gasifier unit consists of a reactor with inbuilt tar cracking system. The catalysts bed has been made outside the periphery of the oxidation zone so as to maintain a temperature of catalyst bed around 700°C which is necessary for maximum tar cracking. The air flow rate in the gasifier can be varied for an output of 15-20 kW depending on the biomass and gas composition.

The unit is equipped with two gas cleaning columns. In the first stage, gas is passed through a cyclone separator to separate the large particles of char and then passed through a cooling column filled with steel sponges. The cooling tower is jacketed and water is used for indirect cooling. By this method, gas temperature can be lowered down to 55°C and major part of tar is condensed here. In the second stage, the gas is allowed to pass through a column filled with wood chips and sawdust, and finally through a bag filter for separation of smaller char particles. The unit has been tested with 8mm pellets made from chick pea stalks with an average calorific value of 18 MJ/kg. The average gas composition was found to be 19% CO, 8% H_2, 16% CH_4 and 9% CO_2. Char based catalysts made from pigeon pea stalks and loaded with 2% Ni was used for tar cracking.

Fig. 8.63 Portable gasifier with in-built tar cracking system

8.43 Non-thermal plasma pyrolysis reactor

A non-thermal plasma reactor has been designed and developed to study the thermal degradation of crop residues (Fig. 8.64). The system consists of stain-less steel (SS) main reactor equipped with viewing glass, needle valve for allowing carrier gas in the reactor, passage for high vacuum system and plasma gun. The plasma gun has been designed for generation of plasma arc inside the reactor using molybdenum plate as the cathode and SS sample holder as anode. High vacuum system has been attached with the reactor to generate different levels of vacuum. It consists of the rotary pump, diffusion pump, penning and pirani gauge for vacuum pressure measurement, integrated three ways to control the vacuum inside the reactor. It can generate the vacuum as high as 10-8 bars. The thermal degradation behaviours of crop residues can be studied under different levels of vacuum and plasma intensity in different environment. Generation of free and charged radicals in plasma under different levels of vacuum is one of the important functionalities of the system.

Fig. 8.64 Non thermal plasma reactor

8.44 Production of high porous carbon from pigeon pea

High-porosity carbon was produced from pigeon pea stalk through a two-stage activation process. First, the stalk was carbonized at 300–450°C in an annular core biochar reactor, allowing volatiles to escape and enhance porosity. The resulting char was then activated under a CO_2 atmosphere at 800–900°C. The activated carbon showed an iodine value of 720 mg/g and a methylene blue value of 160 mg/g, comparable to standard activated charcoal (179 mg/g). It contained 85% total carbon, and the average activation energy was 84 kJ/mol.

8.45 Tar cracking in producer gas using Ni-loaded char catalyst

Tar in producer gas creates substantial economic and efficiency loss in gasifier based power plants. Study was conducted to synthesize char based Ni infused catalyst for in situ tar cracking. A Taguchi orthogonal L_9 array has been adopted for the optimization study using chickpea straw pellets. The temperature of catalysts bed was varied from 500 to 700 °C, particle size of char catalysts from 1 mm to 15 mm and bed depth from 200 to 400 mm. The experimental setup consisted of a mini gasifier, an electrically heated tubular reactor, temperature sensors, tar collecting scrubbers and gas analyzer. Producer gas was passed through the hot catalyst bed at various conditions (Fig. 8.65). The samples were passed through two scrubbing bottles filled with isopropanol at 30°C followed by tar-isopropanol separation by distillation at 70°C. Tar cracking efficiency increased with increasing temperature and Ni-loading and observed to achieve in the range of 81 to 86% at optimum loading and bed depth of 0.2 Ni and 300 mm respectively. The final tar content in producer gas varied between 32 to 236 mg N/m^3.

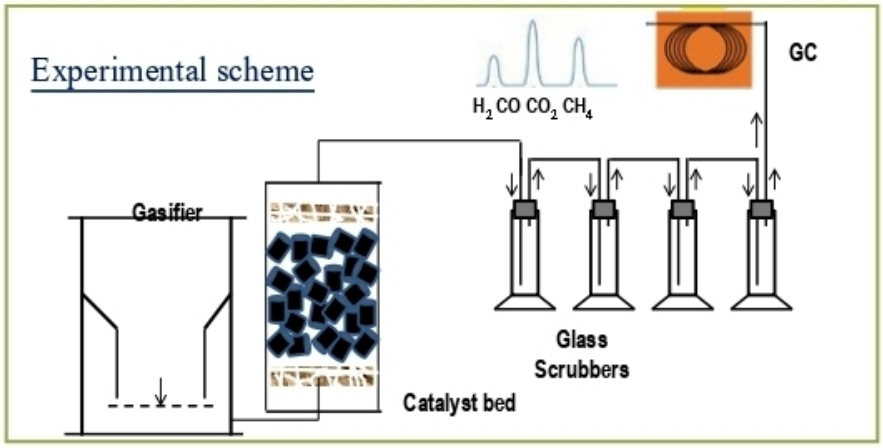

Fig. 8.65 Experimental setup for tar cracking

8.46 Torrefaction system for 200 kg biomass capacity

A pilot-scale torrefaction system with a 200 kg biomass capacity has been developed, equipped with six 9 kW electric heaters and a tilting mechanism for easy discharge of torrefied material (Fig. 8.66). During torrefaction, moisture and hemicellulose are removed, making the biomass dry, brittle, and enriched in cellulose and lignin. Experiments on paddy straw were conducted at 200–300°C for 60–180 minutes to study biopolymeric changes. Samples are being analyzed for moisture content, bulk density, proximate composition, TC, TOC, and TGA. The size and compaction of raw material also affect the process, with recovery ranging from 90–98%.

Fig. 8.66 Torrefaction system

8.47 Synthesis of bio-crude and its fractionation

A bio-crude production unit has been developed to accommodate about one kilogram powdered biomass (Fig. 8.68). The novelty of condenser is that it uses the principle of tube-cell heat exchanger. Water is used as a condensing medium which is allowed to flow in the outer jacket of the condenser unit by a centrifugal pump.

The cleaning of the tubes can be done easily by opening the condenser system. The bio crude vapour is immediately passed through the heat exchanger to condense the bio crude from gas. The institute has also developed a process and technology for value added products from segregated bio-crude. For that a bio-crude segregation unit is developed which has annular core concept. The output of the main reactor was connected with segregated collection system for collection of segmental condensate in five different chambers to segregate the biocrude in different segments having different carbon chains. Unit has been tested for dry run. The on-load runs are under progress.

Fig. 8.68 Bio-crude production unit

8.48 Single Step Activation of Pigeon Pea Stalk Char for Higher Adsorption Capacity

A single-step activation process was developed to enhance the adsorption capacity of pigeon pea stalk char (Fig. 8.69). The biomass was first carbonized at 450 °C for 45 minutes to remove volatiles, after which the temperature was raised to the desired activation level and CO_2 was introduced for activation. Process parameters were controlled using a profile PID controller. The resulting activated carbon showed iodine values between 449 and 751 mg/g, with recovery ranging from 7–25%. Activation temperature and time had a strong influence on product quality, with the highest iodine value achieved at 900 °C for 60 minutes. A second-order polynomial model effectively correlated process variables, showing strong agreement between experimental and predicted values (R = 0.96 for recovery and 0.94 for iodine value).

Fig. 8.69 Single Step Activation of Pigeon Pea Stalk Char

8.49 Inbuilt Tar Cracking in Portable Gasifier

A portable downdraft gasifier has been developed to generate low-tar producer gas without relying on water-based scrubbing (Fig. 8.70). Tar reduction is achieved through the use of char-based nickel catalysts integrated into the system. The main reactor features a conical throat design to ensure smooth downward flow of the feed material. A grate positioned below the throat supports the fuel bed and separates ash, while a stirrer enables intermittent agitation to maintain uniform fuel movement and prevent clinker formation. The catalyst bed is strategically placed around the oxidation zone and directly after the reduction zone, allowing the hot producer gas to pass through it immediately. This ensures effective thermal cracking of tar compounds. The gasifier can hold up to 60 kg of fuel pellets, and provisions have been made for intermittent fuel feeding to support continuous operation. The final range of tar in the gas is observed in the range of 28-56 mg/Nm^3 having a heating value of 5.1-6.9 MJ/m^2. The fuel consumption in the developed gasifier is observed as 10-12 kg/h. The composition of producer gas is CO: 16-24%, H_2:18-20%, CH_4: 2.7-6.7%, and O_2: 3.4-7.7%.

Fig. 8.70Portable dual stage downdraft gasifier

8.50 Portable Gasifier Based Gen-set

Portable gasifiers offer a practical solution for decentralized biomass-to-power conversion, making them ideal for rural energy needs and for utilizing locally available biomass and crop residues. A portable gasifier system with a dry-type tar cleaning unit has been developed and integrated with a diesel generator to produce 2 kW of electrical power from biomass pellets (Fig. 8.71). The system uses a downdraft gasifier (450 mm diameter, 1000 mm height) capable of holding 30 kg of pellets, providing up to 8 hours of continuous operation. The overall unit dimensions are 1000 × 1200 mm. A microcontroller-driven rotating grate ensures smooth fuel movement, while a 20 W DC blower supplies primary air. Temperature sensors are installed at the gas outlet and cooling water tank for real-time monitoring. The system consumes an average of 3.5 kg/h of fuel, with charcoal catalyst requirements of 5.2 kg for every 30 hours of operation. It delivers a gas production rate of 17.8 m^3/h at an airflow rate of 8.5 m^3/h, with tar content maintained between 0.6 and 6.2 mg/Nm^3.

Fig. 8.71 Portable Gasifier Based Gen-set

8.51 Screw Pyrolyzer for Continuous Biochar Production

Biochar improves soil water-holding capacity, reduces methane emissions, and enhances crop yield, but conventional biochar production relies on energy-intensive processes that emit CO_2. To address this, a continuous auger-type pyrolysis unit was developed for eco-friendly, large-scale biochar and bio-oil production (Fig. 8.72). The reactor (1200 mm × 300 mm) is heated using producer gas from an auxiliary gasifier, with the screw driven at 2–30 rpm. Biomass is fed and discharged through rotary airlock valves, enabling a feeding capacity of 28 kg/h with an energy use of 1.2 kWh/h. At 450°C, biochar yield is about 34%, and production cost is approximately Rs. 23/kg. Pyrolysis gas is recycled to maintain reactor heating, making the system suitable as a pilot-scale model for industrial adoption.

Since powdered biochar is difficult to apply in the field, a granulator was also developed to produce biochar granules using clay or starch as binders. The 2 hp granulator operates at 360 rpm with a capacity of 128 kg/h and an energy consumption of 1.5 units, producing granules at Rs. 3.4/kg. Weighing only 60 kg, the unit is easy to operate, maintain, and compatible with common fertilizer applicators.

Fig. 8.72 Screw Pyrolyzer

8.52 Biomass based hot air generation system

Large quantities of biomass generated from farms, agro-industries, and post-harvest operations can be efficiently utilized for hot air generation in drying applications. A biomass-fuelled hot air generator (HAG) was designed and developed to convert biomass briquettes into hot air for industrial and commercial use (Fig. 8.73). A 25 kW prototype HAG was developed consisting of a biomass combustor and a heat exchanger to recover heat from flue gases. The combustion chamber, fabricated from 16-gauge stainless steel (SS-304), is equipped with a manual fuel feeder, a grate for ash removal, and an 85 W forced-draft fan to ensure efficient combustion. The heat exchanger incorporates parallel, cross, and counter-flow heat exchange paths with baffles to enhance heat transfer efficiency. Preheated air at about 40 °C enters the heat exchanger, and three separate fans are provided for primary air supply, preheated air circulation, and exhaust air removal. Using biomass briquettes at a feed rate of about 5 kg h^{-1}, the system produced hot air velocities ranging from 1.5 to 4.0 m s^{-1} with corresponding outlet temperatures of 210–220 °C and 115–120 °C, respectively.

The HAG was integrated with a tray-type drying chamber fitted with wire-mesh trays and evaluated for drying tomato slices. The system achieved an overall drying efficiency of 31% over a drying period of 15 h, reducing the moisture content of tomatoes to about 14%. The overall thermal efficiency of the unit was 40%, with combustion and heat-exchanger efficiencies of 54% and 76%, respectively. The operating cost of the hot air generator was estimated at ₹195 h^{-1}, while the total unit cost was approximately ₹2.5 lakh. The developed biomass-based HAG

effectively reduces fuel consumption and drying costs, making it suitable for micro- to small-scale processing units and domestic drying applications.

Fig. 8.73 Hot Air Generation System

8.53 Bio-hydrogen generation from methane through catalytic reforming

This research focuses on the production of hydrogen (H_2) from methane through catalytic pyrolysis, aiming to develop an efficient and sustainable process. A reactor for methane pyrolysis was fabricated, equipped with a 12 kW heating element with an effective length of 1000 mm and a diameter of 300 mm, insulated with ceramic blankets to ensure uniform heat distribution (Fig. 8.74). Catalysts were prepared using coconut husk–derived char and alumina balls (2–3 mm), with nickel (Ni) impregnated at 5, 10, and 15% to enhance catalytic activity. The porous structure of the sawdust char and alumina support provides a large surface area, facilitating the adsorption and activation of methane molecules, while strong metal-support interactions between Ni nanoparticles and the support improve catalyst stability.

Preliminary experiments with char-based catalysts at 800 °C and a methane flow rate of 2 L/min showed hydrogen concentrations of 88–92% during the first 40 minutes, stabilizing at 55% after 120 minutes. Methane conversion reached up to 98% initially and maintained 80% over 120 minutes, indicating high catalytic performance and stability (Fig. 8.75). During the process, multi-walled carbon nanotubes (MWCNTs) were formed, with diameters and wall thicknesses measured at 13 nm and 11 nm, respectively, through SEM and TEM analyses.

The study systematically evaluated the effects of temperature, gas flow rate, and catalyst loading on hydrogen production, providing insights for process optimization. Overall, the alumina-sawdust char–supported Ni catalyst demonstrates strong potential as an efficient and sustainable material for hydrogen generation from methane pyrolysis, combining high hydrogen yield, catalyst stability, and value-added byproduct formation in the form of carbon nanotubes.

Fig. 8.74 Reactor for methane pyrolysis

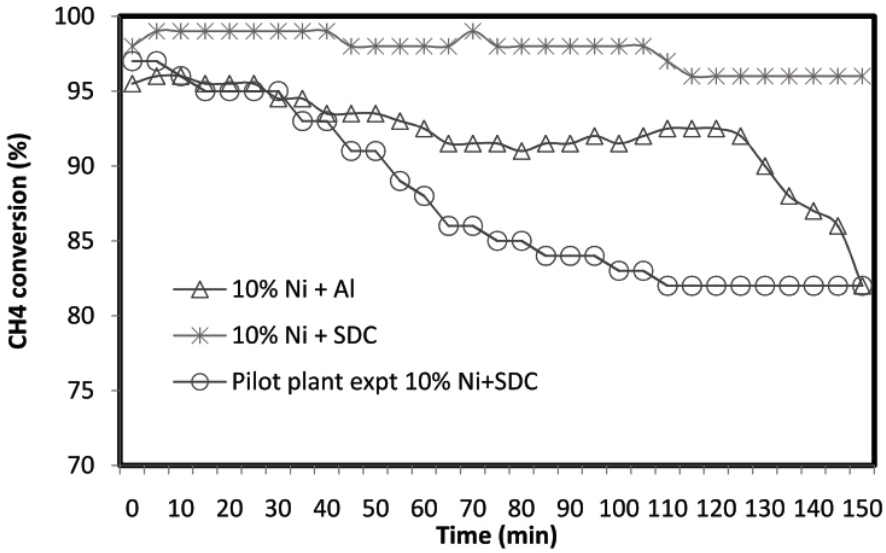

Fig. 8.75 Methane conversion rate (%) using methane pyrolysis reactor

8.54 Generation of supercapacitor grade carbon from crop residues

The synthesis of nanoporous carbon from chickpea stalk through chemical and thermal activation using potassium hydroxide (KOH) was studied (Fig. 8.76). The synthesized nanoporous carbon was thoroughly characterized and applied in for energy storage. Activation of the chickpea stalk was performed under an inert nitrogen atmosphere at varying activation times (30, 60, and 90 minutes) and temperatures (750, 800, and 850 °C). The chemically activated nanoporous carbon was successfully tested as a super capacitor electrode material for the first time, demonstrating its potential in energy storage applications. Comprehensive characterization of the raw chickpea stalk and the prepared nanoporous carbon was conducted using Thermogravimetric analysis (TGA), proximate analysis, adsorption analysis, BET surface area analysis, SEM, XRD, and FTIR spectroscopy. Thermogravimetric analysis revealed that the chickpea stalk undergoes mass loss in three stages, with major volatile degradation occurring between 143–374°C.

Adsorption analyses revealed that the nanoporous carbon exhibited high microporosity and mesoporosity.

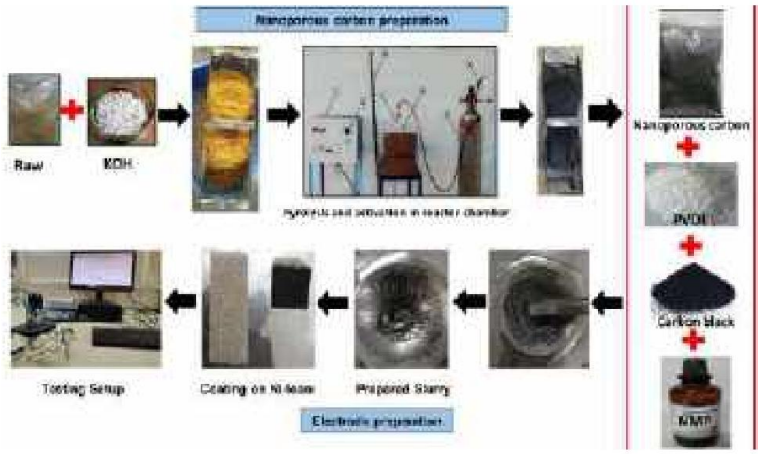

Fig. 8.76 Process for generation of supercapacitor grade carbon

The BET surface area analysis showed that all the prepared nanoporous carbon samples possessed micro and mesopores. The highest surface area (1239 m^2/g) and pore volume (0.60 cm^3/g) were recorded for sample CT9 (temperature 850°C, holding time 90 min, and heating rate 10°C/min). SEM imaging revealed interconnected micro and mesopores in the prepared nanoporous carbon. FTIR analysis indicated functional groups such as alcohol group (O–H), ester group (C–O), carbon dioxide (O=C=O), and carboxylic acid (O–H) significantly improved the interaction between the material and electrolyte ions. Electrochemical performance was evaluated using a three-electrode setup with 1M KOH as the electrolyte. Cyclic Voltammetry (CV), Galvanostatic Charge-Discharge (GCD), and Electrochemical Impedance Spectroscopy (EIS) were employed to analyze the nanoporous carbon as an electrode material. The results showed that the nanoporous carbon-based electrode exhibited a specific capacitance of 343.29 F/g at a current density of 1.0 A/g, an energy density of 48 Wh/kg, and a power density of 495 W/kg, along with excellent cycling stability. The equivalent series resistance was measured at 1.06 Ω. These findings indicate that chickpea stalk-derived nanoporous carbon is a promising biomaterial for high-performance super capacitors and energy storage devices.

8.55 Plasma treatment of crop residues for improved characteristics

Plasma-based treatment of lignocellulosic biomass is an emerging, innovative, and eco-friendly approach to modifying structural and physicochemical properties of crop biomass. In this study, chickpea stalk powder was subjected to cold plasma exposure for 15, 30, 45, and 60 minutes under controlled low-pressure conditions. The high-voltage plasma generated reactive species that interacted with lignocellulose components, inducing significant molecular and surface-level alterations. XRD analysis revealed notable changes in crystallinity, with 15 and 60

minute treatments enhancing crystalline structure, while the 30-minute exposure caused partial amorphization, reflecting plasma-driven rearrangement of hydrogen bonding networks. BET surface area analysis showed an initial reduction from 0.859 to 0.045 m^2/g after 15 minutes, followed by an increase in pore diameter and volume at 30 minutes, indicating expansion of microporous structures due to plasma etching.

CHAPTER – 9

9.Liquid Biofuel Technologies

Liquid biofuels are renewable fuels derived from biological sources such as vegetable oils, animal fats, agricultural residues, and algae. The most common types are bioethanol and biodiesel, which can partially or fully replace conventional petrol and diesel in engines. They help reduce dependence on fossil fuels, lower greenhouse gas emissions, and promote the use of agricultural by-products. Liquid biofuels are considered an important component of sustainable energy systems, especially in the transportation and agricultural sectors.

9.1 Oil extraction from Jatropha oil seed for bio-diesel production

The physical properties of the Jatropha seed were assessed. Based upon 100 seeds, the average length anti diameter of the seed were 18 mm and 8.9 mm respectively. Average weight, moisture content and bulk density of the seeds were 7.6 g, 7.38% (wb) and 0.45 g/cm^3, respectively. The hull content and oil content of the seed (on dry seed weight basis) were 34.4% and 30%, respectively.

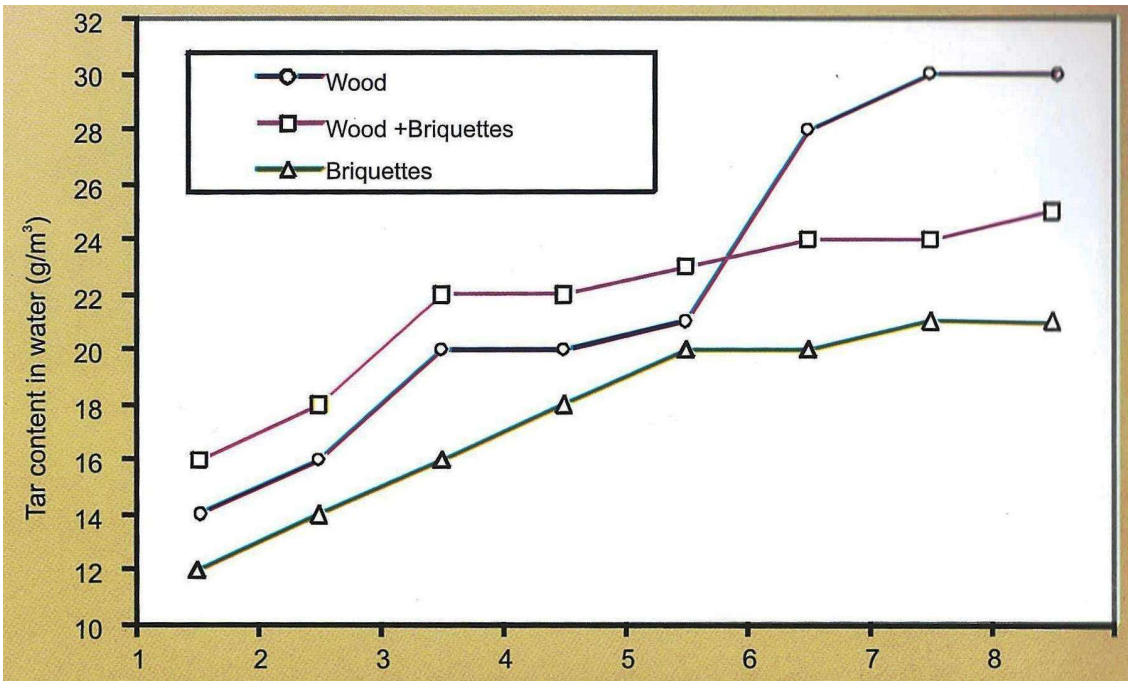

Fig. 9.1 Influence of fuel type on tar content of conditioning water of updraft gasifier

The oil extraction study of Jatropha seed was carried out in a commercial screw press type oil expeller (40 kg/h capacity) with different treatments. The steam pre-treatment to the seed (for one hour at 90-95°C) was favourable for oil extraction. Oil recovery was improved by mixing the groundnut hull or paddy husk with the cake after first pass of oil expelling. Steam pretreated seed, without adding hull, gave poor (11-13%) oil recovery. The pre-treated seed mixed with groundnut hull gave. 30-35% recovery and seed mixed with paddy husk gave recovery up to 75% of available oil.

9.2 Evaluation of selected vegetable oils as alternate fuel for the C.I. engines

The soybean oil–diesel and Mahua oil–diesel blends were evaluated as alternative fuels for a 5 hp, single-cylinder, water-cooled, naturally aspirated CI engine (Fig. 9.2). Soybean oil blends ranging from pure diesel to pure oil were tested for one hour at different loads after steady-state conditions were reached. Results showed that specific fuel consumption increased with both load and higher soybean oil content (Table 9.1). Exhaust gas temperature rose slightly by 0.33–1.93% for the 20:80 SO:HSD blend, while the 40:60 and 60:40 blends caused small temperature drops at moderate loads but increases at higher loads. CO emissions decreased up to 40% load for the 20:80 and 40:60 blends but rose with higher soybean oil content. CO_2 emissions were lower at low loads for the 20:80, 40:60, and 60:40 blends but increased with load. Importantly, NO emissions consistently decreased for the 60:40 blend, and selective reductions were observed for the 20:80 and 40:60 blends. A notable decline in SO emissions occurred at 60% and 80% loads for the 20:80 blend. Engine performance with Mahua oil–diesel blends (20:80 and 40:60) showed similar trends. With the 20:80 MO: HSD blend, SFC and exhaust temperature increased only slightly compared to diesel. At 100% load, MO: HSD (20:80) produced CO: 4086–4384 ppm, NOx: 876–896 ppm, and SO_2: 16–50 ppm (Table 9.2).

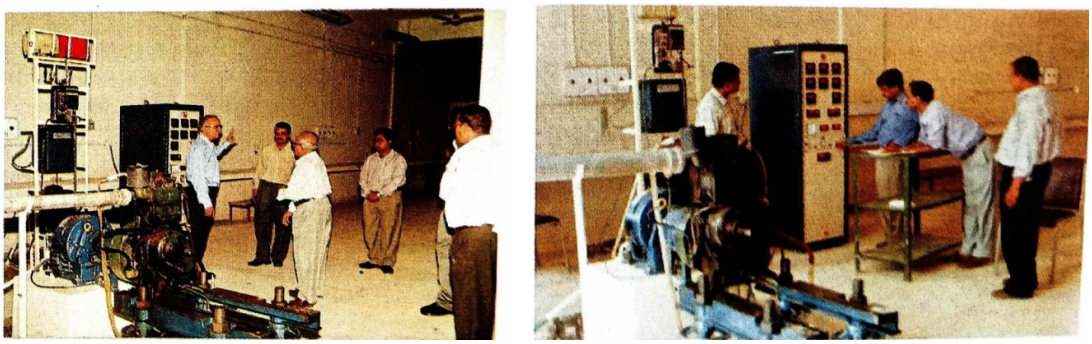

Fig. 9.2 Test set up for conducting the performance test of the engine using prepared fuels

Table 9.1 Percentage variation in SFC and exhaust gas temperature of the engine fuelled with the various blends of soybean oil and HSD at various loads

Load	Test fuel blends									
	SO:HSD (0:100)		SO:HSO (20:80)		SO:HSD (40:60)		SO:HSD (60:40)		SO:HSD (80:20)	
	SFC (g./kWh)	Exhaust gastemp. (°C)	Percentage increase in SFC of the test engine fueled with the various test fuels as compared to HSD at various loads							
			SFC	LGT	SFC	LGT	SFC	LGT	SFC	LGT
20	594.5	104	0.841	1.031	2.943	-4.64	6.442	-1.031	10.345	5.67
40	387.5	248	1.239	+0.806	1.239	-2.016	7.742	2.823	47.974	32.66
60	321.2	303	0.903	0.33	1.526	-0.33	8.500	4.62	NR	NR
80	288.1	362	2.360	1.934	4.339	3.591	10.864	8.84	NR	NR
100	275.1	448	4.653	0.67	6.289	2.23	12.032	8.03	NR	NR

Note (+) indicates percentage increase, (-) indicates percentage decrease

Table 9.2 Percentage increase/ decrease in the exhaust emissions of the test engine fuelled with the various blends of soybean oil: HSD at various loads

Measure engine exhaust emissions	Load (%)	Test fuel blends			
		SO : HSD(0:100)	SO:HSD (20:80)	SO:HSD (40:60)	SO:HSD (60:40)
		Exhaust emissions	Percentage increase/ decrease in the exhaust emissions of the test engine fuelled with various blends of soybean oil and HSD as compared to HSD at various loads		
CO (ppm)	20	1097	2.92	5.01	20.42
	40	1175	6.89	0.51	20.68
	60	1101	3.63	12.44	34.15
	80	1130	46.02	71.15	63.72
	100	1639	45.21	118.36	80.29
CO_2 (%)	20	3.03	1.65	8.91	35.97
	40	4.48	0.89	2.23	4.91
	60	5.64	1.24	2.84	1.77
	80	6.32	25.47	19.3	10.6
	100	8.04	2.36	9.95	10.82
NOx (ppm)	20	173	10.4	17.92	4.62
	40	325	1.54	0.31	4.92
	60	532	0.75	0.38	13.72
	80	645	1.55	10.85	16.21
	100	752	4.26	13.43	16.22
SO_2(ppm)	20	0	0	0	3
	40	0	0	9	19
	60	9	66.67	177.78	322.22
	80	24	8.33	245.83	287.5
	100	51	15.69	264.7	298.04

Noise measurements with neat diesel showed levels rising from 92 dB(A) at minimum load to 99.1 dB(A) at full load (measured at 1 m distance and 1.2 m height). Using MO:HSD (20:80) did not significantly change noise levels. The equivalent continuous sound pressure level (Leq) increased linearly from 89.1 to 94.5 dB(A) from 0–100% load and crossed the 90 dB(A) permissible limit at 40% load, limiting safe operator exposure to 2–4 hours at higher loads. One-octave spectrum analysis showed sound levels peaking near the engine's rated rpm (around 1000 Hz) and decreasing beyond 2000 Hz (Table 9.3).

Mechanical vibrations measured at various engine components showed that vibration displacement exceeded the recommended 100 μm limit on the rocker-arm cover at all loads, and on engine mounting bolts above 40% load, indicating the need for improved vibration control.

Table 9.3 Mechanical vibrations at various engine components

Components	Mechanical vibrations in mm					
	No load	20% load	40% load	60% load	80% load	100 load
Engine mounting base bottom	69	80	67	72.5	76	79
Engine mounting base top	60	56	52	62	65	60
Engine mounting bolts	84.5	90	200	153	190	120
Timing gears cover	60	65	70	61	67	50
Crankcase body	65	72	65	100	70	66
Cylinder head top	85	79	340	100	95	88
Rocker-arm covering	122	152	173	176	166	133
Top of eddy current dynamometer	5.5	3.8	3.75	3.8	1.5	2.0

9.3 Esterification of non-edible oils for production of quality bio-diesel to energize stationary IC engines

Jatropha and Karanja seeds were procured for biodiesel research, and preliminary characterization showed Jatropha oil density in the range of 0.9274–0.9278 g/ml. Oil extraction through a commercial expeller yielded about 20% oil. An experimental setup was developed for esterification of non-edible oils, and process parameters for Karanja oil were optimized using 20% methanol, NaOH/KOH catalyst, a reaction temperature of 60 ± 5°C, and 400 rpm stirring for one hour, resulting in 90–91% Karanja Methyl Ester (KME) (Fig. 9.3). Based on these results, a 5-litre laboratory biodiesel production unit was designed (Fig. 9.4).

Further optimization was carried out for Jatropha oil, where KOH catalyst concentration and alcohol quality were standardized. Using commercial ethanol, Jatropha Ethyl Ester (JEE) recovery ranged from 84–88%, while methanol-based transesterification resulted in 90–93% ester yield. A 50-litre batch-capacity biodiesel plant consisting of a reactor, settling tank, washing tank, and drying unit was developed and evaluated (Fig. 9.5). The calorific values of diesel and biodiesel were found to be 47.4 and 35.9 MJ/kg, respectively.

Fig. 9.3 Laboratory scale unit for production of bio diesel

Fig. 9.4 Prototype of 50 L/batch capacity bio-diesel plant

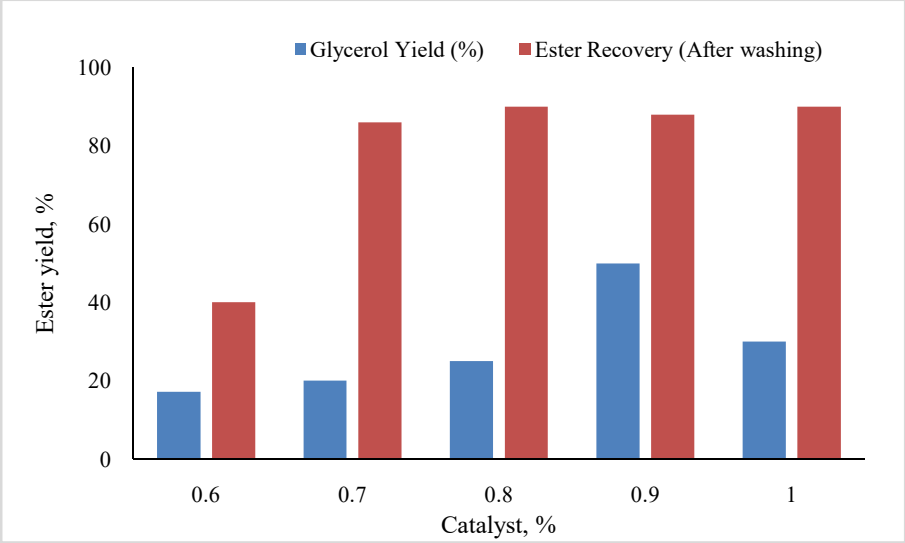

Fig. 9.5 Effect of catalyst on yield of ester from Karanja

Engine Evaluation with Biodiesel

A 3.7 kW CI engine was tested using blends of KME and diesel (B-0 to B-100). Brake specific fuel consumption (BSFC) decreased with load but increased with biodiesel proportion because of its lower heating value. Minimum BSFC was 306.8 g/kWh for diesel and the highest was 361.8 g/kWh for B-100 at full load. Brake thermal efficiency improved with load across all blends. Exhaust temperatures were 472–505°C at full power; CO emissions increased with load, NO/NOx showed increasing trends with brake power, while SO_2 emissions were negligible (Table 9.3). Smoke opacity and engine vibration increased with biodiesel content.

Table 9.3 Effect of various fuel blends on brake specific fuel consumption at various power ratings

Fuel blends	Brake specific fuel consumption (g/kW h)					
	0.27 kW	0.69 kW	1.49 kW	2.23 kW	2.97 kW	3.70 kW
B-0	1551.7	658.7	404.3	338.7	310.0	306.8
B-20	1617.5	694.6	431.5	357.3	330.4	315.9
B-40	1750.2	730.8	459.1	376.2	350.9	342.7
B-60	1822.3	760.9	469.5	389.5	356.1	348.5
B-80	1895.6	771.7	477.6	393.4	361.7	353.4
B-100	2057.1	808.4	480.9	397.7	372.4	361.8

A tractor engine was also tested using blends of Jatropha ethyl ester (Fig. 9.6). BSFC decreased with increasing load but increased with higher biodiesel substitution. At rated power, BSFC ranged from 321 to 391 g/kWh, showing up to 21.8% increase due to biodiesel's lower calorific value. Brake power efficiency improved with higher JEE blending. CO emissions decreased significantly with higher biodiesel blends (B-30 to B-50), while NO emissions increased slightly. Smoke opacity increased with load but was about 10.9% lower for biodiesel than diesel.

Fig. 9.6 Testing of tractor with blending of JEE in petro-diesel at load.

9.4 Evaluation of tractor engine using blends of treated jatropha oil and petro diesel

The properties of jatropha oil such as density, viscosity, flash point, fire point, cloud point, pour point and calorific value were determined for various fuel blend ratio (5:95 to 30:70). The effect of temperature on density and viscosity of jatropha oil was measured for both raw and treated oils. The brake specific fuel consumption (BSFC), engine efficiency, exhaust gas temperature, smoke density, noise, and vibration levels were determined during the engine operation with different blends of raw jatropha oil with petro-diesel, for different power ratings. The BFSC increased with increase in blend ratio, and decreased with increased in engine load. The engine efficiency increased with the increase in blend ratio and engine load. The exhaust gas temperature increased with increase in blend ratio and engine load. The smoke opacity also increased with increase in blend ratio and engine load.

9.5 Adoption of suitable process for production of alcohol from agro-residues and development of a laboratory scale plant for alcohol production

Ethanol production from agro-residues such as paddy straw and maize stalk was studied using heat and alkali-pretreated biomass followed by enzymatic hydrolysis and fermentation with Saccharomyces cerevisiae (Fig. 9.7 & 9.8). Pretreated paddy straw hydrolysed with commercial cellulase produced a suitable substrate for fermentation. Enzymatic treatment significantly enhanced saccharification, yielding a maximum of 34.68% (w/w) reducing sugars in 2 hours, compared to only 0.42% without enzymes. Yeast metabolism further improved release of fermentable sugars, and the alcohol yield after enzyme-assisted fermentation reached 1.1 g%, with a fermentation efficiency of 44.35%, whereas only 0.18 g% alcohol was obtained without enzymes.

Energy consumption analysis showed that size reduction and grinding required 0.066 kWh/kg for rice straw and 0.056 kWh/kg for maize stalk. Further grinding to 0.1–1.5 mm sizes required 2.1 kWh/kg for paddy straw and 1.42 kWh/kg for maize stalk. The cellulose content of paddy straw, standardized using Updegraff's method, was 55% (dry basis), and the maximum volumetric ethanol productivity achieved was 0.230 g/L/h (11 g in 48 h). Based on the optimized parameters, a 0.5L per batch laboratory-scale alcohol production plant was designed, fabricated, and installed. The system consisted of a fermentation reactor, filtration assembly, and primary plus fractional distillation units. About 6 kg of paddy straw and maize stalk powders were pretreated with 2% NaOH, autoclaved at 15 psi, washed, and

enzymatically hydrolysed (Palcosoft Super 720). Yeast inoculum and nutrients were added to initiate fermentation, followed by distillation of the fermented broth.

The plant operated satisfactorily, producing approximately 0.6 L of ethanol per batch from paddy straw. The yield corresponded to 290 mL alcohol/kg of paddy straw (45% alcohol), equivalent to 120 mL/kg in absolute alcohol. Maize stalk performed better, yielding 330 mL/kg (57% alcohol), equivalent to 188 mL/kg absolute alcohol. These results demonstrate the feasibility of producing bioethanol from agro-residues using optimized pretreatment, enzymatic hydrolysis, and controlled fermentation in a small-scale plant.

Fig. 9.7 Fermentation and primary distillation unit

Fig. 9.8 Fractional distillation unit

9.6 Alcohol production from agro-residues

A 5.0 L/batch capacity alcohol production pilot plant (laboratory scale) was designed for alcohol production from agro-residues. The pilot plant consisted of filtration unit, fermentation unit, primary distillation and fractional distillation unit. The absolute ethanol yield from the ground alcohol from paddy straw and maize stalk were 100-120 ml/kg and 160-180 ml/kg, respectively. The maximum energy (55-60%) was required for process of distillation (primary distillation and fractional distillation). Energy for other processes, physical treatment, thermochemical treatment, hydrolysis wore 15-22%, 16-17%, 6.3-6.8% respectively.

9.7 Process Protocol for Extraction of Lipid from Microalgae for Biofuel Production

Microalgae are important organisms for the production of value-added products and lipids in the field of renewable energy. A facility to extract lipid from microalgae biomass has been developed in the institute. This system can handle biomass up to 3 kg and a solvent of 15-20 L. Trials have been conducted to extract lipids from the microalgae biomass with five extraction cycles for each operation. The lipid from 0.5 kg micro-algae biomass has been extracted using seven litre hexane at 70 °C for 2 h. Separation of lipids from the solvents and recovery of solvents have been carried out at 70 °C through a rotary evaporator, with a solvent recovery of 65%. The average lipid content of the microalgae harvested using hydrolysate media is about 17% (Fig. 9.8).

Fig. 9.8 Process protocol for lipid extraction from microalgae biomass for biofuel production.

Chapter - 10

10.Energy Management in Agriculture

10.1 Energy Inflow and Outflow Analysis for Production of Soybean Crop

Energy input in the soybean crop is increasing due to the increasing demand for fertilizers and chemicals. The energy input scenario has been assessed for central India. Data collected from 120 farmers from the eleven villages of the Vindhya plateau based on the random selection method have been analysed. Farmers under marginal (2 ha) have been considered to calculate the energy requirement for soybean crop production. The total energy inputs and outputs have been depicted in the figure. Fertilizer is the most energy-intensive source followed by fuel and seed. The contribution of fuel energy in the energy matrix has been maximum in seedbed preparation (62%) followed by harvesting, threshing (21%), and sowing operation (16%)(Fig.10.1). Energy inputs and grain productivity are increased from marginal to other categories of farmers.

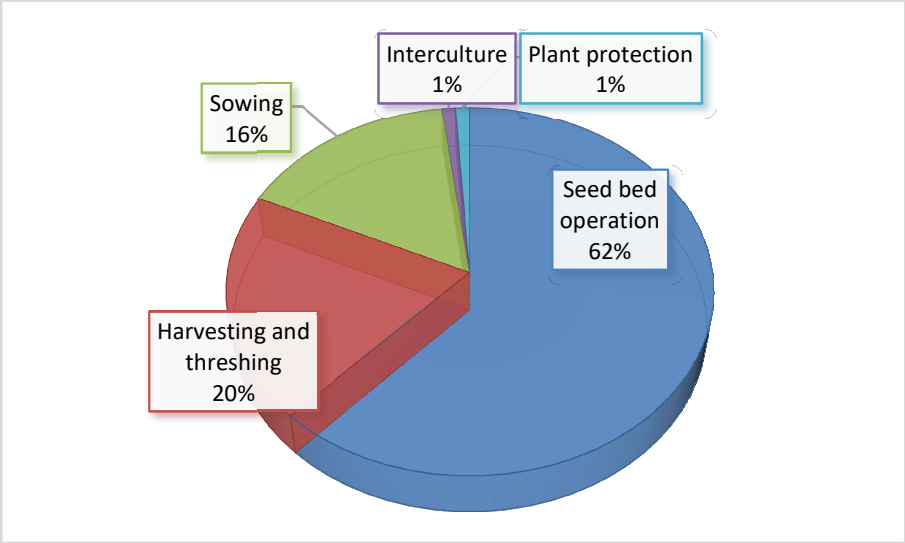

Fig.10.1 Contribution of fuel energy in different operations

10.2 Crop Residue Availability Assessment in Madhya Pradesh

A study was conducted across 30 villages in different agro-climatic zones of Madhya Pradesh to assess the availability of crop residues. Data were collected through farmer interviews, field visits, and crop sampling at harvest to determine straw-to-grain ratios and estimate total and recoverable residues. Wheat–soybean was the dominant cropping pattern, with about 60% of farmers using combine harvesters for wheat and most using them for soybean.The average straw-to-grain ratios were 1.5:1 for wheat and 1.8:1 for soybean, varying by variety. Based on field samples, the theoretical residue generation was 5.8 t/ha for wheat and 2.8 t/ha for soybean, whereas farmers reported lower values (3.8 and 1.6 t/ha), indicating collection losses. Using the estimated ratios, total residue availability in Madhya Pradesh was calculated at 12 Mt for wheat and 8.5 Mt for soybean (Fig. 10.2).

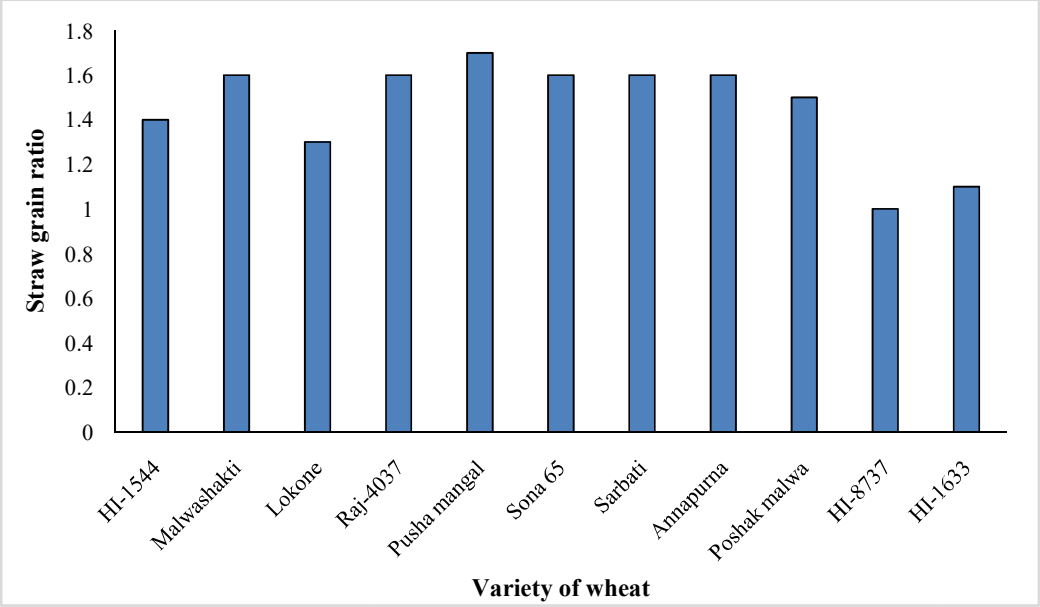

Fig.10.2 Straw grain ratio for different wheat variety

A study of 300 soybean–wheat farmers in Madhya Pradesh revealed total energy inputs of 9,923 MJ/ha for soybean and 19,453 MJ/ha for wheat, with energy productivity of 0.11 and 0.23 kg/MJ, respectively. Using Data Envelopment Analysis (DEA) through CCR and BCC models, efficient and inefficient farmers were identified. DEA indicated potential operation-wise and source-wise energy savings of 27% and 35% in wheat, and 36% and 38% in soybean. Fertilizer application was the most energy-intensive operation in soybean (45%), followed by sowing (27%) and seedbed preparation (13%). For wheat, irrigation consumed the most energy (36%), followed by fertilizer application (34%) and sowing (15%)(Fig. 10.3).

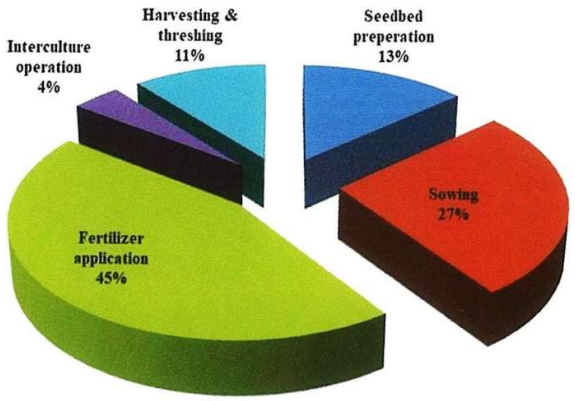

Fig.10.3 Operation-wise energy input distribution in soybean and wheat cultivation

10.3 Analysis of energy and carbon footprint in rice milling

The study collected data from three rice milling plants in Bramhapuri, Maharashtra, with capacities of 4 TPH, 8 TPH, and 12 TPH. The energy consumption and carbon emissions were analysed across various stages of rice milling, including cleaning, hulling, whitening, polishing, and others. The process flow for each milling stage was mapped, and energy usage and CO_2 emissions for each stage were

recorded. A breakdown of energy input (in MJ per tonne of rice) and CO_2 emissions (in kg CO_2 equivalent per tonne) was calculated for each mill capacity, providing insight into the energy demands and environmental impacts of each operation (Table 10.1). The study revealed varying trends in energy consumption and CO_2 emissions across different milling capacities. While larger mills (8 TPH and 12 TPH) showed improved efficiency in most processes, certain stages like whitening and polishing remained major energy consumers, contributing over 50% of total energy and emissions in the 4 TPH mill, and 45%-50% in the 8 TPH and 12 TPH mills.

Table 10.1 Process-wise energy input and carbon dioxide emissions of rice mills

S. No.	Process	Energy input, MJ.T^{-1}			Carbon-di-oxide emission, kg CO2eq. T^{-1}		
		4 TPH	8 TPH	12 TPH	4 TPH	8 TPH	12 TPH
1	Cleaning	59.65	42.01	37.66	4.41	3.11	2.80
2	Hulling	59.29	61.54	59.66	4.42	4.58	4.44
3	Paddy	14.17	10.41	6.94	1.04	0.77	0.51
4	Thick grading	5.79	2.31	6.07	0.43	0.17	0.45
5	Whitening	278.40	213.24	177.03	20.74	15.89	13.19
6	Tip separation	8.31	11.44	8.54	0.61	0.85	0.63
7	Polishing	278.80	172.75	157.47	20.78	12.88	11.74
8	Colour sorting	23.98	24.84	27.90	1.78	1.84	2.07
9	Length grading	30.74	29.56	37.83	2.28	2.19	2.81
10	Dust cyclone	42.33	24.50	23.01	3.16	1.83	1.72
11	Bran cyclone	98.08	118.10	117.30	7.31	8.81	8.75
12	Bran & Tip	53.53	42.39	38.60	3.99	3.16	2.88
13	Packaging	25.29	11.52	10.30	3.16	1.71	1.42
	Total	978.37	764.61	708.31	74.09	57.79	53.41

10.4 Energy inflow outflow assessment of soybean wheat cropping system of selected villages of MP

The survey and data collection from the farmers was carried out in the 30 selected villages of Madhya Pradesh and a total 600 farmer's data were collected and analysed. To evaluate efficiency, Data Envelopment Analysis (DEA), a non-parametric statistical method, was employed to identify efficient and inefficient farmers and to calculate the projected energy saving.

The introduction of a solar-operated knapsack sprayer in a soybean field significantly reduced energy consumption. For herbicide application, energy input with solar sprayer was 150.35 MJ/ha, compared to 174.35 MJ/ha with a conventional power knapsack sprayer, resulting in the energy saving of 13.77%. In case of insecticide application, the energy consumption with the solar-operated knapsack sprayer was observed 51 MJ/ha. In Madhya Pradesh energy consumption for insecticide application with the manual knapsack sprayer was 59 MJ/ha, whereas with the power knapsack sprayer it was 116 MJ/ha, resulting in a 14% and

56% energy saving respectively with the solar-operated sprayer, showcasing its efficiency and sustainability.

Intervention of technologies like laser land leveller (LLL), seed cum fertilizer drill and solar-operated knapsack sprayer were carried out in the farmer's field. It was observed that, energy saving of 5.59% is possible with the use of LLL. A seed cum fertilizer drill was introduced for sowing soybean (variety RVS 1135) with a seed rate of 85 kg/ha, reducing total energy consumption to 1932 MJ/ha compared to the regional average of 2615 MJ/ha. This intervention achieved around 26.10% energy saving.

Fig.10.4 Energy inflow outflow and savings through improved technologies in the soybean wheat system of selected villages in Madhya Pradesh

CHAPTER - 11

11. Utilizations of Wind Energy

Notation

a	Axial speed induction factor
a′	Angular speed induction factor
B	Number of blades
c	Chord length of blade (m)
Cd	Drag coefficient
C_1	Lift coefficient
Cp	Power coefficient
F	Tip-loss factor
P	Power from wind turbine (W)
Q	Rotor torque (Nm)
r	Radial distance from rotor axis to blade element (m)
R	Radius of rotor (m)
T	Rotor thrust (N)
v∞	Wind or approach velocity (m/s)
W	Relative velocity (m/s)

Greek letters

α	Angle of attack (deg)
ε	Minimum drag-to-lift ratio of airfoil of rotor blade
θ	Blade setting angle (deg)
Λ_0	Tip speed ratio of rotor
λ_r	Local speed ratio of rotor
ρ	Air density (kg m^{-3})
σ	Local solidity ratio
φ	Angle of relative wind (deg)
Ω	Angular velocity of rotor (rad s^{-1})

The enormous potential of wind as natural energy source, mainly because of its decentralized availability, makes it a promising energy option. The horizontal axis windmills are most common of all wind machines. Most recent works on wind energy appears to be related to the generation of electrical power and little effort has been directed to water pumping windmills for irrigation.

11.1 Uses of Wind Power

Low-speed multi-bladed horizontal axis windmills are suitable for irrigation pumps due to their high starting torque and efficient operation in low wind conditions. However, design parameters of Horizontal Axis Wind Turbine (HAWT) rotors vary widely, requiring optimization.At low Reynolds numbers typical of such windmills, cambered steel plates are preferred over NACA or Wortman air foils. Since blade camber and angle of attack vary significantly with changing tip speed ratios, it is essential to determine lift and drag characteristics of cambered blades across a wide range of angles for accurate performance prediction and camber optimization.

The design of a HAWT involves selecting the number of blades, air foil type, and radial variations in chord length and twist. Early aerodynamic designs assumed frictionless flow and infinite blades, allowing simple analytical solutions. Later studies, following renewed wind energy interest in the 1970s, incorporated effects of drag and finite blade numbers, but these introduced complex iterative methods to satisfy aerodynamic relationships, making closed-form solutions difficult.

To achieve maximum power extraction, aerodynamic analysis must include drag and tip-loss effects while simplifying design relations for practical use. Moreover, increasing the number of blades at a constant solidity reduces chord length and Reynolds number, lowering aerodynamic efficiency and power output. Since existing models use the Prandtl tip-loss factor without accounting for Reynolds number effects, optimizing the number of blades (ranging from 6–48 in current designs) through wind tunnel experiments is necessary. For rotors with a design tip-speed ratio of around 2.0, the ideal blade count lies between 4 and 12, emphasizing the need for systematic optimization of low-speed HAWT designs.

The following investigations were carried out on utilization of wind energy.

11.2 Generation of performance characteristics of a 5 m diameter horizontal axis wind rotor.

To ensure proper load matching, it is essential to know the torque and power characteristics of wind rotors. These characteristics can be obtained through computer simulation or wind tunnel testing. However, simulations are limited by incomplete airfoil data across wide angles of attack and by difficulties in accounting for Reynolds number effects, while wind tunnel models cannot accurately represent wind shear or structural interferences from supports and towers.

To determine rotor performance, testing with a loading device, similar to that used for IC enginesis necessary over a wide range of torque and speed. A 12-bladed, 5 m diameter rotor was tested using a hydraulic loading device to measure torque, speed, and wind velocity at rotor height. Variations in output power with wind speed and in power and torque coefficients with tip-speed ratio were analysed.

The rotor frame comprised six spokes, inner and outer rings, and a hub mounted on a 50 mm shaft. Each MS sheet blade (1.6 mm thick) was attached to supports providing the required twist, with roots positioned 0.5 m from the axis. A 4 m long tail vane enabled automatic alignment with wind direction. The 6.5 m high truss-type tower, made of MS angles and a 115 mm diameter top pipe, had a 2.2 m square base.

An automatic furling device deflected the rotor axis up to 75° from the wind direction when wind speed exceeded 36 km/h, preventing over speeding. Based on the experimental tests, the power and torque characteristics of the 12-bladed HAWT were successfully evaluated, providing useful data for optimizing low-speed windmill designs.

From the test results of the horizontal axis wind rotor, the following conclusions were drawn:

i. The power output of the windmill was upto 360 W at 5 m/s of wind speed. The practical cut-in speed of the wind mill is 3 m/s.

ii. The rotor efficiency of 0.26 to 0.29 was obtained when the wind rotor was operated in the tip speed ratio range of 1.8 to 2.6.
iii. Torque coefficient of 0.11 to 0.15 was obtained when the rotor was operated in tip speed ratio range of 1.0 to 1.9.
iv. From power as well as torque point of view the optimum tip speed ratio for the rotor was 1.8 to 2.0.

11.3 Aerodynamic characteristics of cambered steel plate in relation to their use in wind energy conversion systems

Two-dimensional wind tunnel studies were conducted to determine lift and drag characteristics of steel blades with 0, 4, 6, 8, 10, 12 and 14 per cent camber. The aerodynamic characteristics of blades were determined at Reynolds number of 2.23×10^5. The span and chord length of the blades were 606 and 304 mm respectively. Two ring transducers were designed and developed for measurement of lift and drag forces. The corrections in angle of attack were made for streamline curvature effect. The variation of lift and drag coefficients and lift to drag ratio with angle of attack was studied.

Findings

1. The maximum lift coefficient (C,) was 1.58 for 8 per cent and 1.60 for 10 per cent cambered blades. The lift coefficient of flat plate was minimum at all angles of attack.
2. The drag coefficient (Ca) of blades increased with increase in camber. It was minimum in the angle of attack range of -2° to +1° and maximum in the range of 80° to 90°. For cambered blades, the maximum values of drag coefficient were obtained in the range of 1.9 to 2.2.
3. The lift/drag ratio was found to be maximum for 8 per cent cambered blade. For angle of attack range of 0 to 20°, the ratio was low for 14 per cent cambered blade. However, at larger angles, it was low for flat plate. The overall maximum C_1/C, ratio obtained was 25 for 8 per cent cambered blade at 4º of angle of attack.
4. Taking into account the maximum C_1/C and the range of angle of attach across which C_2/Ca is high, the 8 per cent cambered blade was found to be the best for its application to Wind Energy Conversion Systems (WECS).

11.4 Optimum design and performance prediction of HAWT rotors

The optimum design of a HAWT rotor is the determination of blade shape and twist at different radial locations such that the power extraction from the rotor is maximum at the design tip-speed ratio. The existing methods for optimum designs either do not take into account the effects of drag and tip-losses or are approximate and based on trial and error. A new method for optimum design and peak performance prediction, based on analytical approach was devised. Through extension of strip theory, which is based on momentum theory and blade element theory, the following relationship was derived as condition for maximum power extraction.

11.5 Conditions for maximum power from horizontal axis wind turbines

Conventional analysis of the performance of a horizontal axis wind turbine rotor combines a momentum balance of the flow upstream and downstream of the rotor with the aerodynamic characteristics of the air foil section concerned. The flow through the rotor is shown in Fig. 11.1 The momentum theory, after application of the Prandtl tip-loss factor, yields following relationships for the thrust and torque of a blade element.

$$dT = 4aF(1-aF)pV_{\infty}^2 \cap rdr \quad \text{... (11.1)}$$

and

$$dQ = 4aF(1-aF)pV_{\cap\Omega}r^3dr \quad \text{... (11.2)}$$

where the tip-loss factor F is given by

$$F = \frac{2}{\cap}cos^{-1}\left\{exp\left[-\frac{B}{2}\left(1-\frac{r}{R}\right)(1+\lambda_o^2)^{1/2}\right]\right\} \quad \text{... (11.3)}$$

Flow around a blade element is shown in Fig. 11.2. Through blade element theory, the thrust and torque of a blade element are as follows:

$$dT = (1-a)^2\frac{\sigma C_{1^{cos\emptyset}}}{sin^{2\emptyset}}\left(1+\frac{C_d}{C_1}tan\,\emptyset\right)\frac{1}{2}pV_{\infty}^2 2\pi rdr \quad \text{... (11.4)}$$

and

$$dQ = (1-a)^2\frac{\sigma C_1}{sin^{\emptyset}}\left(1-\frac{C_d}{C_1}tan\,\emptyset\right)\frac{1}{2}pV_{\infty}^2 2\pi rdr \quad \text{... (11.5)}$$

where the solidity ratio

$$\sigma = \frac{Bc}{2\pi r} \quad \text{... (11.6)}$$

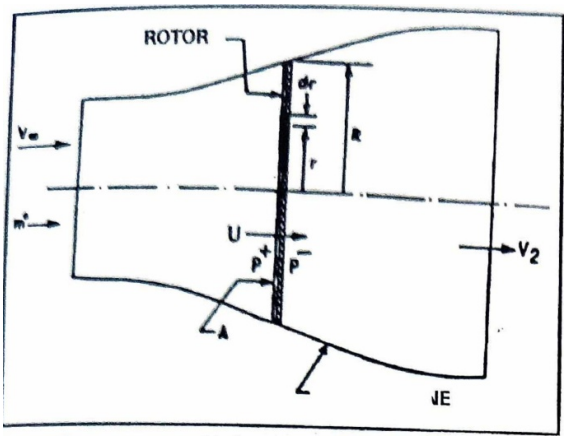

Fig. 11.1 Wind Turbine Control Volume

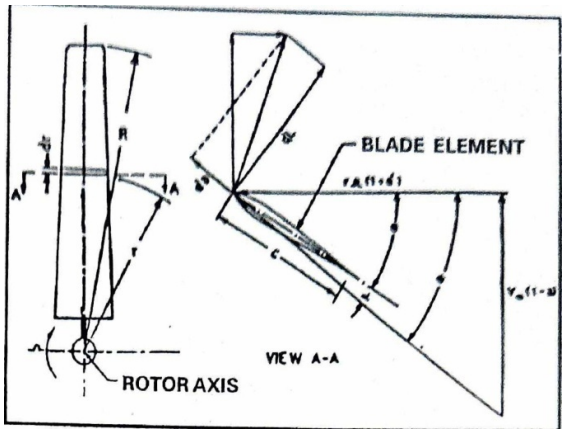

Fig. 11.2 Velocity and force components on a blade element

The power generated by an element of the wind turbine rotor blade is

$$dP = \Omega dQ \qquad \ldots (11.7)$$

and the power coefficient.

$$dC_p = \frac{dP}{\frac{1}{2}p\pi R^2 {V_\infty}^3} \qquad \ldots (11.8)$$

From eqns. (11.5), (11.7) and (11.8)

$$dC_p = \frac{8}{{\lambda_o}^2} a'F(1 - aF)\lambda_r{}^3 d\lambda_r \qquad \ldots (11.9)$$

Where,

$$d_r = \frac{\Omega dr}{V_\infty}$$

At any radial station and a given tip-speed ratio, the values of F and λ_r, are constant. Therefore, at the given radial station, for dC_p to be at a maximum, the term a'(1-aF) has to be at a maximum.

The condition for a'(1-aF) to be at a maximum is,

$$\frac{d\acute{a}}{da} = \frac{F\acute{a}}{1 - Fa} \qquad \ldots (11.10)$$

By equating the expressions for thrust and torque obtained from momentum and blade element theories [eqns. (11.1), (11.2), (11.4) and (11.5)] and dividing the resultant expression for the torque by that for the thrust.

$$\frac{\acute{a}}{a} = \frac{tan\,\emptyset - \varepsilon}{\lambda_r(1 + \varepsilon\, tan\,\emptyset)} \qquad \ldots (11.11)$$

Where,

$\varepsilon = C_d / C_1$

By substituting, $tan\,\emptyset = \frac{1-a1}{1+\acute{a}\lambda_r}$ ... (11.12)

$$\frac{\acute{a}}{a} = \frac{(1-a) - \varepsilon(1+\acute{a})\lambda_r}{\lambda_r[(1+\acute{a})\lambda_r + \varepsilon(1-a)]}$$

or

$$\acute{a}^2\lambda_r^2 + \acute{a}(\lambda_r^2 + \varepsilon\lambda_r) + a^2 + a(\varepsilon\lambda_r - 1) = 0 \quad \ldots (11.13)$$

By differentiating eqn. (11.13) with respect to a,

$$\frac{d\acute{a}}{da} = \frac{1 - 2a - \varepsilon\lambda_r}{\lambda_r^2\, 2a' + \lambda_r^2 + \varepsilon\lambda_r} \quad \ldots (11.14)$$

By comparing the values of da'/da from eqns. (11.10) and (11.14),

$$2F\lambda_r^2\acute{a}^2 + F(\lambda_r^2 + \varepsilon\lambda_r)\acute{a} - (1 - Fa)(1 - 2a - \varepsilon\lambda_r) = 0 \quad \ldots (11.15)$$

By substituting $\lambda_r^2\acute{a}^2$ from eqn. (11.13) in eqn. (11.15),

$$\acute{a} = \frac{(1 - \varepsilon\lambda_r - a)(3Fa - 1) + a(1 - Fa)}{F\lambda_r(\lambda_r + \varepsilon)} \quad \ldots (11.16)$$

Where, a = axial speed interference factor;

a' = angular speed interference factor;
λ_r = speed ratio of blade element;
F = Prandtl tip-loss factor; and
ε = drag to lift ratio of airfoil.

Therefore, eqn. (11.16) is the condition relating two speed induction factors, the drag-to-lift ratio and the tip-loss factor for maximum power from an element at a given radial station on a blade.

11.6 Design of rotor and its peak performance prediction

For the design of the rotor for maximum power a blade was divided into a number of radial elements, each node representing a radial station. The blade chord, its twist and the local power coefficient at each station were determined as described below:

Speed induction factors

The axial and angular speed induction factors (a and a') for any radial station were determined by solving eqns. (11.13) and (11.16). The solutions were obtained using the Newton-Raphson method.

Chord length and twist of blade

At the given radial station, the relative wind angle ϕ was determined using eqn. (11.12). The twist of the blade θ = ϕ - a, where a is the angle of attack for the airfoil section of the blade at which the C_d/C_l ratio is at a minimum. By equating the thrust from eqns. (11.1) and (11.4), the solidity ratio is,

$$\sigma = \frac{4aF(1 - aF)\, sin^2\, \emptyset}{(1-a)^2 C_l (1 + \varepsilon\, tan\, \emptyset)\, cos\, \emptyset} \quad \ldots (11.17)$$

After calculating from eqn. (40), the chord length was determined using eqn. (11.6). C_l is the lift coefficient at the minimum C_d/C_l value for the given airfoil section.

Power coefficient

The power coefficient for the element at the radial station was determined using eqn. (11.9). For numerical integration, eqn. (11.9) was modified as follows:

$$dC_p = \frac{8}{\lambda_o} a' \; F(1 - aF)\lambda_r^3 \frac{dr}{R} \qquad \ldots (11.18)$$

The total number of radial stations was taken to be 19, in steps of 0.05R. The first radial station was at 0.05R and the last at 0.95R. The right-hand side of eqn. (11.16) contains F and λ_r in the denominator. At r=0, λ_r becomes zero. At r=R, F becomes zero [eqn. (11.3)]. Therefore, computations at the two extremes of the blade could not be carried out and the contributions to the power from the inner 5% and outer 5% lengths of blade were not included. In the design process, the iterative treatments required for convergence of the speed induction factors and for maximization of the power through comparison were obviated, because of the exact relationship established for a, a', ε and F corresponding to maximum power. The only iterative process required in the new method is for solution of an equation by the Newton - Raphson method, which requires a maximum of 10 iterations for an accuracy of 10^{-5} for a. Because of the exact relationship established, the design process begins right at the maximum power point rather than searching for the point of maximum power and then performing the computations. This leads to a simplification of the optimum design and accurate peak power prediction and at the same time to a saving of computer time. The whole design and peak power prediction for a windmill using the new method takes about 40s on an 8-kbyte computer.

In the new method, use of the above relationship obviated the iterative process involved in conventional optimum design and peak performance prediction methods for locating the point of peak power from a blade element. For optimum design and peak performance prediction of HAWT rotors, a computer programme was developed. The new method also enabled determination of different flow parameters and study of them with design conditions of a rotor. The results of the new- method were compared with those of the methods of other researchers.

A computer programme was also developed for off-design performance prediction of HAWT rotors. The airfoil data for 8 per cent cambered blade were utilized and performance characteristics of rotors with different number of blades were found out for design tip-speed ratios of 2.0 and 3.0.

Findings

1. A relationship among speed interference factors, minimum drag/lift ratio and the tip-loss factor for maximum power extraction from a horizontal axis wind turbine has been established and through use of this, the iterative processes required in conventional optimum design and peak performance prediction methods have been obviated.
2. The increase in design tip-speed ratio greatly reduced the rotor solidity and relative wind angle. The increase in drag reduced rotor solidity but increased the relative wind angle. Lessening the number of blades reduced both, the rotor solidity as well as the relative wind angle, however, the effect of number of blades was negligible at high design tip speed ratios.

3. For speed ratios less than 2.0 (in the range where major portion of low speed wind rotor blades operates), the influence of drag and tip-loss factor on axial and angular speed interference factors was high.
4. From peak performance prediction of HAWT, it was found that the power coefficient (C_p) increased with increase in tip-speed ratio (λ). At high tip-speed ratios, the power coefficient decreased for high values of drag/lift ratio. Increasing tip-speed ratio beyond the optimum value increased the energy loss due to drag whereas below the optimum value, effects of slip stream rotation and tiplosses were more prominent.
5. From the off-design performance prediction for HAWT rotors it was found that the power coefficient of the rotors decreased at tipspeed ratio lower or higher than the design value. At off-design tip speed ratios, the different parts of blades operated at angles of attack away from the optimum value and thus the aerodynamic performance was poor.
6. The results of off-design performance prediction for HAWT rotors revealed that the increase in number of blades improved the performance of a rotor, however, the extent of improvement was more at the lower number of blades in rotor.

11.7 Design, development and testing of rotor models

The results of peak and off-design performance prediction methods suggest that the performance of the rotor improves with increase in number of blades. However, increase in the number of blades reduces its chord length resulting in the reduction of its Reynolds number. At low Reynolds numbers, the aerodynamic performance of airfoils deteriorates, and output power is reduced. The peak and off-design performance prediction methods do not take into account the effect of Reynolds number. Keeping the effects of tip-losses as well as Reynolds number in view, optimum number of blades was determined by testing the rotor models of following tip-speed ratios and number of blades:

Design tip speed ratio	Number of blades in rotor
2.0	4, 6, 8, 10, 12, 14 and 16
3.0	3, 4, 6, 8, 10, 12 and 14

The rotor models with design tip-speed ratio of 2.0 were tested in wind tunnel at four air velocities in the range of 7 to 14 $m.s^1$ and models with design tip-speed ratio of 3.0 were tested at two air velocities ranging from 11 to 14 $m.s^1$. The power and torque coefficients, tip-speed ratio and Reynolds number at peak power were determined. The effects of tip- speed ratio, number of blades and peak power Reynolds number on power coefficient were studied. The torque characteristics of the rotor models were also studied.

Findings

1. For rotor models with design tip-speed ratio (λ_d) of 2.0, maximum power coefficients at all air velocities were found to be highest with 8-bladed rotor. The highest value of power coefficient for 8- bladed rotor was however 12 per cent less than the value obtained through off-design performance prediction method. This may be attributed to transmission losses in test set up and lower Reynolds number.

2. For bladed rotor models with design tip-speed ratio of 3.0, 3- and 4- rotors performed better than the other rotors. The maximum power coefficients with the 3- and 4-bladed rotors 3.00. ranged from 0.35 to 0.36 in the tip-speed ratio range of 2.73 to 3.00.
3. For the rotor models with design tip-speed ratio of 2.0 as well as 3.0, the performance of the rotors improved when the number of blades was increased from 4 to 10 for λ_d=2.0 and 3 to 4 for λ_d =3.0. When the number of blades was very high (12 to 16 for λ_d=2.0 and 8 to 14 for λ_d=3.0), the performance of the rotors was, however, poor. For fewer number of blades, the tip-losses are reduced greatly when the number of blades is increased, but for large number of blades the reduction in tip-losses is only marginal and loss of power through reduced Reynolds number becomes more dominant.
4. For design tip speed-ratio of 2.0, 8- and 10-bladed rotors performed better than the other rotors at the same Reynolds number. Although there was no noticeable difference in the performance of 8- and 10-bladed rotors at similar Reynolds numbers, the 8-bladed rotor was better because it attained higher Reynolds number at a given air velocity through its larger blade chord.
5. The maximum torque coefficient for rotors with design tip-speed ratio 2.0 varied from 0.140 to 0.207 whereas for rotors with design tip-speed ratio of 3.0, it varied from 0.092 to 0.141. Therefore, for low speed applications where better torque characteristics are desirable, the HAWT rotor with design tip-speed ratio of 2.0 is better than that with design tip-speed ratio of 3.0.

11.8 Development and testing of 5 m diameter rotor

From testing of rotor models in wind tunnel, an 8-bladed rotor with design tip-speed ratio of 2.0 was found to be the best for low speed horizontal axis windmill. A scaled-up rotor of 5 m diameter with design tip-speed ratio of 2.0 and eight blades was developed (Fig. 11.3). The blades were made of 1.02 mm GI sheet. Pipe sections were provided for reinforcement at high pressure side of the blades. The blade chord length and twist were linearized. The rotor was mounted atop a truss type tower. The rotor shaft height above ground level was 7.0 m. A turn table and tail vane assembly facilitated yawing of the rotor. A furling mechanism was provided as protection device against wind speeds above 36 kmph. Two bevel gear boxes were provided to obtain rotary power at ground level with speed step up of 3.6 times from the rotor.

Fig. 11.3 View of CIAE Multibladed Horizontal Axis Wind Mill

The rotor was tested for its power and torque characteristics across wind speed range of 3.8 to 8.5 ms^{-1}. During testing, wind speed at rotor height, rotor speed and rotor torque were measured. An in-line torque pick up was used for measurement of rotor torque. A hydraulic loading device was used for loading of rotor. The gear pumps of the loading device were run with wind rotor. The outlet pressure of the pumps was set with pressure relief valves. Increase in outlet pressure of pump increased the torque on pump and in turn the torque on rotor. By setting different loads (torques), the rotor was tested across the tip-speed ratio range of 0.5 3.5.

Findings

a) The output power of the 5 m diameter rotor was 0.224, 0.807 and 2.00 kW at 4, 6 and 8 $m.s^{1}$ of wind speed, respectively.
b) The power coefficient of the rotor increased with increase in wind speed. The maximum power coefficient increased from 0.288 to 0.325 with increase in wind speed range from 3.8-4.5 to 7.5-8.5ms^{-1}. The maximum power coefficient was obtained in tipspeed ratio range of 2.2 to 2.3.
c) The maximum power coefficient of 5 m diameter rotor was 19 to 28 per cent less than that obtained from off-design performance prediction method. It was 8.2 to 18.6 per cent less than the maximum value for the 8-bladed (λ_d = 2.0) rotor model tested in wind tunnel. This difference may be due to wind shear, drag of reinforcement members, tower shadow and transmission losses.

CHAPTER - 12

12. Other Areas of Energy Research

12.1 Development of tractor operator's workplace layout based on ergonomical considerations

Operating a tractor imposes considerable physical and mental stress on the operator, and improper seat or control design can severely diminish work performance and increase the risk of accidents (Fig. 12.1). For four-wheel tractors, the comfortable and safe operation hinges on the proper design of controls, including their location and the required strength limits for their use. Optimal workplace layout is achieved by integrating anthropometric data with the technical design features. The control dimensions of frequently operated componentssuch as the steering wheel, hand accelerator, brake and clutch pedals, gear shift lever, and accelerator pedalwere designed using compiled anthropometric and strength data of Indian agricultural workers, analysis of existing tractor layouts, and user feedback. Specifically, the accelerator pedal, a frequently toe-operated control, requires a limiting force of 75 N (considering 30% of the 5th percentile right foot strength), with its minimum length equal to the 95th percentile toe length and its width exceeding the 95th percentile foot breadth. Conversely, the brake pedal, requiring high force and operated by the right leg, necessitates a limiting force of 250 N (the 5th percentile value of right leg strength sitting). Similarly, the clutch pedal, operated by the left leg, utilizes the 5th percentile value of left leg strength sitting as the limiting force. Both the brake and clutch pedals should have a minimum length of 60 mm (optimum 75 mm) based on ergonomic guidelines, with their breadth determined by the 95th percentile value of foot breadth.

Fig.12.1 Tractor operator's seat

12.2 Evaluation of tractor exhaust mufflers

The performance of different tractor exhaust mufflers of HMT, IIT design, Escorts, and the existing standard mufflerwas evaluated on HMT and MF tractors. Noise levels at the operator’s ear were measured under three conditions: no load in the laboratory, no load during transport on tar road, and ploughing with a two-bottom MB plough, following IS:12180-1987. One-octave band spectral analysis

(31.5–16000 Hz) was also conducted, along with measurements of exhaust back pressure, exhaust gas temperature, and fuel consumption.Noise increased with engine speed for all mufflers. Maximum noise occurred at 1 kHz for most mufflers and at 2 kHz for the Escorts muffler and without muffler. On HMT tractor, IIT muffler showed noticeable improvement, reducing noise by 1.6 dB(A) under stationary no load and 5.6 dB(A) during ploughing compared to the existing muffler. On the MF tractor, IIT muffler reduced noise by 5.5 dB(A) at rated speed. Noise reduction was more prominent in higher frequency bands.

Back pressure, exhaust gas temperature, and fuel consumption all increased with engine speed. IIT muffler produced lower back pressure than the standard HMT muffler (2.73 vs 6.08 kPa). Exhaust gas temperatures ranged from 225–267°C on HMT and 248–264°C on MF tractors across mufflers. Fuel consumption at rated no-load was slightly lower with IIT mufflers on both tractors compared to the standard mufflers.

12.3 Decision support system for farm machinery management for their optimum selection and matching with power source

The increasing number of tractor modelsover 75 options ranging from 12 to 60 hphas made the selection of appropriate tractors and matching implements more complex for farmers. Proper matching of machinery plays a crucial role in improving operational efficiency, reducing fuel and operating costs, and ensuring optimum capital utilization. To address this challenge, a system-based decision support tool was developed for the optimal selection and matching of tractors, implements, and other farm machinery.

A mathematical model was formulated and incorporated into computer-based software (Fig. 12.2), enabling users to determine the required drawbar power based on implement draft and operating speed. The software further estimates PTO power needs by considering only 80% of the tractor's maximum engine power, ensuring realistic field performance. Using these computed requirements, the system recommends suitable tractor makes and models from a comprehensive databank.

The decision support system also helps reduce energy use, as studies by PCRA indicate that proper implement matching, gear selection, engine throttling, and ballasting can save up to 30% diesel. By integrating technical specifications of more than 50 tractor models from major manufacturers such as Mahindra & Mahindra, HMT, Eicher, TAFE, Escorts, Punjab Tractors, Bajaj Tempo, and Sonalika, the tool helps users make informed choices. Market data incorporated in the system also show that 31–40 hp tractors dominate with about 55% share, helping guide practical selection decisions.

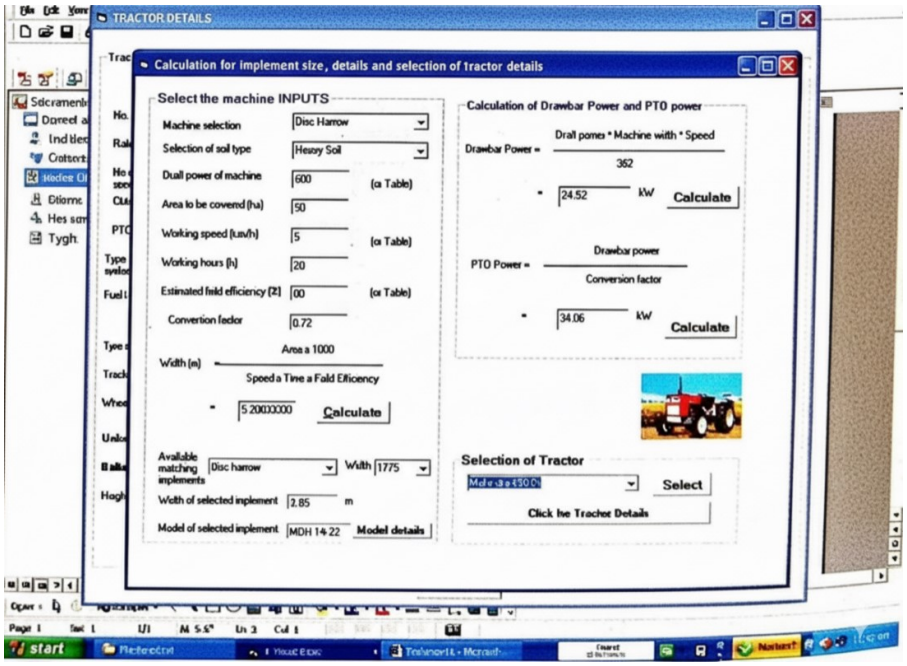

Fig.12.2 Software screen for calculating implement and tractor size

12.4 Reduction of ride and hand transmitted vibrations to tractor operators

Hand-arm vibration levels on tractors were evaluated using an OR36 eight-channel sound and vibration analyser (OROS, France) equipped with a tri-axial accelerometer mounted on the steering wheel. Tests were conducted during transport mode on both tar-macadam and farm roads. On tar roads, measurements were taken at forward speeds of 10.5 and 17.2 km/h, while on farm roads, speeds of 4.8 and 10.6 km/h were used. Travel speed was accurately determined by timing the tractor over marked distances of 100 m (tar road) and 50 m (farm road).The measured hand–arm vibration levels were compared with ISO 5349 (1986) limits. Results showed that ISO-weighted RMS accelerations were consistently higher on farm roads than tar roads at all speeds. Vibration levels in the X and Y axes generally remained within the ISO 2, 4 and 8hour exposure limits, except at 32 Hz in the X-axis at 17.2 km/h on tar road, where the limits were exceeded. More notably, 63 Hz vibrations in the Z-axis surpassed ISO limits under several operating conditions (Fig.12.3), indicating a critical concern.The study highlights the need for targeted vibration-reduction strategiesparticularly at 63 Hz, where excessive steering-wheel-transmitted vibrations pose increased risk to operator comfort, safety, and long-term health.

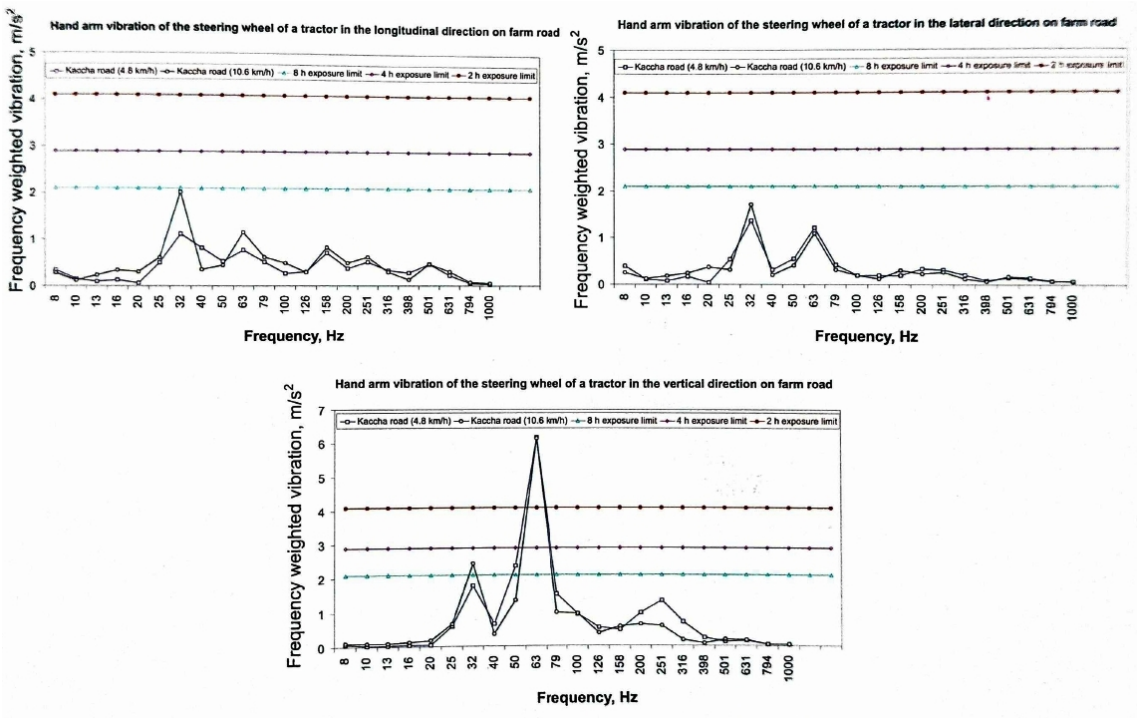

Fig. 12.3 Vibration level at man-seat interface on farm road at different forward speeds

12.5 Investigation on greenhouse gas emission in different energy conversion processes for efficient utilization of surplus crop residues

The field burning of different crop residues in the state of Madhya Pradesh was assessed using Image processing Software (Erdas Imagine 9.3) and the results were validated on sample basis by surveying. A typical example for extraction of crop burned area is given Fig. 12.4. Wheat was the major crop dominant in the rabi season covering 76.582.2% area. Using satellite image analysis the field area burnt was found to the extents of 35.7-49.4 % in Rabi season. A study was conducted to assess the char produced during open field burning of crop residues (wheat straw) in three villages namely Sadalatpur, Barbatpur and Mandideep of Raisen district. The study revealed that the amount of char from crop residue burnt fields varied from 67-129 kg/ha whereas the potential of conversion of biomass to char is 700 kg/ha.

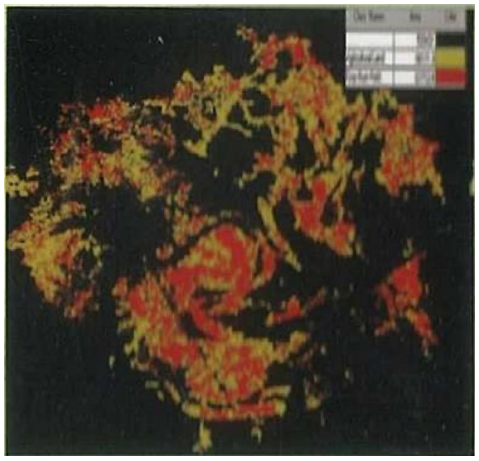

Fig. 12.4 Satellite-based assessment of crop residue burning and char generation from wheat straw

12.6 Energy auditing of a Dal mill

The energy auditing of a Dal mill (1 t/h), in Raisen district has been conducted. It has been observed that in the process of dal making electrical and thermal energy is used. Electrical energy is used for operating motors and thermal energy for drying operation. Dal mill has five electrical motors of 5.5- 15 kW capacity. The electrical energy use was measured with help of clamp on power meter. Power factor for operation of different motors has been found in the range of 0.9-1.0. The motor of 11.25kW capacity has been suggested to be replaced with 7.5 kW motor to improve utilization factor from 67 to 71%. The replacement of motor can save 1200 kWh/year, worth Rs 7,200/year with payback periodof three years. Sixtyfour tonne of wood is being used annually by this Dal mill for drying purpose, which can be replaced with biomass briquettes. The replacement ofwood with briquettes would save Rs. 73,000/- annually apart from reducing deforestation.

12.7 Microalgae production and harvesting system

The laboratory scale production and isolation of microalgae have been carried to select suitable strain for large scale cultivation. Three stains of microalgae such as Scendesmus sp., Oscillatoria sp. and Chlorella sp. have been isolated and grown in 5 litre container in BG-11 media in a growth chamber under controlled environment (by controlling light, CO2, temperature and nutrients). The growth of algae (selected strain of Scendesmus sp. and Chlorella sp.) was up-scaled in a 20polythene bag, followed by a final production in a raceway open pond (Fig. 12.5) of 2500 L capacity (Fibre reinforced plastic (FRP) pond). The FRP pond was specially designed to grow the algae. The pond is provided with FRP paddles for stirring the content which is powered by a geared motor (0.25 hp) to maintain the speed of 10 rpm. Growth of the algae is accelerated in the race way pond by using different combinations of fertilizer leading to production of algae at the rate of 350 mg/100ml with an optical density (OD) of 686 nm.

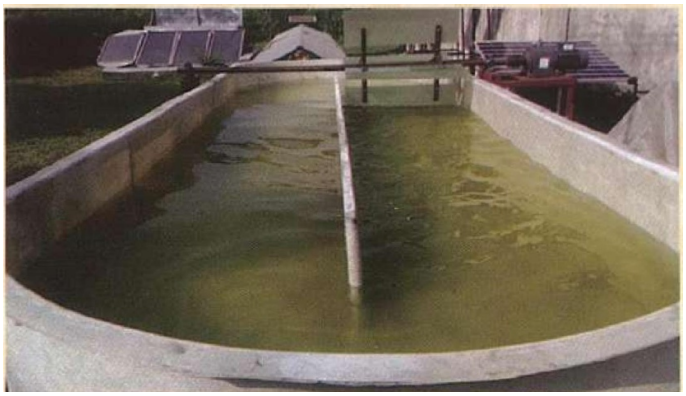

Fig. 12.5 Microalgae production system

Different harvesting techniques such as chemical flocculation, electrolysis and filter paper have been tried to harvest micro algae cultivated in the open pond. It is observed that the performance of filter paper harvesting was best in terms of

OD (0.015-0.077) and yield (0.4 g/l) of algae obtained after harvest is dried by using vacuum dryer at temperature 55-60°C.

12.8 Energetics of soybean-wheat cropping system in Madhya Pradesh

Energy input and output analysis of soybean-wheat crop production is used to identify the energy intensive farm operations and find the way to minimize the energy input at different levels of productivity. The energy productivity and energy use efficiency for soybean crop have been found to be 0.08 k/MJ and 2.26, respectively, whereas the values are (022 kg/MJ and 5.26, respectively for wheat crop. Cost of production for soybean and wheat varies from Rs. 16580-17438 and Rs. 31047-33381 per ha, respectively according to land holding size of the farmers. It has been observed that the tillage operation with MB plough and cultivator is energy intensive operation at the farmer's field in both the crops. The intervention of rotavator in seedbed preparation has the potential to save 25.41% and 39.18% of energy input required in soybean and wheat crop, respectively. The post production energy requirement for soybean and wheat has been found to be 41.46 and 44.01MJ/q, respectively when using tractor for transport operation.

12.9 Energy inflow and outflow for maize-chickpea cropping system of Madhya Pradesh

Analysis of energy requirement for different farm operation is important for minimization of energy input for growing crop and enhances the input use efficiency without hampering crop productivity. Energy input and output analysis for maize-chickpea cropping system has been carried out for this purpose. The total energy required in maize crop for seed bed preparation, sowing, fertilizer application, inter culture, plant protection, harvesting and threshing operation has been found to be 1476.1, 650.5, 7987.9, 126.5 and 259.3 MJ/ha, respectively. In seed sowing, manual method is followed to place the seed in channel. Fertilizer application requires the maximum 75.9% of total energy input. Diesel is the second highest contributor in the input energy matrix with 16.8% of total energy input. The average energy consumption for maize cultivation in Madhya Pradesh is found as 10510.3 MJ/ha. The analysis shows energy use efficiency and energy productivity of 5.01 and 0.34 kg/MJ, respectively. Input energy requirement for seedbed preparation, sowing, fertilizer application, irrigation, plant protection and harvesting & threshing of chickpea cultivation has been 936.5, 2236.1, 1943.1, 1915.7, 93.4 and 258.3 MJ/ha, respectively. Source wise energy contribution indicates that fertilizer share is more than other inputs. Diesel contributes 17.9% in total input energy matrix due to involvement of tractors and reaper. Similarly, the average total energy input, energy use efficiency and energy productivity for chickpea cultivation is 7381 MJ/ha, 3.41 and 0.19 kg/MJ, respectively.

12.10 Conversion of tractor diesel engine to 100% compressed natural gas engine

To substitute fully or partially the gasoline or diesel fuel with Compressed Natural Gas (CNG) and bio-CNG an attempt has been made to develop a CNG based

system to retrofit in the tractor engine by modification of engine components (Fig. 12.6). A three cylinder tractor engine has been selected for the study.

Fig. 12.6 CNG based system retrofit in the tractor engine

Frame for mounting CNG cylinder (60 l water capacity) has been fabricated, assembled and installed in front of the tractor. The CNG kit is fitted with CNG cylinder. The reduction in compression ratio of tractor engine from 17:1 to 10.33:1 has been done by using 5.2 mm thick spacer and placed below the engine head. The fuel pump has been replaced with spark distributor and fitted/aligned in the timing gear mechanism of the tractor with modified flange. An inlet air manifold has been fabricated and carburetor has been suitably fitted to regulate the air-CNG mixture. All the arrangements with air cleaner have been made to connect carburettor and air cleaner.

Contact us

Agricultural Energy and Power Division
ICAR-Central Institute of Agricultural Engineering
Nabibagh, Berasia Road, Bhopal – 462038
Ph: 07552521117